

Measurement of air content in the Greenland ice sheet

**Master thesis of
Sebastian Bender**

**Supervisor
Thomas Blunier**

**co-supervisor
Bo Vinther**

ABSTRAKT

I dette speciale beskriver jeg, hvordan jeg har opbygget et apparat, der kan måle luftindholdet i gletsjeris. Jeg har målt luftindholdet i 10 stykker is fra Indlandsisen i Grønland (Eurocore) med en rimelig præcision. Jeg har sammenlignet målinger fra litteraturen. 3-4 målinger stemmer godt overens, mens 6 målinger giver et lidt højere luftindhold end forventet.

ABSTRACT

In this thesis I describe how I have build an apparatus to measure the total gas content in glacier ice. I show the measurement of 10 adjacent samples from a Greenland ice core (Eurocore), estimate the accuracy and compare the result with earlier studies from the literature. 3-4 measurements are in good agreement and 6 measurements gave a higher air content than expected.

Content

Introduction	3
PTV-Method	4
Effects of variations in ice sheet elevation	5
Setup overview	6
Heat fluxes in the system	7
Effects of vapour pressure	8
Refreezing and solubility of gasses	10
Measure instruments	19
On temperature sensors.	19
Building circuits for the measurements and resolution considerations	20
Data logging	24
First temperature instrumentation	26
On calibration of sensors.....	29
Calibration of pt1000-sensors with a precise pt100-sensor – initial considerations.	29
Refined calibration with 2 dataloggers.....	32
Calibration over an time interval with slowly rising temperatures.....	38
Calibration of sensor 3 and 4 (around 25°C).....	38

Calibration of Sensor 1 and 2 (near -30°C)	43
Further calibration of pt1000 sensors.	49
Measuring the saturated vapour pressure – test of the pt1000 calibration. A possible better way of calibrating	53
Rejecting the sensor calibration.....	55
Stability of electronics	56
Pressure measurement	57
The pump	57
Calibration of the pressure gauge	58
Automatic logging with the pressure gauge	64
Dimensions of the setup	66
Valve corrections	67
Leak corrections	67
Volume calibration	68
Appendix Volume and additional calibration	73
Calibration of V_{ex}	76
Summarizing the calibrated volumes needed for measurements	77
Measurements on air contained in a volume with variable temperature	77
Summarize of calculations	81
Ice core measurements	82
Estimate of the air content	88
Individual errors on all measurements	88
Correction for the cut bubble effect.....	91
Possible explanations for the deviation from Raynaud	94
Suggestion for changes in the setup	98

Introduction

The subject for this thesis is measurements of the total gas content in glacier ice. I have build up an apparatus for such measurements, where I mainly follow the system described in (Lipenkov, 1995). The focus will be on the building of the setup, and the troubles of getting high accuracy measurements. I finally present 10 measurements I have done. These measurements mainly serve as a test of the apparatus and the method.

The amount of air trapped in glacier ice is determined during the densification process by the porosity in the firn at the bubble close-off level and by the ambient air pressure. Measurements of the gas content variations as a function of depth and thus age of the ice, can therefore be interpreted as a combination of variations in climatic conditions at the formation site and variations in the ice thickness over time, because formation of ice at greater height will trap less dense air leading to a smaller air content.

Temperature affects the air content. (Raynaud,1997) gives an empiric derived linear relation between the temperature at the close off level in the ice and the total air content.

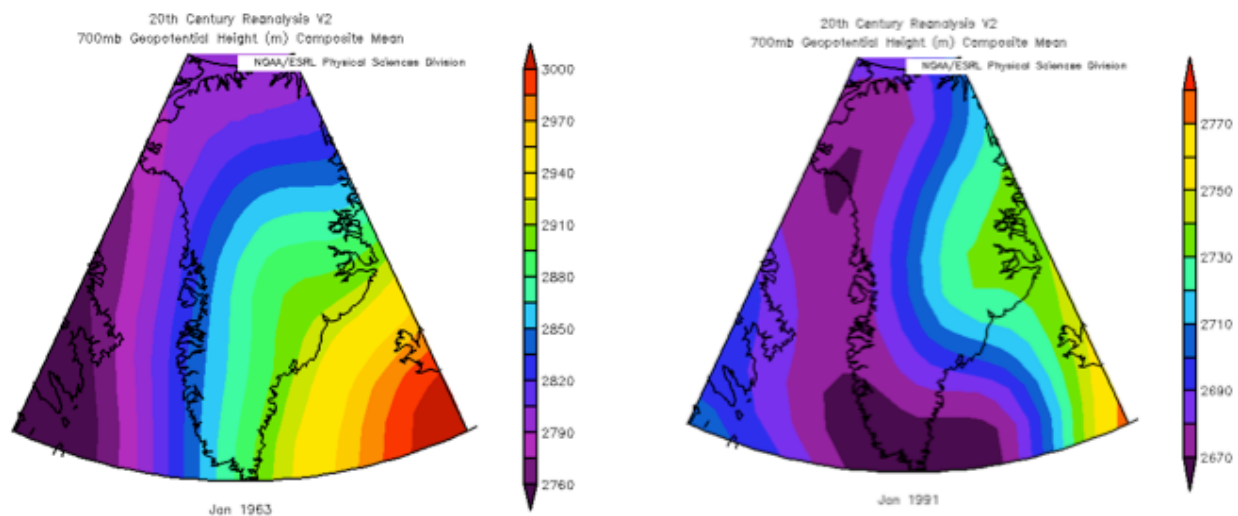
Wind packing of the snow can as well give variations in air content.

Change in precipitation pattern and relative summer/winter precipitation affects the content.

Longer time scale variations are caused by insolation variations (Raynaud, 2007).

The most interesting climatic effect on the air content for this thesis is height changes in the ice shield. Raynaud finds that at least half of the air content variation in the GRIP core only can be explained by changes of 250 in the ice shield height.

Another interesting implication is the influence of pressure field changes. As seen on Figur 1 the mean geopotential in 700 hPa, that is near the ice shield top differs with 150 gpm over the central Greenland for jan63 and jan91. These to month are chosen, as it was significant NAO- and NAO+ periods. The difference in pressure on the ice shield top is equivalent to a height change of the same magnitude, 150 m. Air content variations could then reflect main changes in such weather patterns in the past.



Figur 1. Reanalysis of the mean geopotential in 700 hPa (near the ice sheet top) for jan1963 (NAO-) to the left and jan 1991 (NAO+) to the right.

Source: www.noaa.gov.

PTV-Method

To measure the air content we must extract the air from the ice to a volume, V , where we can measure the pressure and the temperature.

The method is based on the gas equation $pV = nRT$. The equation is assumed to hold then ice is formed at the close off level in the glacier, so for a given mass of just formed ice (for example one gram):

$$\frac{p_c V_c}{T_c} = nR$$

Here V_c is the pore volume (the porosity) of the ice mass, and p_c and T_c is the actual pressure and temperature at close off level, nR can be regarded as the amount of air contained.

When the ice is brought to the laboratory, the air is extracted to a chamber with volume V_L . The pressure, p_L , and temperature, T_L , is measured and hence the amount of air is given as

$$\frac{p_L V_L}{T_L} = nR = \frac{p_c V_c}{T_c}$$

To give a precise definition of *the total gas content in ice*, I follow Raynaud et al, who normalize with a standard pressure and temperature:

$$V = V_L \frac{p_L T_0}{p_0 T_L} = V_c \frac{p_c T_0}{p_0 T_c}$$

This gives a measure of volume/mass with the trapped air at standard pressure and temperature, $p_0 = 1013$ hPa and $T_0 = 273$ K. A reasonable unit to use is STP cm^3 air per gram of ice. The formula shows the governing factors that control the air content is porosity, pressure and temperature at the close off level.

Effects of variations in ice sheet elevation

One reason for determining the gas content is to detect past variations in the ice sheet elevation. This affects p_c , and we must establish a relation between height and V (assumed that all other factors are constant). The air pressure variation with height can be calculated assuming hydrostatic balance

$$\frac{\partial p}{\partial z} = -\rho g = -\frac{p g}{R_d T}$$

Assuming that p and T have been constant, p_0 and T_0 , at height, z_0 , over the ice shield for a period, it follows that a height change (of the close off level) gives a linear response in p_c and hence in V .

(Raynaud, 1997) says that $\frac{\partial p}{\partial z}$ can vary and be difficult to estimate. But we can try a quick consideration:

If we for example assume $T = -30^\circ\text{C}$ on the ice sheet and look at the effect of a small change in height $\Delta z = 10\text{m}$ the relative change in p from the above would be 0,14%. To estimate height changes we must then be able to measure the air content with a high precision. Then comes the question of the magnitude of the absolute pressure we measure in such an experiment. This depends on the size of the volume the air is extracted into in the laboratory. For practical reasons it will be a very low pressure. In this project we have build an equipment that will give pressures in the range 10 to 20 hPa to measure, so a height change of 10 m would be reflected in 2 ice samples where the difference in pressure measurements is only 1,4 to 2,8 Pa. That says, we need a very precise pressure gauge.

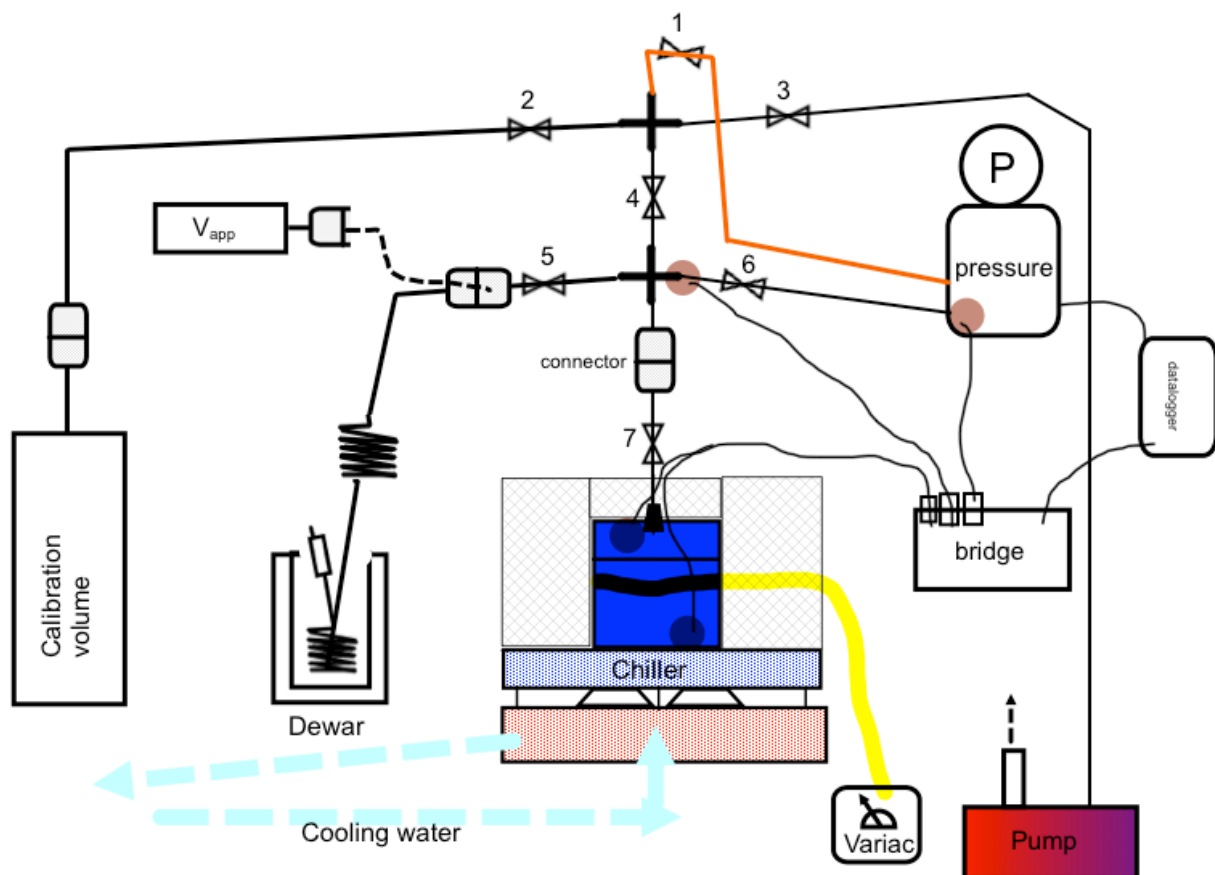
Setup overview

Following setup was build for this experiment (Figur 2). The air is extracted in the blue extraction cell. The cell can be cooled from the bottom by the peltier chiller. The top and sides are isolated with Armaflex – a material with very low heat diffusivity. A thin heating wire is wrapped around the upper part (17Ω) and a heat flux of 20W can be provided to the cell. The lid is fastened with 9 bolts and a rubber O-ring provides leak tightness. The cell can be closed with a valve (valve 7), and can be connected/disconnected to the line with a special VCR-connector. The cell also serves as a vessel for the ice samples on their final travel from the freezer to the laboratory. Two temperature sensors are stuck to the cell (top and bottom) and their wires can easily be plugged in or out the bridge with banana plugs when the cell is going to the freezer.

All tubes are $\frac{1}{4}$ " stainless steel. 7 valves (numbered on Figur 2) make it possible to separate chosen volumes from others to keep vacuum or a constant amount of air in given volumes. When the extraction cell is connected to the line, it is immediately evacuated while chilling from the bottom; when all air is removed valve 7 is closed, the ice sample is melted and refrozen, valve 4 and 5 are closed and valve 6 and 7 are opened, and the pressure is thus measured in the volume limited by valve 4 and 5, which I will call the *Main Volume*, V_M . The pressure is measured by a big pressure gauge of the model Lektra P-BADR. Two temperature sensors are stuck to the tubes and pressure gauge to determine the temperature of the part of extracted air above the cell.

3 special VCR connectors is incorporated: one for the cell, and two others that can be connected to a dry air inlet, a calibration volume and an appendix volume, V_{app} , that is sometimes necessary for increasing the main volume.

The chiller was constructed by the staff at the NBI-workshop. The chilling is provided by two 3-steps peltier elements. When current is sent through them, they transfer heat from one side to the other to a certain temperature difference. The peltier elements are fastened between two aluminium plates of which the cold one serves as the cooling base for the extraction cell. It is necessary to keep the temperature down in the warmer plate. This is done by circulating water through it with a fountain pump in a bucket. To reach temperatures below -30°C it further showed to be necessary to cool the cooling water with circa 5 kg ice in the bucket. This in turn gives the cooling water a stable temperature and hence secures a stable equilibrium temperature during the measurement, which is important.



Figur 2. Setup.

Heat fluxes in the system

Different materials for the extraction chamber were considered: glass, aluminium, steel. It was finally decided to be aluminium. The advantages of this material are for the first the high thermal conductivity and for the second it is cheaper and easier for the university smiths to work with. The drawbacks are that we cannot follow the melting/refreezing of the ice sample, and from the

sample enters the chamber and until the extracted air is measured we must rely on the temperature sensors on the outside walls. It will be impossible to see if the refrozen ice is bubble free. It can be done by looking at the sample after the measurement is conducted, but then it will be too late to re-measure as the main part of the air is gone.

We will measure the temperature on the top and on the bottom of the outside wall of the chamber to estimate the air temperature inside. We will first give an estimate of how big temperature difference we can expect by calculation the heat flux through the walls.

The chamber is cooled from the bottom; at equilibrium temperature there will be a flux of energy, Q/t , going in through the tube and the insulating material and out through the bottom.

Effects of vapour pressure

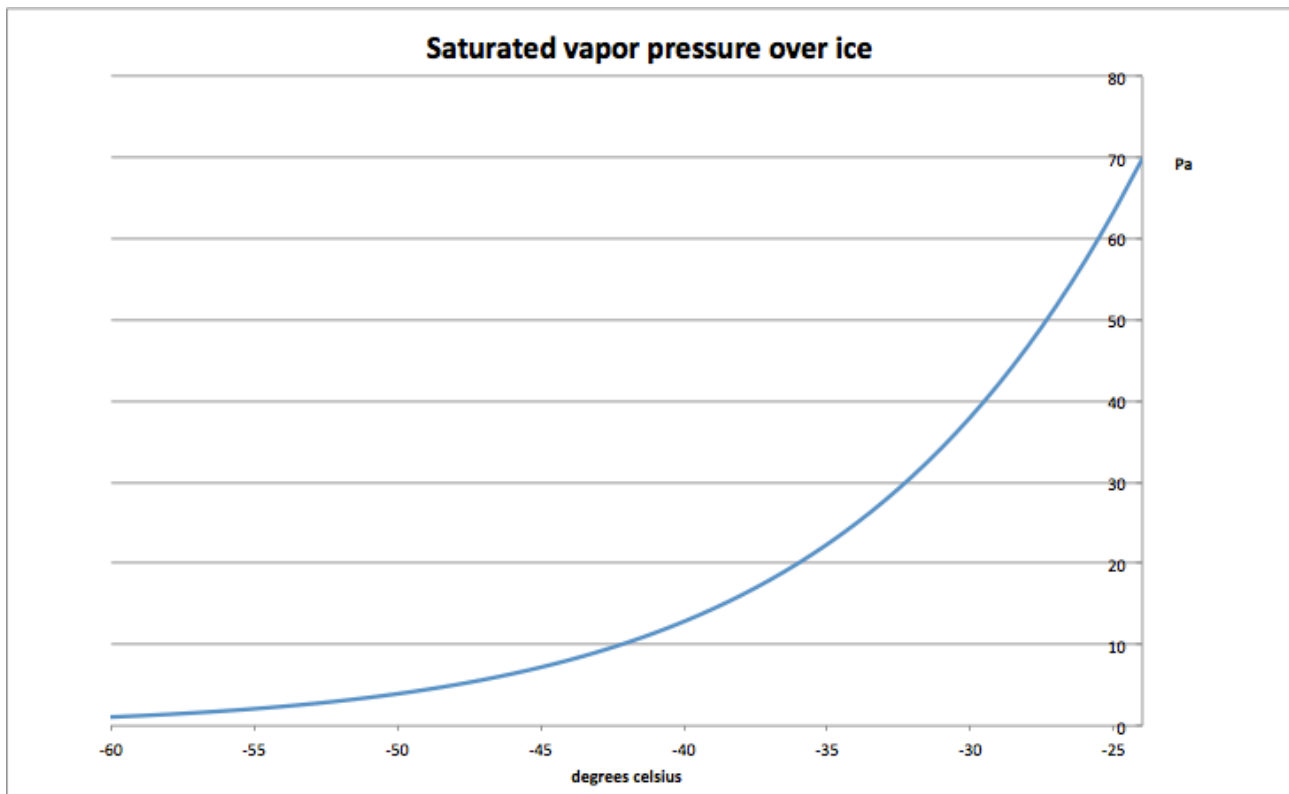
During the extraction of the air by ice melting some ice/water will evaporate and we cannot avoid the contribution of the vapour partial pressure to the measured pressure. To reduce this effect we let the melted ice refreeze and dry the released air by cooling it to -30°C . The colder it gets the more vapour will condense hence reducing the error on the pressure measurement. On the other hand the colder also the pressure - and hence the resolution on the measurement - will fall. To reach lower (and stable) temperatures also requires higher technical efforts. To decide a acceptable temperature in this trade off, we look at the saturated vapour pressure over ice. Several formulas exist; (WMO, 2008) gives this

$$e_{ice}(T) = 6,112 \exp[22,46T/(272,62K + T)] \quad (\text{eq 1})$$

eq 1

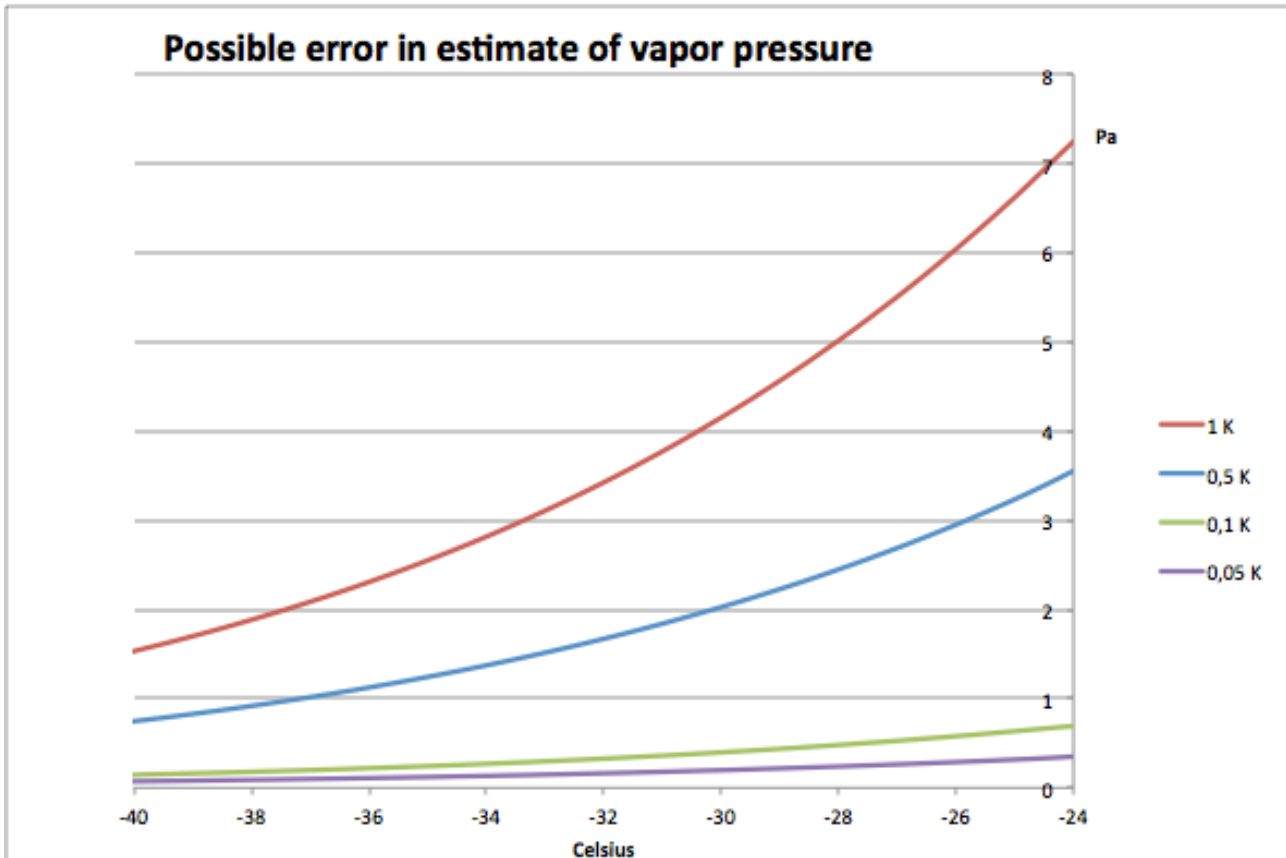
where T is in $^{\circ}\text{C}$ and e_{ice} is in hPa, for ice (-65°C to 0°C) (pure phase).

which is shown on Figur 3



Figur 3. Saturated vapor pressure over ice from WMO-formula.

It is seen that to reduce the vapour pressure to less than 7,5 Pa (as discussed in the chapter on pressure measurement) requires temperatures below -45°C . At higher temperatures we must assume that the air is saturated and correct for the vapour pressure. This again sets criteria to the temperature accuracy; at high temperatures even a small error in the temperature measurement can lead to a significant error in the determination of the vapour pressure. This is shown on Figur 4 for 4 different temperature accuracies. It is seen that, if we can determine the temperature within 0,1 K the error is negligible, but for an accuracy of 1 K the possible error in the vapour calculation becomes intolerable big for temperatures higher than -25°C . From this we decide to aim at a temperature near -30°C and calculate with a vapour contribution at 38 Pa to the measurement.



Figur 4. The possible error in the calculation of the vapor pressure for different accuracies in the temperature determination.

Refreezing and solubility of gasses

In this method of extracting air from ice, it must be considered, that during the process some air is dissolved in the water from the molten ice, and hence will the pressure measurement underestimate the original amount of trapped air. To avoid the problem the intention has been to degas the molten sample by refreezing it slowly from the bottom, so that ice crystals are forming on the cell bottom and slowly growing upwards until the whole sample is frozen. Thereby it should push out the dissolved air. This technique is used for creating bubble free ice at CIC, where a column of water is frozen from the bottom and heated from the top creating ice at a rate of 10 cm/day.

In this setup the extraction chamber is cooled from the bottom by a peltier chiller. On the top part heating wires are wrapped around it. By cooling from the bottom and heating from the top, the hope is, that the ice crystals will grow slowly from the bottom. Several experiments with freezing tap water this way

has been conducted, but they all end the same way: the water is super cooled and suddenly the whole lot freezes in few seconds. The experiments were inspected with a light torch through a Plexiglas lid and certainly no ice crystals had formed on the bottom before the sudden freeze. Different regulations of heating and cooling speeds were tried but with no success. I assume the problem is for the first the shallowness of the sample (bottom area is 3,2cm x 3,2 cm and height is 0-3 cm); water density is highest at 4°C so as the bottom water cools to temperatures near its freezing point it will shift place with the top layer until the whole column is super cooled. Either the temperature difference on top and bottom must be larger than 4°C, or the bottom cooling must be so fast that ice crystals form and stick to the bottom before they are convected to the top. I doubt that it will be possible without changing the design.

It must therefore be considered to correct for dissolved air or at least estimate the error that it can induce.

The nature of solubility of a gas, x, in water under equilibrium is stated in Henry's law,

$$p_x = k_H(T) \cdot c_x$$

where p_x is the partial pressure of the air component x (O_2 or N_2), c_x is the concentration of that component dissolved in the water (fx in mole/L), and k_H is its Henry coefficient which is dependent on the water temperature. The solubility decreases with temperature and is almost twice as high at 0°C as at 25°C – the range at which the ice sample in this experiment can be exposed to. I assume though that even if air is degassed from the heated sample to Henry equilibrium, some will dissolve again during the cooling and refreezing process, such that the amount of dissolved air is given with the equilibrium of 0°C water. When further the water freezes no more air will dissolve and the already-dissolved air will be kept in the ice.

Assume that the air consists of 79% N_2 and 21% O_2 . The number of mole of air in V_{ex} is $n = n_N + n_O$ where $n_N = 0,79n$ and $n_O = 0,21n = 0,266n_N$.

The temperature dependence of k_H is calculated by the *van t' Hoff equation*

$$k_H(T) = k_H(T_\theta) \exp \left[-C \left(\frac{1}{T} - \frac{1}{T_\theta} \right) \right]$$

where $C = \begin{cases} 1700K & \text{for } O_2 \\ 1300K & \text{for } N_2 \end{cases}$.

For $T_\theta=298\text{K}$, I use values $k_H(T_\theta) = \begin{cases} 76923 \frac{\text{m}^3 \cdot \text{Pa}}{\text{mole}} \text{ for } O_2 \\ 163934 \frac{\text{m}^3 \cdot \text{Pa}}{\text{mole}} \text{ for } N_2 \end{cases}$

(taken from: http://en.wikipedia.org/wiki/Henry's_law)

For 0°C this gives

$$k_H(0^\circ\text{C}) = \begin{cases} 456 \cdot 10^2 \frac{\text{m}^3 \cdot \text{Pa}}{\text{mole}} \text{ for } O_2 \\ 1099 \cdot 10^2 \frac{\text{m}^3 \cdot \text{Pa}}{\text{mole}} \text{ for } N_2 \end{cases}$$

In this experiment we have the special condition of a closed system: water and air are contained in the volume

$$V_{\text{ex}} = V_w + V_a,$$

where V_{ex} is calibrated from the beginning, $V_w = \frac{m_{\text{ice}}}{\rho_w(T)}$ and $V_a = V_{\text{ex}} - V_w$. The mass

of the sample, m_{ice} , is measured first and hence follows V_w , which is slightly

dependent on T_w ; in the following I use $\rho_w = \begin{cases} 0,9998 \frac{\text{g}}{\text{cm}^3} \text{ for } T=0^\circ\text{C} \\ 0,9991 \frac{\text{g}}{\text{cm}^3} \text{ for } T=15^\circ\text{C} \end{cases}$. So the

volumes depend on the mass of the sample and on the water temperature. We must consider what happens with the air when the ice melts.

When the sample is enclosed in V_{ex} the amount of mole of air is

$$n = n_N + n_O = \overline{n}_N + \underline{n}_N + \overline{n}_O + \underline{n}_O$$

where $\overline{n} = \overline{n}_N + \overline{n}_O$ is the free air and $\underline{n} = \underline{n}_N + \underline{n}_O$ is the dissolved air.

$$V_a = V_{ex} - V_w$$

$$\bar{n} = \bar{n}_N + \bar{n}_O$$

$$V_w = \frac{m_{ice}}{\rho_w(T)}$$

$$\underline{n} = \underline{n}_N + \underline{n}_O$$

Figur 5. In the closed extraction chamber, V_{ex} , the air molecules are either dissolved or participating to the pressure.

For each of the gasses we then have the partial pressure

$$p_x = \frac{\bar{n}_x RT}{V_a} \tag{eq 2}$$

eq 2

and the concentration in the water

$$c_x = \frac{n_x}{V_w} \tag{eq 3}$$

eq 3

Combining these relations with the constraint condition, $n_x = \overline{n_x} + \underline{n_x}$, we get the linear relation between p_x and c_x :

$$p_x = (n_x - c_x V_w) \frac{RT}{V_a} \quad (\text{eq 4})$$

eq 4

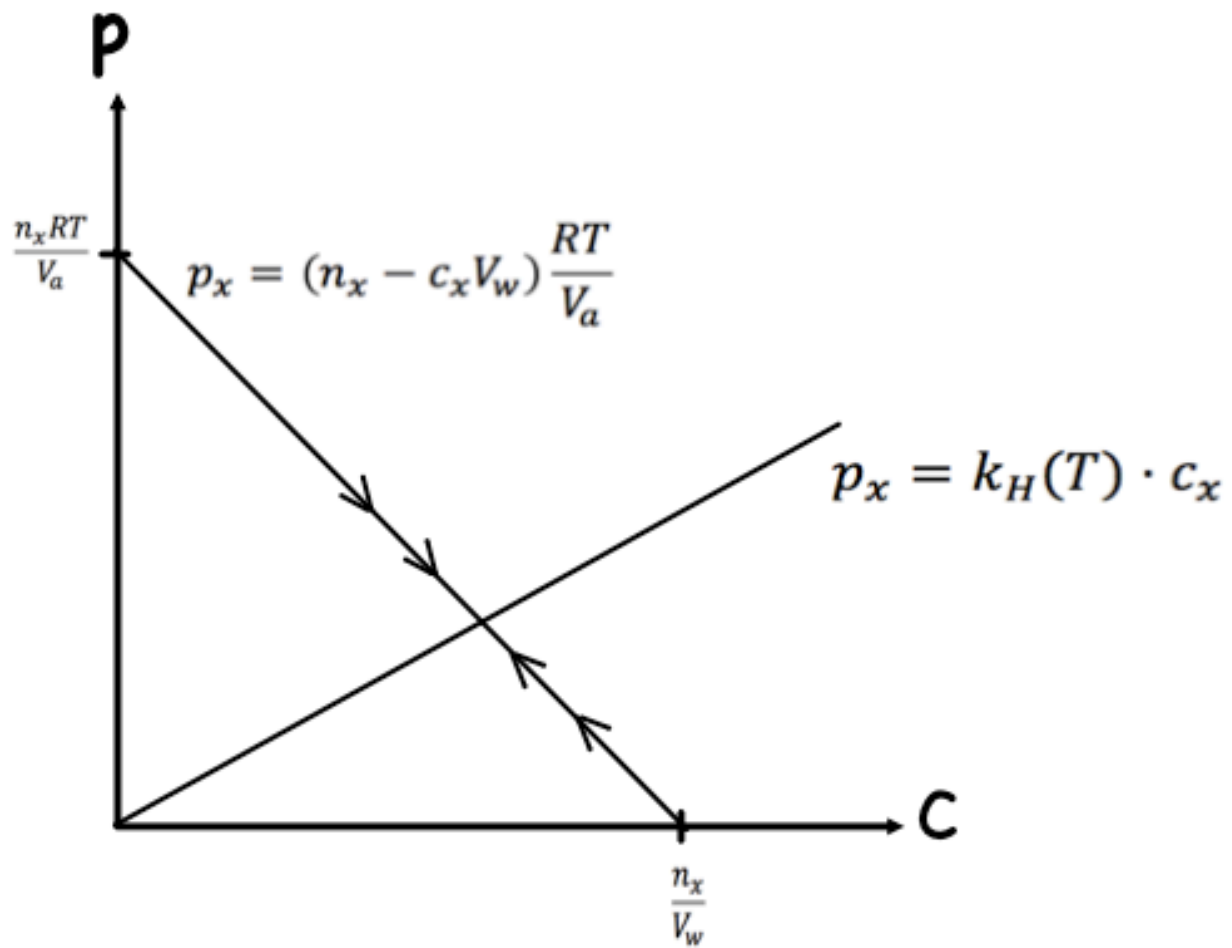
If all air bubbles were relieved to the air during the melting, we would have:

$$c_x = 0 \text{ and } p_x = \frac{n_x RT}{V_a}$$

If on the contrary all air was dissolved we would have:

$$p_x = 0 \text{ and } c_x = \frac{n_x}{V_w}$$

In either case there would be Henry equilibrium and dissolving or degassing would begin to take place, changing both concentration and partial pressure until equilibrium is reached for a given constant temperature. This is illustrated on Figur 6.



Figur 6. Henrys Law and the constraint of a closed chamber determine the partial pressure and concentration of each gas.

The slope of Henrys Law increases with increasing temperature, and both slope and offset of the constraint condition depends on temperature and the mass of the sample.

Substituting (eq 3) and (eq 2) into Henrys Law we can express the ratio between dissolved and free air:

$$\frac{n_x / n_x}{n_x} = \frac{RT}{k_{H,x}} \frac{V_w}{V_a} = \frac{RT}{k_{H,x}(T) \left(\frac{V_{ex}}{V_w} - 1 \right)} \quad \text{eq 5}$$

eq 5

It is preferable with a low ratio to give the smallest error. To obtain this we could heat the water up and hope that the air would not dissolve again during the re-cooling. It is also seen how the smaller the sample is, the lesser air will be dissolve (since the free space is then bigger and the partial pressure smaller). With small samples follows though other sources of error: higher cut bubble effect and lower measured pressure.

When we try to calculate directly from the pressure measurement the total gas content, it is essentially \bar{n} we determine, but we does not a priori know the composition of the air in V_a . Therefore we must now calculate the amount of O_2 and N_2 in dissolution and free air respectively. O_2 dissolves more easily than N_2 , therefore the partition in the chamber will be different than that in atmospheric air (with a higher part of N_2). We use (eq 4) and Henrys Law to derive an expression of the concentration given the input parameters (water temperature, mass of sample and its air content), and getting rid of the partial pressure:

$$c_x = \frac{n_x RT}{k_{H,x}(T) \cdot V_a + RTV_w} \quad (\text{eq 6})$$

eq 6

We can now derive ratio between oxygen and nitrogen in V_a in three steps using first (eq 2) then Henrys Law and finally (eq 6) (and we let F denote the O_2/N_2 -ratio):

$$F \equiv \frac{\bar{n}_O}{\bar{n}_N} = \frac{p_O}{p_N} = \frac{k_{H,O}c_O}{k_{H,N}c_N} = \frac{n_O}{n_N} \frac{V_a + \frac{RT}{k_{H,N}}V_w}{V_a + \frac{RT}{k_{H,O}}V_w} \quad (\text{eq 7})$$

eq 7

$$= \frac{n_O \left(\frac{\rho_w(T)}{m_{ice}} V_{ex} - 1 \right) + \frac{RT}{k_{H,N}(T)}}{n_N \left(\frac{\rho_w(T)}{m_{ice}} V_{ex} - 1 \right) + \frac{RT}{k_{H,O}(T)}}$$

The last step is formulated to show the influence of the input parameters directly. It is seen as expected, that

$$\bar{n}_O/\bar{n}_N \rightarrow \begin{cases} \frac{n_O}{n_N} & \text{for } V_w \rightarrow 0 \text{ (small samples)} \\ \frac{k_{H,O}}{k_{H,N}} & \text{for } V_w \rightarrow V_{ex} \text{ (big samples)} \end{cases}$$

$\frac{n_O}{n_N}$ is assumed to be 21%/79%. From the determination of \bar{n} and (eq 7), we get:

$$\begin{aligned} \bar{n}_N &= \frac{\bar{n}}{1+F} \\ \bar{n}_O &= \frac{\bar{n}}{1+F^{-1}} \end{aligned} \quad (\text{eq 8})$$

eq 8

From (eq 8) and (eq 5) we calculate \underline{n}_N and \underline{n}_O , and then have the complete estimate for n.

Summarizing, the scheme for determining the air content could be:

- 1) The measurements are: m_{ice} , temperatures, pressure in V_M .
- 2) From the pressure we calculate \bar{n}
- 3) Calculate \bar{n}_N and \bar{n}_O by (eq 7) and (eq 8)
- 4) Calculate \underline{n}_N and \underline{n}_O by (eq 5)

We prefer though to derive a formula for dissolved air as a whole, so we will not have to consider the individual constituents. We calculate the ratio of dissolved air to free air by combing (eq 5), (eq 7) and (eq 8), and this leads to the general theorem:

In a closed chamber of volume V_{ex} containing water of temperature T and mass m_{ice} and air composite of two components (N_2 and O_2) with relative occurrence $\frac{n_O}{n_N}$ the fraction of dissolved to free air is given by

$$\frac{n}{\bar{n}} = RT \left(\frac{\rho_w(T)}{m_{ice}} V_{ex} - 1 \right)^{-1} \frac{\left((1+F)k_{H,N}(T) \right)^{-1} + \left((1+F^{-1})k_{H,O}(T) \right)^{-1}}{(1+F)^{-1} + (1+F^{-1})^{-1}} \quad \text{eq 9}$$

eq 9

$$\text{where } F = \frac{n_O \left(\frac{\rho_w(T)}{m_{ice}} V_{ex} - 1 \right) + \frac{RT}{k_{H,N}(T)}}{n_N \left(\frac{\rho_w(T)}{m_{ice}} V_{ex} - 1 \right) + \frac{RT}{k_{H,O}(T)}}$$

It is seen that it only depends on temperature and sample mass (density, k_H and F depends on temperature and F depends on mass as well), but not on the air content of the ice. The ratio is plotted as function of sample size on Fig 7 in the range of ice mass used in the experiments. It is shown for 0°C and 15°C. If the sample is heated before refreezing clearly it will drive out significant more air. It is though not clear how much air will re-dissolve while re-cooling it; will equilibrium with 0°C be reached before freezing or will concentration be in the field between maximum reached temperature and 0°C? It will have to be tested experimentally. Attempts have been done by extracting air 2 or 3 times from the same ice sample, removing the extracted air before the second and third extraction. For example: for a sample of 10g, it would be conjectured that the second extraction would give circa 1% of the air extracted first time, and that the third extraction would give only 10^{-4} of the first, which will be below the measurable limit. Experiments to test this are discussed later (Fig 62).

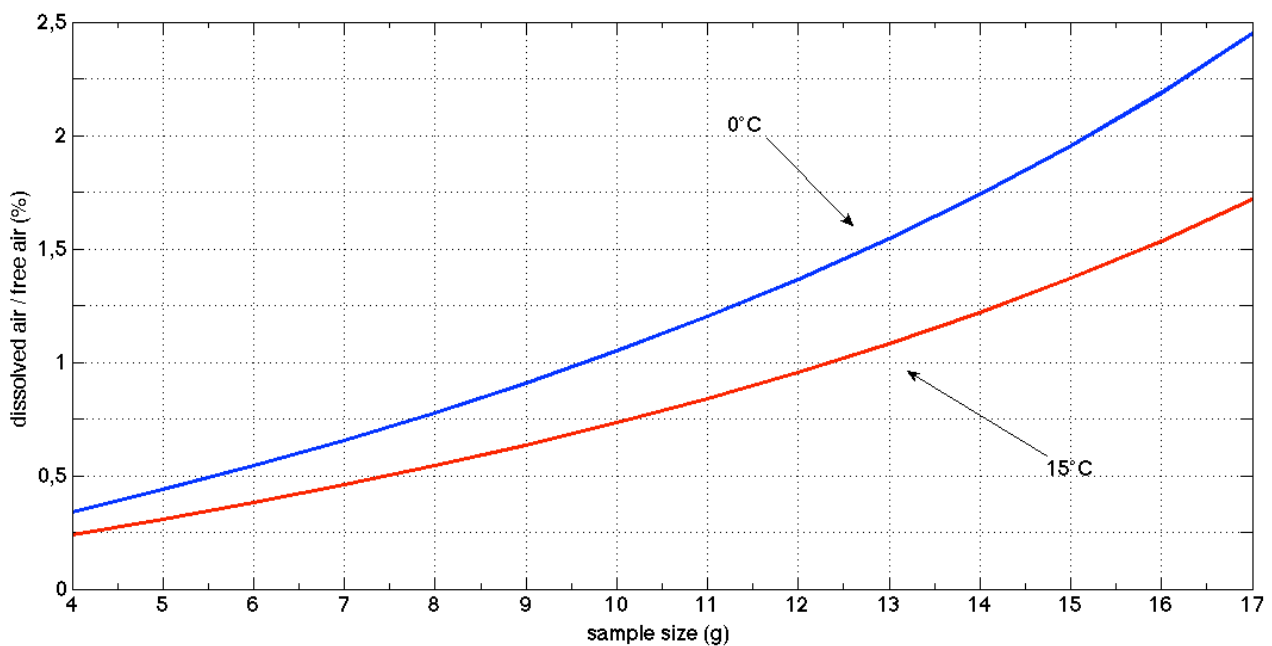
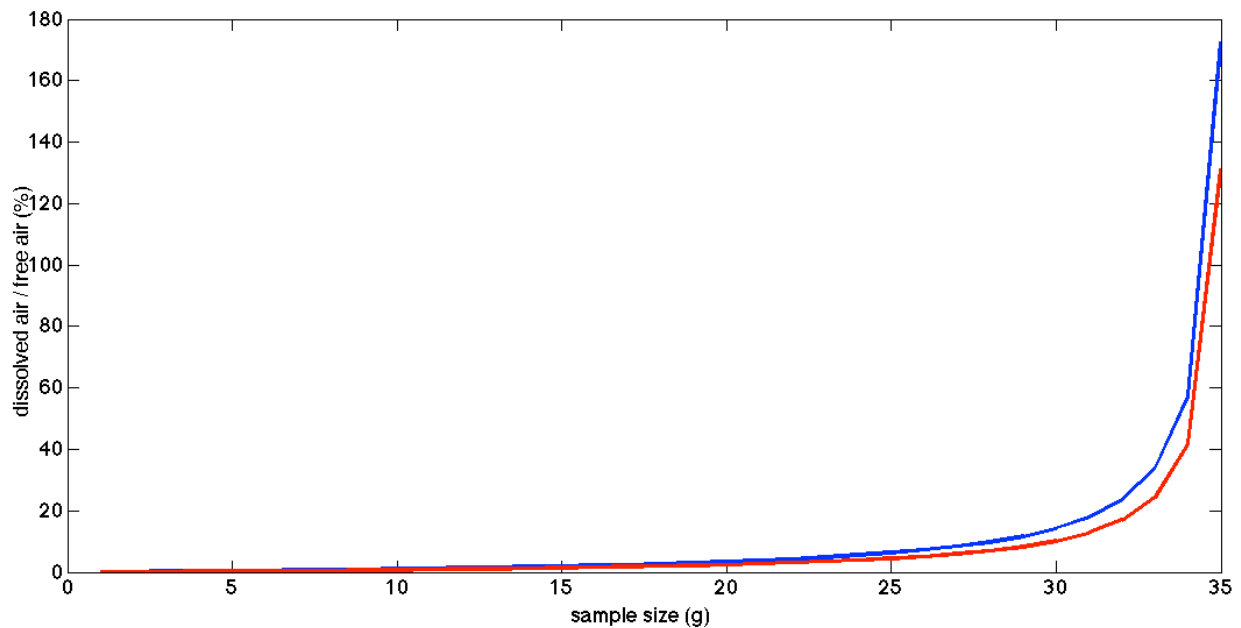


Figure 7. Given an ice sample in the closed V_{ex} ($35,47 \text{ cm}^3$). Fraction of dissolve air/free air in equilibrium from (eq 9) with 0°C and 15°C for the span of sample sizes used.



Figur 8. Same as (Figur 7) but here the full range is shown – the practical size limit is 25 g ice in this setup.

Measure instruments

On temperature sensors.

The temperatures are measured with pt1000-sensors, that is small pieces of platinum connected to 2 wires. The resistance in the material is close to but not exactly linear dependent on the temperature in an interval covering the temperatures relevant in this experiment (-30°C to +30°C). The measurement is hence conducted by building the pt1000 into a balancing bridge (Wheatstone Bridge), pushing a stable voltage on the whole circuit, and measuring the voltage an appropriate place in the bridge (see diagram). The measurement of the output voltage must have a resolution, which makes it possible to calculate the temperature in the pt1000 with a resolution of 0,1°C.

A standard formula, which relates temperature and resistance in the platinum-sensors, the so-called Callendar – Van Dusen formula, established in 1925, is given by

$$R = R_0[1 + AT + BT^2 + CT^3(T - 100)]$$

where R is the resistance in the sensor, R_0 is the resistance at 0 °C, T is the temperature in Celsius and A, B, C are constants given by

$$A = 3,9083 \cdot 10^{-3} K^{-1}$$

$$B = -5,775 \cdot 10^{-7} K^{-2}$$

$$C = \begin{cases} -4,183 \cdot 10^{-12} K^{-4} & \text{when } T < 0 \\ 0 & \text{when } T \geq 0 \end{cases}$$

(Wikipedia has a very informative article about pt1000 sensors)

Building circuits for the measurements and resolution considerations.

We want to measure temperatures 4 places during the ice-measurements: 2 places on the extraction cell (top and bottom), 1 (or 2) on the tubes connecting the extraction cell and the pressure gauge, finally 1 to log the air temperature in the laboratory. To that end a circuit is constructed with 4 Wheatstone Bridges.

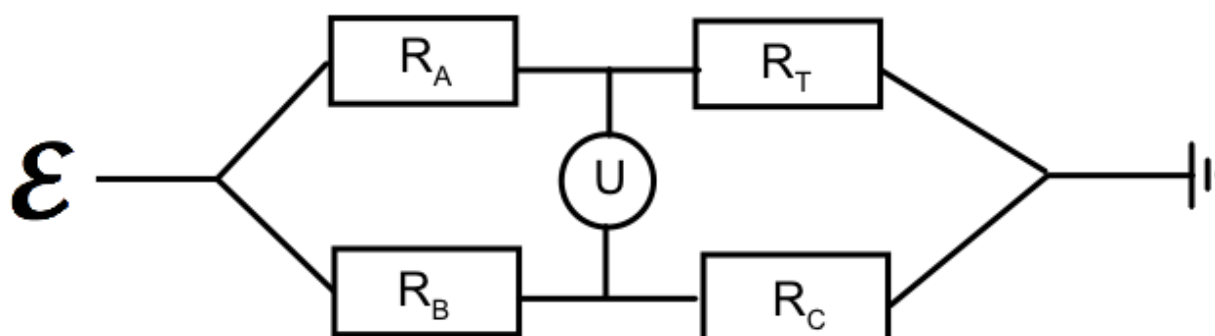


Diagram 1. Wheatstone Bridge used to measure pt1000-resistances.

In each bridge we have

$$U = \mathcal{E} \left(\frac{R_B}{R_B + R_C} - \frac{R_A}{R_A + R_T} \right)$$

and hence

$$R_T = \frac{\mathcal{E}}{\left(\frac{\mathcal{E} R_B}{R_B + R_C} - U \right) \frac{1}{R_A}} - R_A$$

where U is the bridge voltage that is going to be measured, \mathcal{E} is the electromotive force pushed on the circuit, R_T is the temperature dependent resistance in the pt-sensor, and R_A , R_B , R_C are fix valued resistors. How do we

choose values for \mathcal{E} , R_A , R_B , R_C ? As we want the highest possible resolution for the temperature measurement - it could be called the sensibility of the instrument - the circuit should be constructed so that:

a change in R_T gives the highest possible change in U

that is,

we must find maximum for

$$\frac{\partial U}{\partial R_T} = \mathcal{E} \frac{R_A}{(R_A + R_T)^2}$$

with respect to \mathcal{E} and R_A .

Notice that the sensibility is independent of the values of R_B and R_C , but the choice of \mathcal{E} and R_A is not straight forward.

Clearly, \mathcal{E} is directly proportional to U , and in principle we could get any resolution we want by beefing up \mathcal{E} to a mighty voltage. This way is in praxis limited (not only by security but also) because a problem with internal heating in the sensor rises due to the dissipated power. Since $P = \frac{U_R^2}{R}$ where U_R is the voltage across a resistor dissipated power will certainly from some level of U_R begin to heat up the sensor and hence give unwanted and annoying errors to the measurements. So efforts to increase the precision have undesired secondary effects. A doubling of the emf which a priori would double the resolution on the temperature measurement would also quadruple the internal heating in the sensor possibly causing an error of higher magnitude than the increase in resolution and hence ruin the benefit. Therefore it is important to study the internal heating effect and find a threshold value for the emf for which internal heating no longer can be neglected.

Now consider the choice of R_A . The expression $\frac{R_A}{(R_A + R_T)^2}$ has its maximum for $R_A = R_T$; therefore the most canonic choice for R_A will be the expected resistance in the sensor for a central temperature in the interesting range. For example we would choose $R_A \approx 882\Omega$ if the pt1000 is going to be used at temperatures near -30°C since the Callendar formula gives this value for -30°C . This would give the highest resolution in an interval around that temperature.

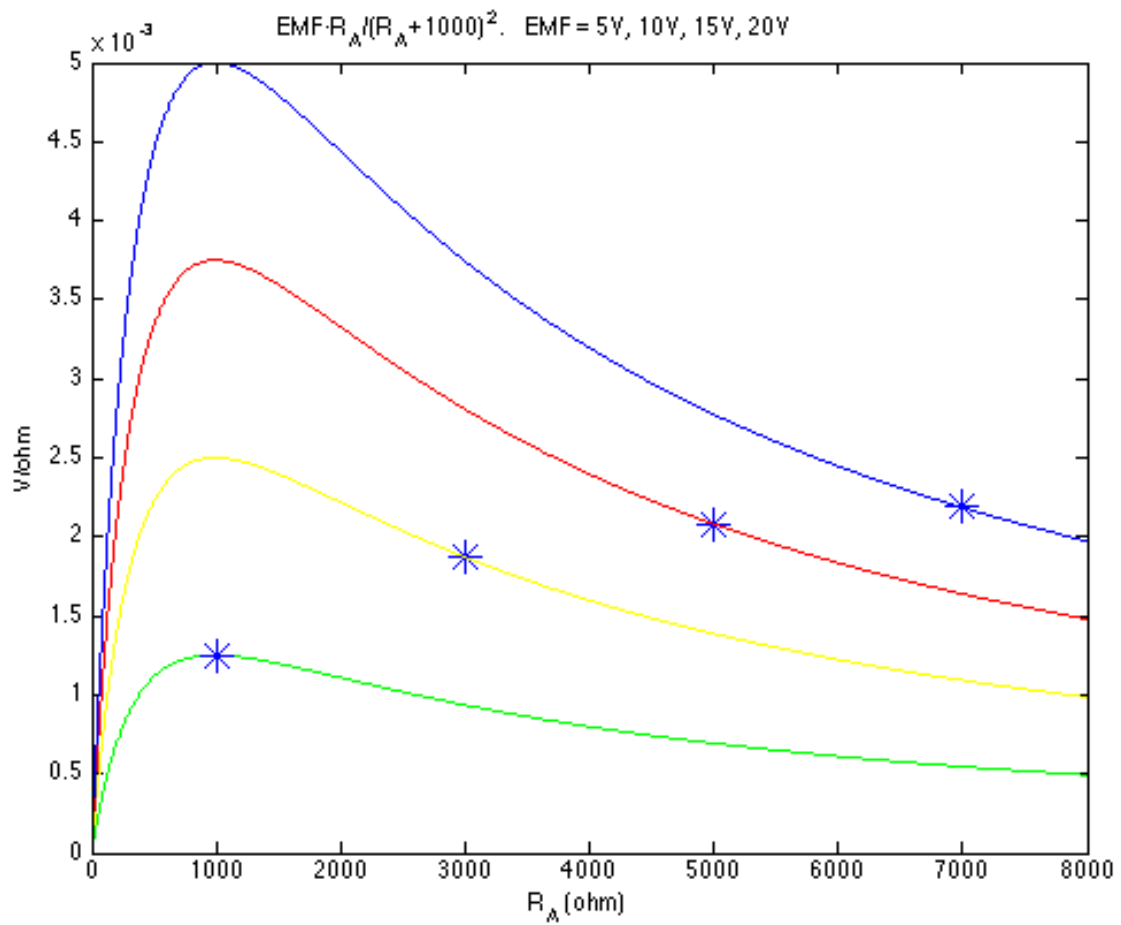
On the other hand there is a benefit in choosing $R_A > R_T$ since the power dissipation in the sensor then will be lesser for a given emf. That is true because the voltage across the sensor is $\mathcal{E} \frac{R_T}{R_A + R_T}$. It must therefore be considered if one should operate with a threshold value for the amount of sensor heating we will tolerate. There from we can decide the optimal values for \mathcal{E} and R_A as shown on

Figur 9. Here is shown plots of $\frac{\partial U}{\partial R_T}$ as function of R_A for different values of \mathcal{E} and also calculated points of constant power dissipation. It is seen that actually with some advantage \mathcal{E} can be increased without increasing the internal heating in the sensors.

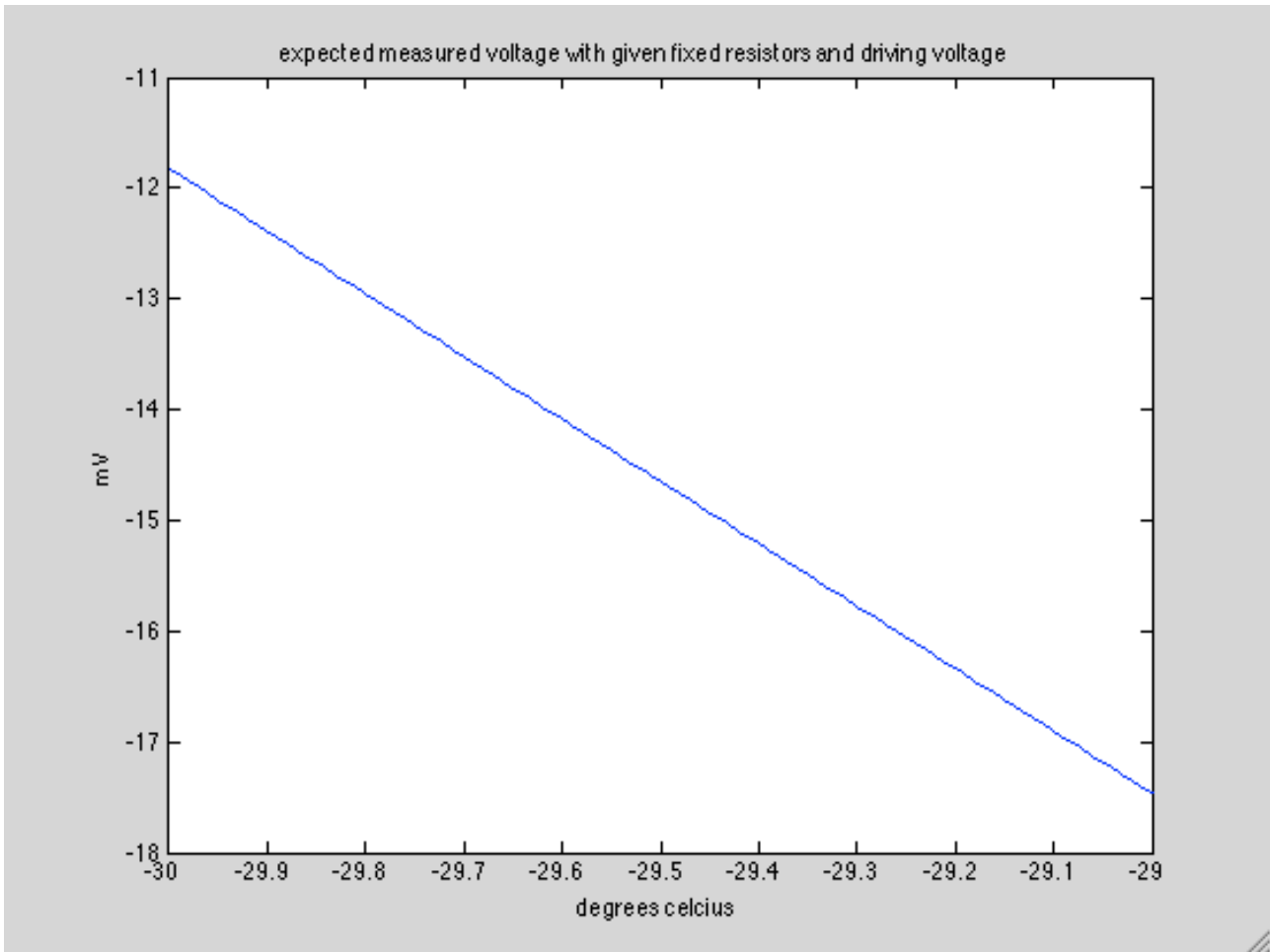
Though it must also be concerned that the stability of a high voltage power supply is probably lower than a low voltage pendant, which could introduce new accuracy problems when using to high voltage.

Another concern is the resolution of the voltmeter used for the measurements. The data loggers we have for use has resolution 1,53 mV.

And what will then the resolution on the temperature measurement be? On Figur 10 is shown an example with emf $\approx 5V$. It is seen that we need a resolution of 0,5 mV in the measurements to give a temperature resolution of 0,1°C. To increase the resolution we must increase \mathcal{E} .



Figur 9. Plot of functions $\mathcal{E} \frac{R_A}{(R_A + R_T)^2}$ dependence on R_A with $R_T = 1000\Omega$ and 4 different values of \mathcal{E} (5V, 10V, 15V and 20V). The 4 stars mark points with the same power-dissipation in the sensor (6,25 mW).



Figur 10. Here is shown the calculation of the expected voltage to measure in the temperature range when the resistance in the pt1000-sensor is calculated by the standard formula, the fixed resistances in the balancing bridge is and the governing voltage is $R_1=872,4 \Omega$, $R_2 = 1000,14 \Omega$ $R_3 = 998,2 \Omega$ and $\mathcal{E} = 5,0564 \text{ V}$.

Data logging

Measurements is logged with 2 data loggers of the model: NI usb-6009. Each logger has 4 analogue input channels for differential voltage. During a measurement 6 voltages are logged: 1 for the pressure gauge, 4 for temperature and 1 for the electromotive force on the circuit made for temperature sensors. The accuracy in the loggers are dependent on the voltage range they are set up to measure. The best accuracy (1,53 mV) is obtained by restraining the input voltage range to $\pm 1 \text{ V}$.

As the Wheatstone bridges is constructed the voltage measurement for the pt1000 sensors will be within this range; it will be close to 0 when temperatures are near -30°C in the extraction chamber and near 25°C in the laboratory, and even if we choose a very high electromotive force, the measured voltage will be within $\pm 1 \text{ V}$.

To log the electromotive force itself with highest accuracy, a voltage divide is made by 2 fixed resistor of sufficient resistances, so the voltage above one is lesser than 1 V. This divide is put parallel to the bridges in the circuit. The emf is the obtained by multiplying the measured voltage by the ratio of the 2 resistances.

Similar a resistor divide is made for pressure logging with highest accuracy and resolution (see below).

The 6 electric signals are logged with the software LabView. I use other software such as Matlab, Excel and LoggerPro to handle the data. For each measurement a textfile is saved containing the signals. To handle the data I remove the header, replace all ',' with '.' and copy the files to a certain input directory on the computer. I use the matlab routine '**totair.m**' to calculate on the measured voltages and obtain temperatures and pressure.

Beside the input file,
totair.m uses:

the textfile '**Fixresistors.txt**' containing the values of the 20 fixed resistors, and the functions:

wstone.m (calculating the resistances from the measured voltage)
pt1R2T.m (calculating the temperature from the resistance in the pt1000s)
pt2R2T.m
pt3R2T.m
pt4R2T.m
U2p.m (calculating the pressure from the measured voltage over the load resistor)

and if wanted a file containing displayreadings from the presssuregauge.

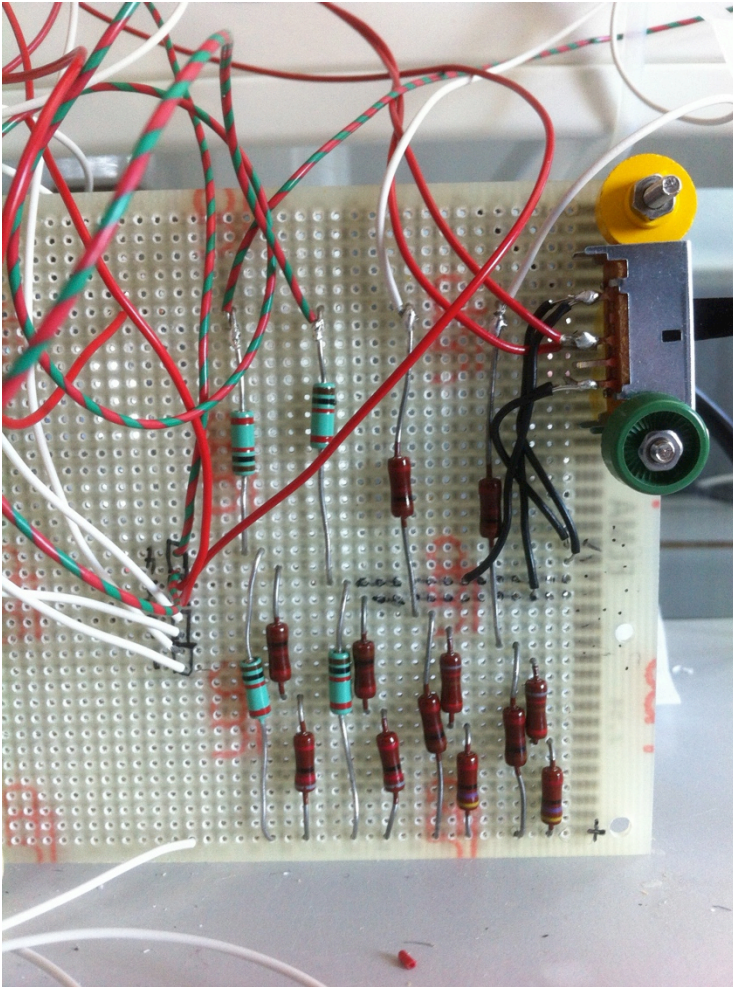
Fixresistor	Resistance (Ω)	sensor	function
1	91,63	pt100	Wheatstone fix 1 (highest sensitivity near -30°C)
2	110,57	pt100	Wheatstone fix 1 (highest sensitivity near 25°C)
3	100,17	pt100	Wheatstone fix 2
4	100,47	pt100	Wheatstone fix 3
5	872,4	pt1	Wheatstone fix 1

6	871,2	pt2	Wheatstone fix 1
7	1085,0	pt3	Wheatstone fix 1
8	1082,4	pt4	Wheatstone fix 1
9	1000,14	pt1	Wheatstone fix 2
10	998,2	pt1	Wheatstone fix 3
11	998,2	pt2	Wheatstone fix 2
12	1009,3	pt2	Wheatstone fix 3
13	1001,0	pt3	Wheatstone fix 2
14	999,4	pt3	Wheatstone fix 3
15	1002,7	pt4	Wheatstone fix 2
16	1003,1	pt4	Wheatstone fix 3
17	100,7	power supply	Measure voltage across this R to calculate emf.
18	1000,3	power supply	Resistor divide - $R=R17+R18$.
19	39,59	pressure gauge	Divide of load resistance. Voltage across this R is measured.
20	209,89	pressure gauge	Divide of load resistance (load= $R19+R20$)(no measurements on R20)

Table 1. Overview of fixed resistances used in the electric circuits.

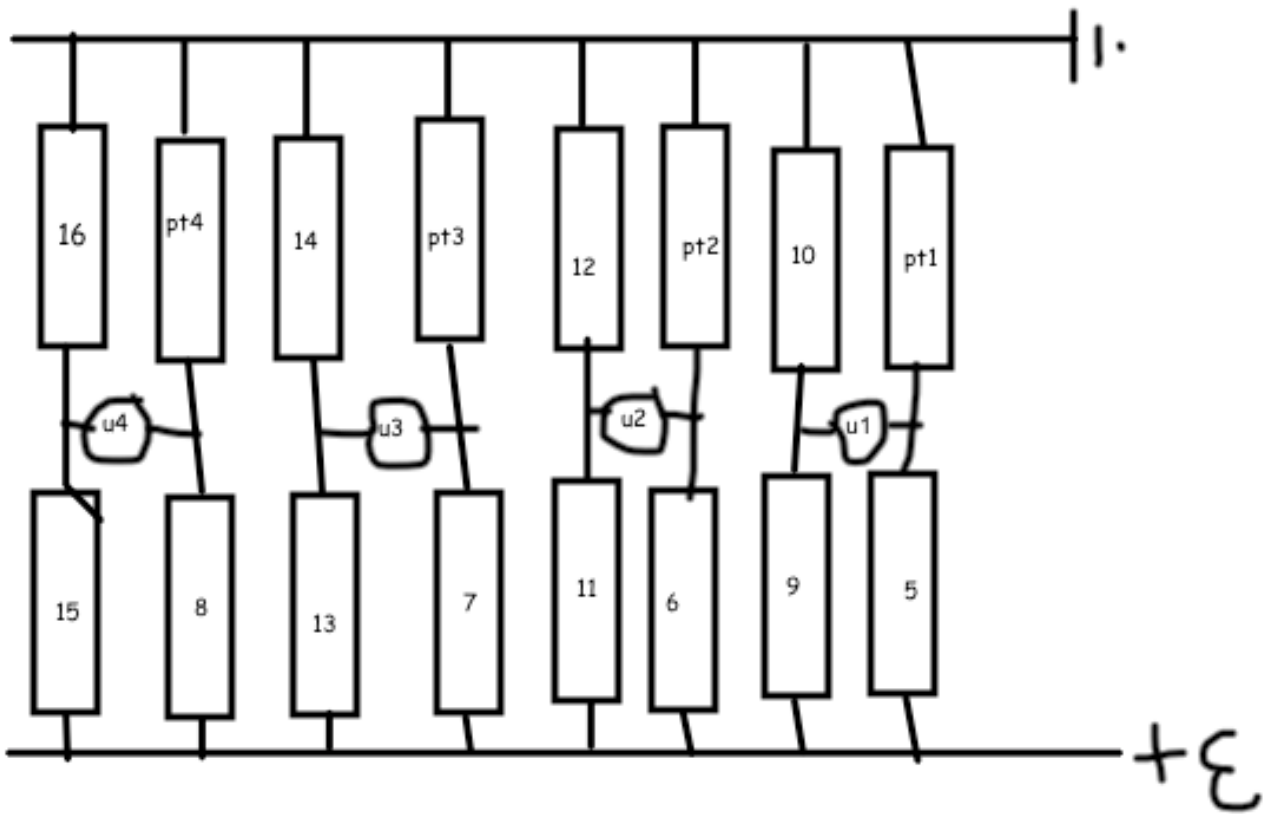
First temperature instrumentation

The fixed resistors in the bridges are chosen to give 2 sensors highest resolution at temperatures near -30°C and 2 other sensors highest resolution at temperatures near 25°C . We get the highest resolution (neglecting the internal heating question for now) when the measured voltage is close to 0 V which is the case when $R_A = R_T$ and $R_B = R_C$. From the Callendar-formula we get pt1000-resistances $882\ \Omega$ and $1097\ \Omega$ for these temperatures and search for fixed resistances near these values to use in the bridges.



Figur 11. 4 Wheatstone Bridges and a system of wires to connect to the pt1000 sensors and to a datalogger. The switch in upper right corner has an output that allows a choice of either the bridge-voltage from circuit 3 or 4. The output from these circuits can as well be taken directly from other wires.

In all 4 times 3 fixed resistors are needed for the bridges which are build into parallel circuits with common \mathcal{E} and ground. They are soldered on a print card together with wires for connections to the pt1000 sensors and inputs to a data logger. These wires are connected to plug-connectors, so that the pt1000-sensors easily can be plug or unplugged.



Figur 12. **DIAGRAM**

All resistors are measured with a multimeter to check their values precisely. Since they could change characteristics with time it can be necessary to re-measure them from time to other. A complication here is that they are a part of a bigger circuit now, and a multimeter-measurement above a single resistor does not simply give its resistance, but is dependent on several of the resistors in the circuit. Let \widetilde{R}_9 be the measured resistance across R_9 (see Figur 12). From Kirchovs Laws it is derived that:

$$\widetilde{R}_9 = \frac{1}{\frac{1}{R_9} + \frac{1}{R_9^*}}$$

where

$$R_9^* = R_{10} + \frac{1}{\frac{1}{R_{11}} + \frac{1}{R_{12}}} + \frac{1}{\frac{1}{R_{13}} + \frac{1}{R_{14}}} + \frac{1}{\frac{1}{R_{15}} + \frac{1}{R_{16}}}$$

and

R_9, \dots, R_{16} are the fixed resistors shown in the diagram.

Similar relations holds for resistors R_{10}, \dots, R_{16} . The 8 values of R_9, \dots, R_{16} must then be found by solving this system of 8 nonlinear equations – a formidable task if it not was for program Matlab, which nowadays has a built in iterative procedure for solving such equations; one must hope that the solution is unique, but it seems reasonable and gives values close to the values marked on the resistors.

The resistors R_5, \dots, R_8 can be measured directly when the pt1000-sensors are unplugged, since they in that case no longer are in a closed circuit.

On calibration of sensors.

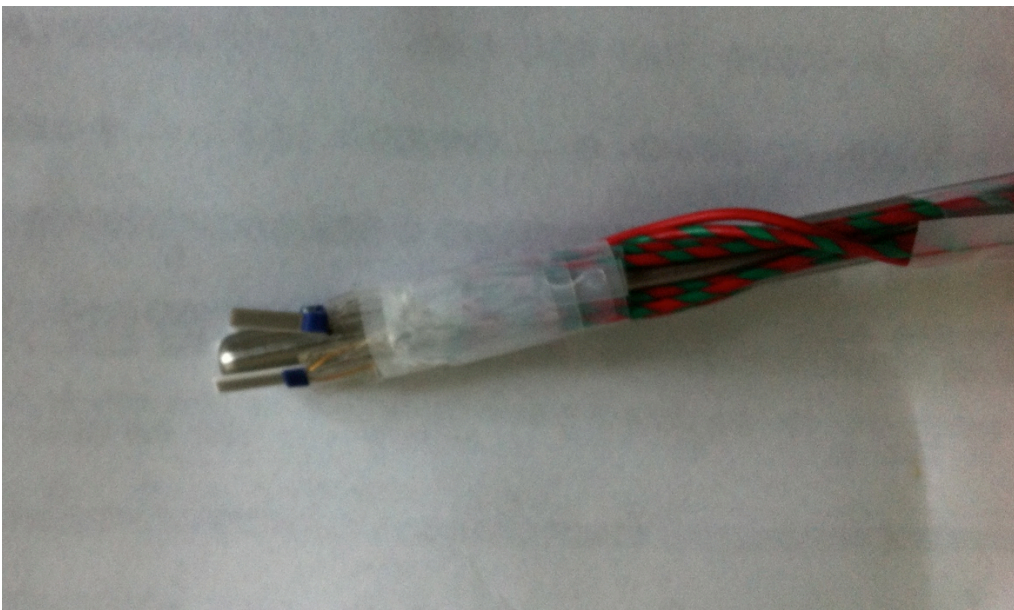
Several attempts to calibrate the sensors have been done. Now the sensors of some of these experiments are broken and the whole work is useless and gone in the sink. The 4 sensors were in some calibration procedures attached on the surface of the chillier and in other procedures to the side of the extraction cell – always as close as possible to each other and with a round handed dose of thermal paste on the contact plane to the cell. They were attached with at piece of armacel tape. Hence it was assumed that the sensors were exposed to the same temperature. The Cell was placed on the chiller and cooled with the same procedure proposed for the experiments. The voltage over each pt1000-senosr was logged every second.

After 5 of the above-mentioned experiments it turned out that the behaviour of the individual sensors was not reproduced with a satisfactory degree of precision. A possible explanation could be that I during soldering had overheated the solder (more than 300°C on the soldering kolb can cause solder pest, I now know) - therefore I changed all soldering on all sensors and wires. During this I broke the legs off 3 sensors and new sensors has been introduced.

Calibration of pt1000-sensors with a precise pt100-sensor – initial considerations.

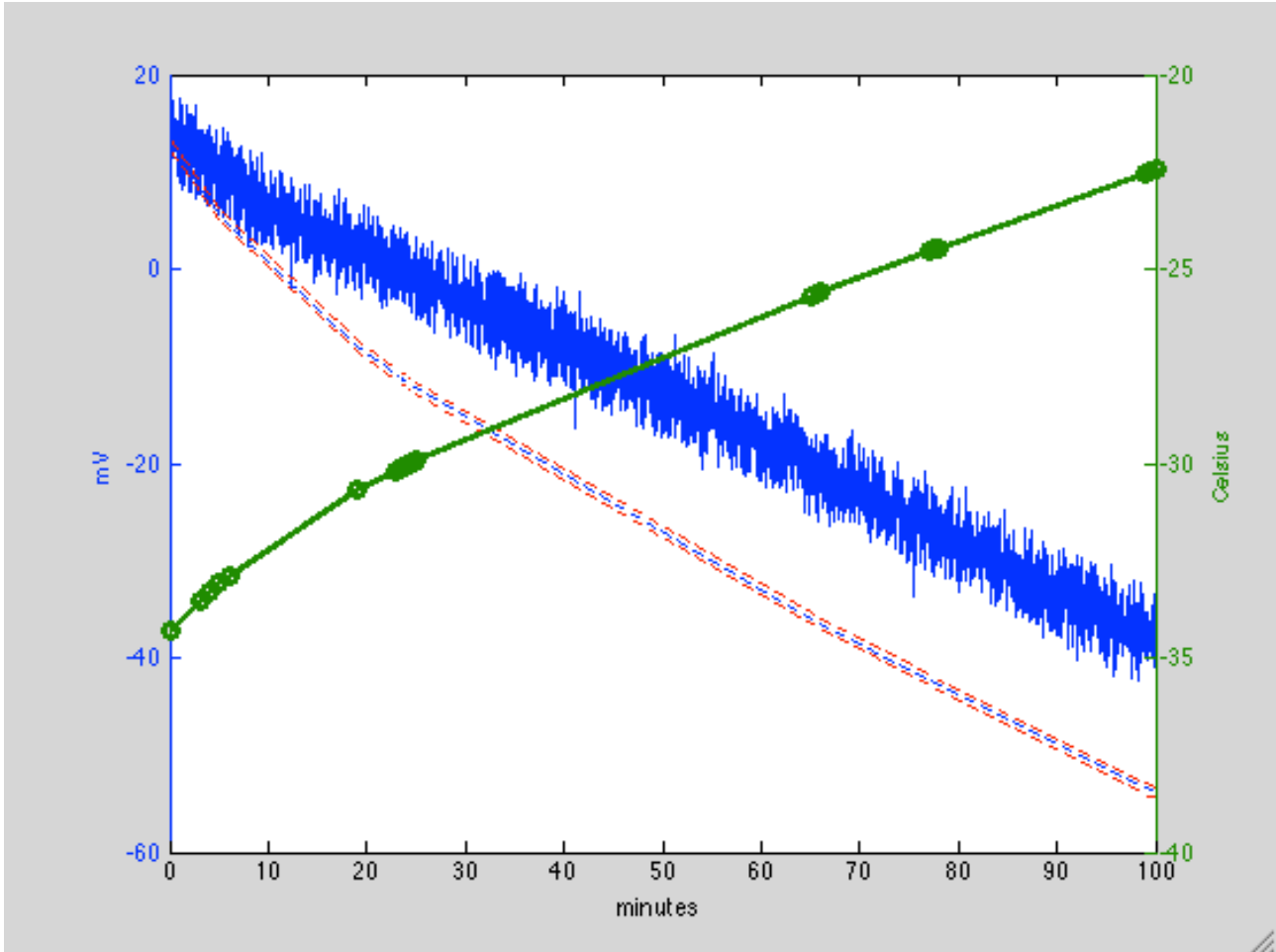
The calibration described in this chapter leads to 5 interval formulas for T as function of R for the different pt1000 sensors. Unfortunately the functions have shown to be erratic and useless. I have discovered this late – to late to redo it. I let the chapter stay.

The pt1000-sensors need to be calibrated against a precise thermometer. The intention from the sensor-producer is to trim them around 0 °C, that is $R=R_0=1000\Omega$ at 0°C, but it has been experienced that there can be an offset up to 5 degrees. Further it must be checked if the temperature dependence of their resistance is exactly as described in the standard formula. The optimal way would be to measure for a period with the sensors kept in an environment with absolute constant and extremely, precisely known temperature; and eventually repeating a series of measurements under different but constant temperatures. Since this is not possible with our facilities, a calibration procedure with slowly and controlled rising temperatures was used.



Figur 13. 4 pt1000-sensors attached to the tip of the pt100-sensor. Further the sensors are wrapped tighter together, placed in a thin rubber-etui and immersed in a spirit-dewar.

The 4 pt1000-sensor are taped to the tip (the sensitive part) of the pt100. Thermal paste is smeared on the sensors to secure good thermal conduction. More tape is wrapped around the sensor tips and the whole aggregate is placed in a rubber glove and immersed in a Dewar containing ethanol. Now measurements of the sensors are logged. After a while when the temperature in the Dewar is stable, the resistances are measured with a multimeter (this is a calibration point at room temperature). Thereafter liquid nitrogen is added to cool the ethanol to a temperature near -40°C. The lid is placed on the Dewar again and while it is slowly heating the resistances are measured, at different temperatures in the operational range. On Figur 14 are shown an example of this procedure.



Figur 14. Blue: measured voltage for pt-sensor1. Green line: temperature calculated from pt100-sensor-measurements taken at discrete time points (marked). Dashed lines: expected measured voltage calculated from standard formula (the 3 lines shows the effect of temperature deviance of $\pm 0,1$ °C).

As seen on the figure the temperature rises 10-15 degrees during 100 minutes with the fastest temperature rise in the beginning at lowest temperature. A simple assumption would be that the rate of temperature is proportional to the (approximately constant) room temperature in the laboratory, that is

$$\frac{dT}{dt} = K(T - T_{lab})$$

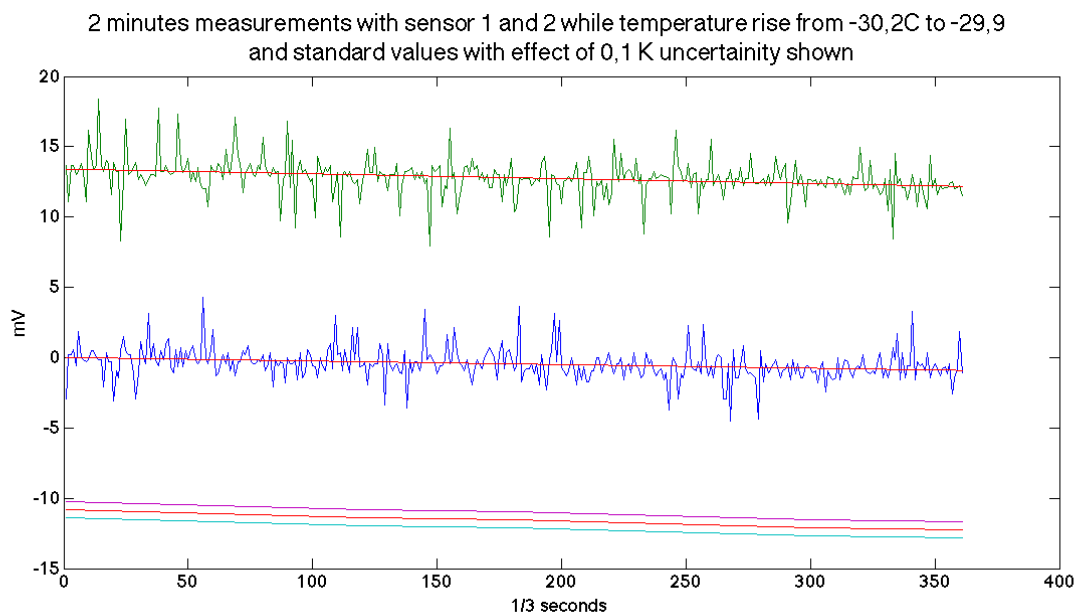
where K is a suiting constant, from which it follows that the temperature converges exponentially towards T_{lab} :

$$T = T_{lab} - \Delta T_0 e^{-Kt}$$

where ΔT_0 is $T - T_{lab}$ at $t=0$.

In small time intervals in the magnitude of 1 minute, it is a proper assumption that there is a linear temperature increase with time; the temperature change in this short time is anyway not much bigger than 0,1 °C which is the aim for the accuracy.

Therefore the first intention was to make a point wise calibration for example by taking the mean of 2 minutes interval as shown on Figur 15.

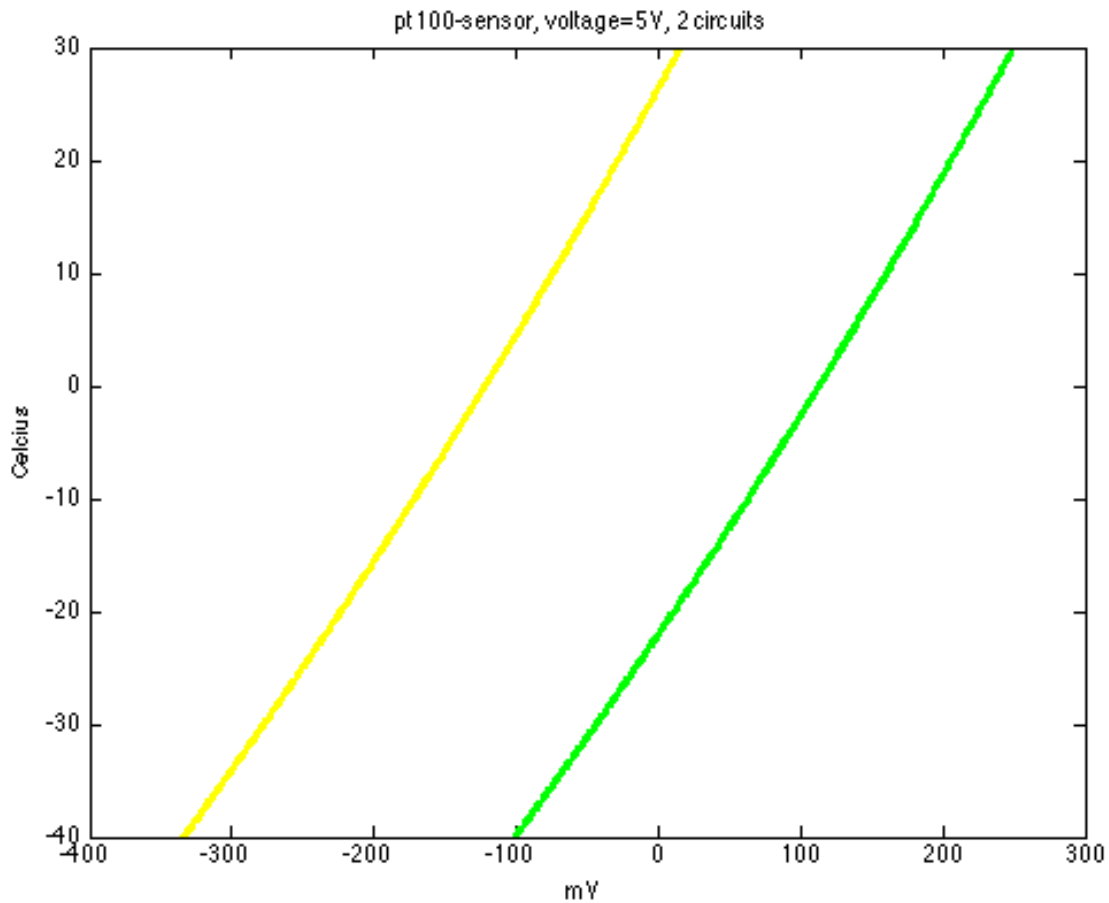


Figur 15. Finding a calibration point. During 2 minutes the temperature rose from -30,2°C to -29,9°C. Direct measurements of 2 sensors are shown including linear regression lines. The 3 lines in the bottom are calculations of the expected measured voltage based on the Callendar-formula and the measured temperature $\pm 0,1^\circ\text{C}$.

Refined calibration with 2 data loggers

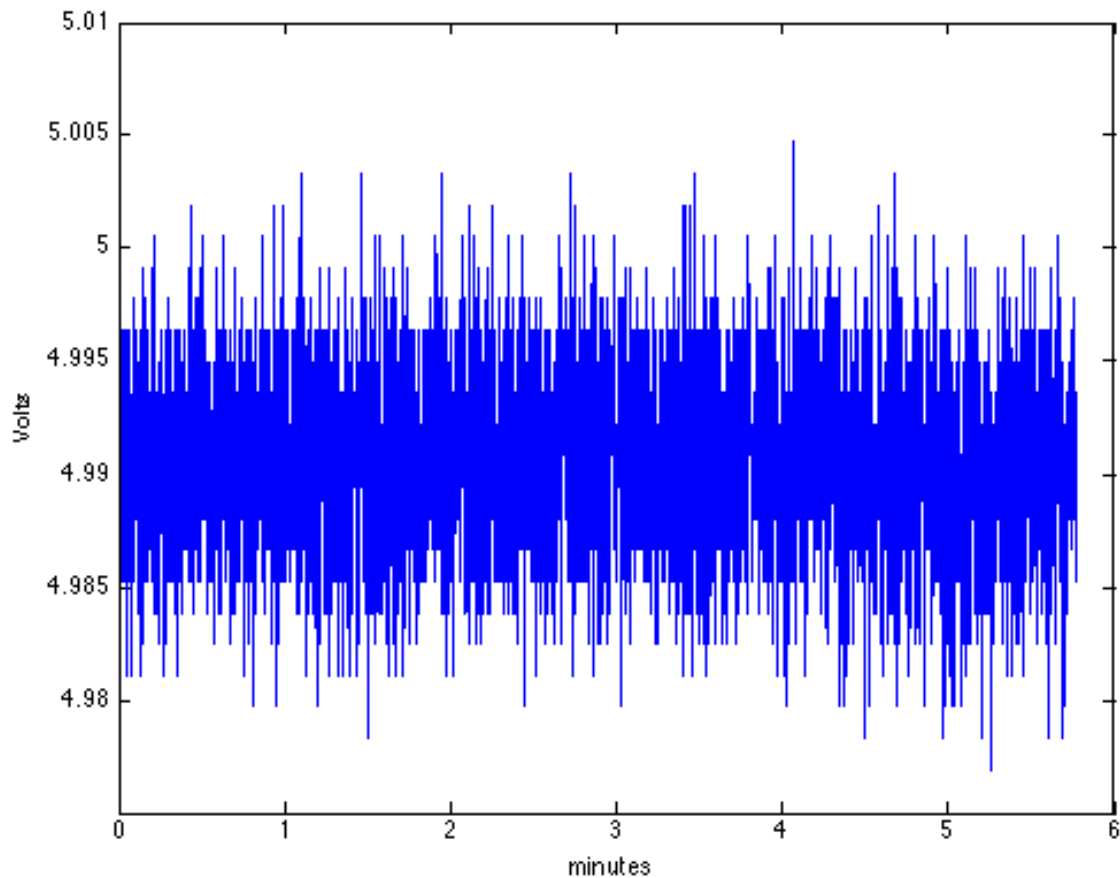
Later the experimental equipment was supplied with an extra data logger, which gives the possibilities of 1) logging the electromotive force on the circuit and 2) logging the measurements of the pt100 calibration sensor to avoid writing a lot of discrete numbers by hand. Two wheatstone bridges was constructed for the pt100-sensor – one to give highest accuracy on temperatures near -30°C and another to give highest accuracy on temperatures near 20°C. The Callendar-

formula is assumed to hold for the pt100-sensor, and on that basis the temperature/voltage relation is calculated as shown on Figur 16.



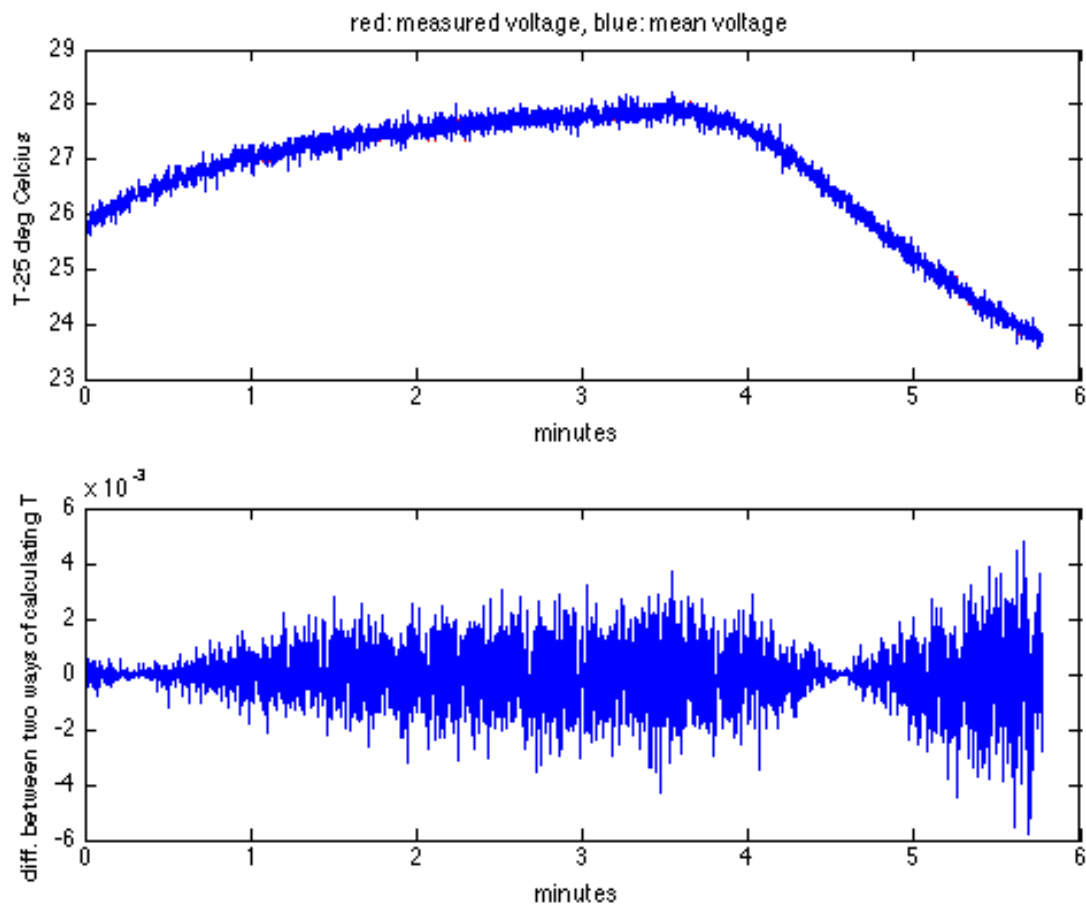
Figur 16. Relation between temperature and measured voltage with the pt100-sensor coupled to the two different balancing bridges.

The data logger was used as power supply for the calibration measurements. The stability of this supply was tested as shown on Figur 17.



Figur 17. Voltage logged 10 times a second during calibration. Mean=4,9907 V. Std=4,4 mV. Linear regression gives a slope of -0,00015 V/min showing that drift is negligible.

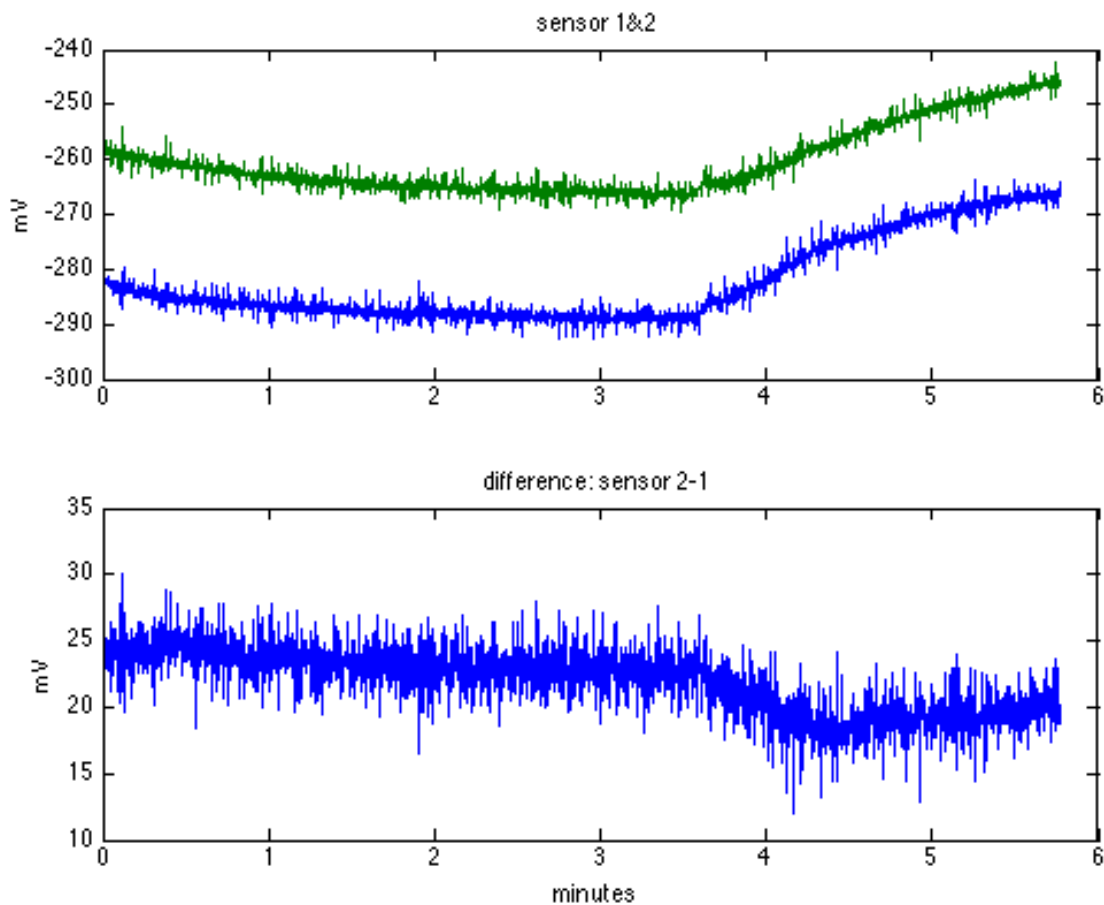
It is concluded that drift can be neglected, but there is spread with $\text{std}=4,4 \text{ mV}$. Now there are 2 ways of implementing \mathcal{E} in the calculations: either we can use the direct measured voltage, or we can use the mean value over a period of interest. I will calculate the temperature in the corresponding time interval in these two ways to see what difference it makes. This will also be a kind of test if the power supply's stability is sufficient. The result is shown on Figur 18.



Figur 18. Temperature is calculated in two ways: by using the direct measured voltage and by using the mean voltage over the period. Top: both temperatures (cannot be distinguished). An initial temperature rise of 2 degrees caused by internal warming in the sensors is seen. After 3 and a half minute liquid N₂ is added to the immersion spirit, and the temperature begins to decrease. Bottom: the difference between the two ways of calculating temperature. The voltage is logged 10 times each second.

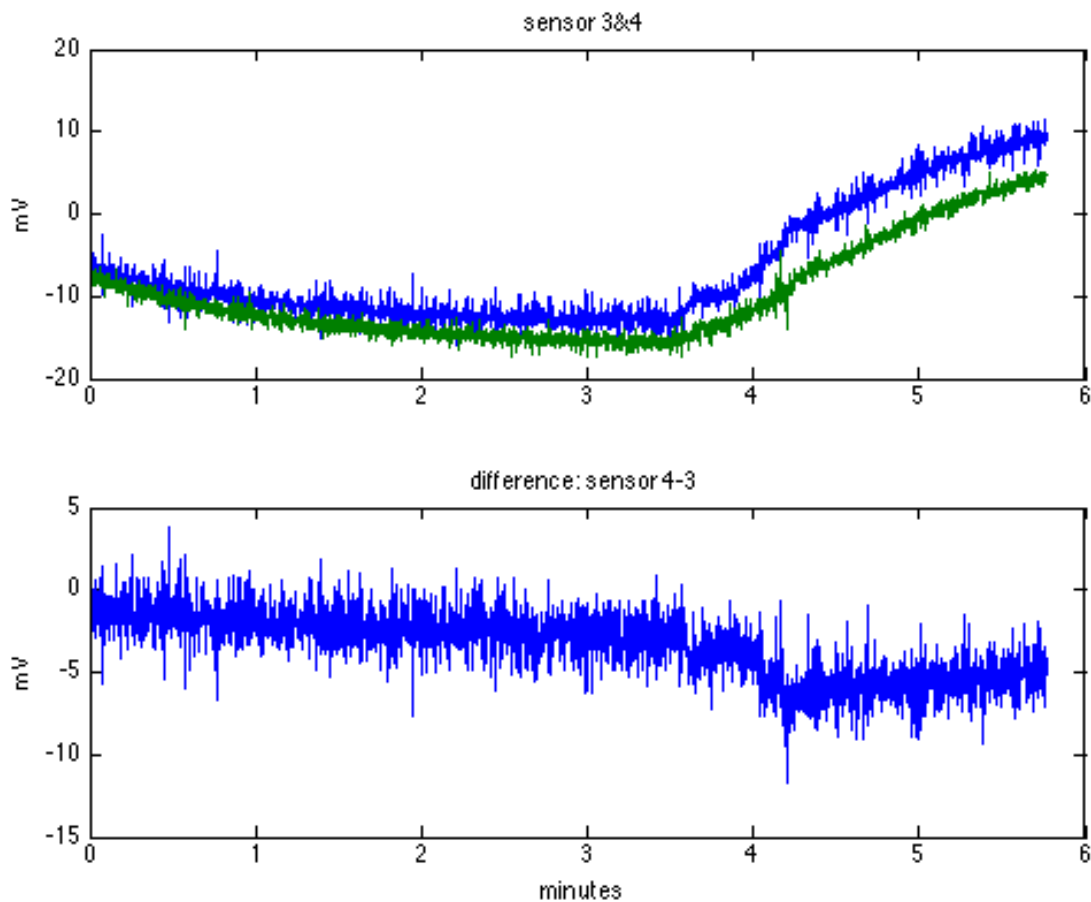
It is seen that it will only give differences of less than 3 mK on the temperature if we choose one or the other way which is negligible compare to the accuracy goal of 0,1 K. Surprisingly a systematic variation is seen on the deviation from mean looking like beats with a long period of 4 minutes. To that I can give no explanation. The conclusion is though that it is defencable to use this power supply regarding the stability.

Now we look at the contemporary measurements on the pt1000-sensors.



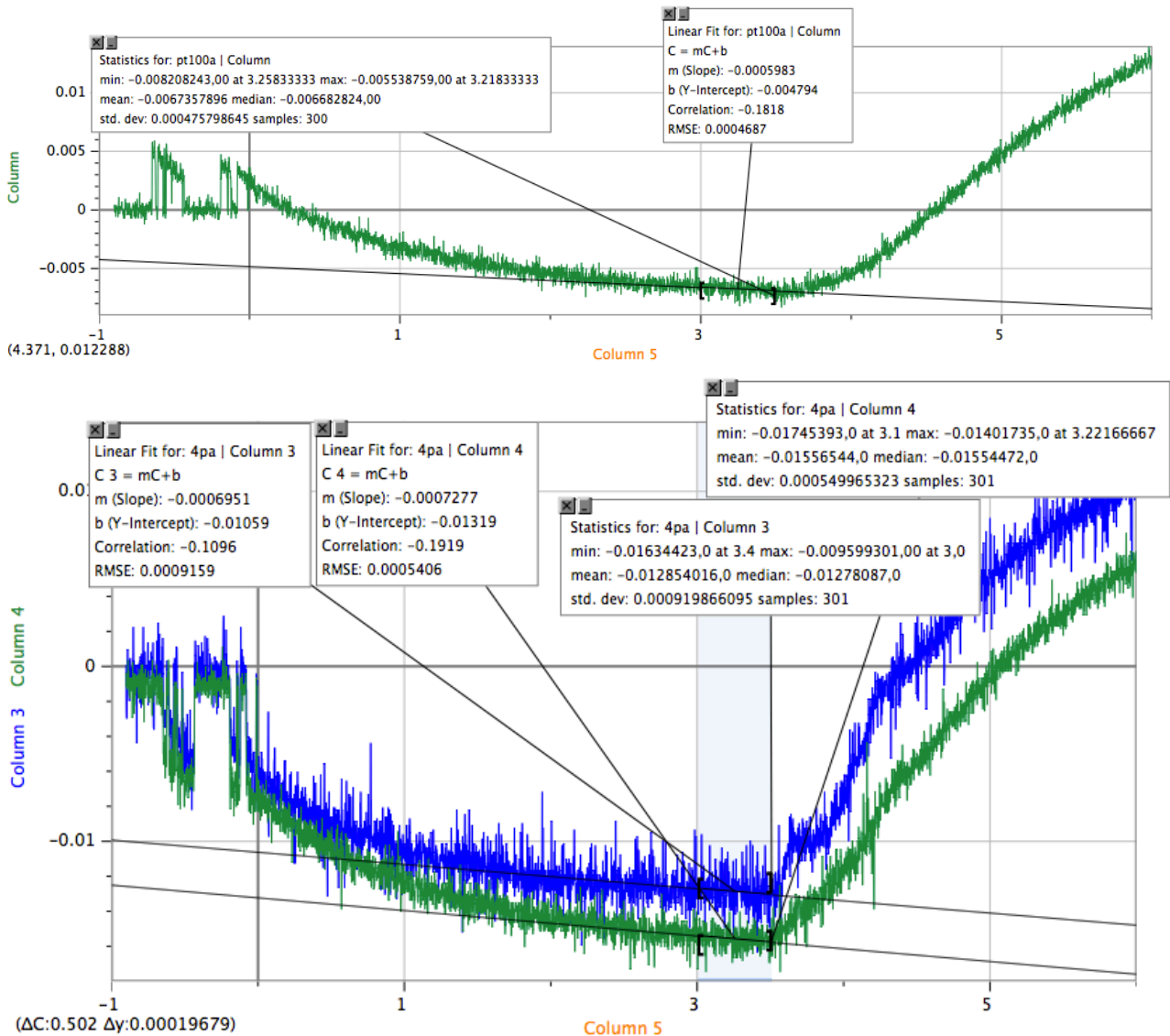
Figur 19. Measurements with pt1000-sensors 1 and 2. (fil: 4pa.txt).

Notice variation during the time period. It shall be noted that this experiment was started after the sensors had been immersed in the Dewar for a long time disconnected from the power supply, so temperature constancy and stability can be assumed at start. I wanted to see if the internal heating was significant in this setup, and this is the case. We see the temperature rise 2 degrees during the first 3 minutes on Figur 18 and equivalently we see the pt1000 sensors react in Figur 19 (yet we cannot see the corresponding temperature). I will later test if this internal heating can be detected when the sensors are attached to the extraction cell. Maybe it will be necessary to correct for this. But assuming that the heating eventually will stabilize the temperature and that the pt100 and pt1000 sensors then will keep the same temperature, we don't have to take this into account in the calibration. It is just a necessary condition that the sensors have the same temperature – not what the actual temperature in the Dewar is.



Figur 20. Measurements with pt1000 sensor 3 and 4. (fil: 4pta)

To calibrate the sensors we need to ensure measurements in a temperature stable environment. Even in the small space in the sensor packet shown on Figur 13 there can apparently be not insignificant temperature differences under circumstances when there is rapid temperature changes, which can be seen on Figur 19 and Figur 20. As liquid N₂ is added there is different lag times for the sensors. It must be a little test to check if we have a constant difference between the sensor measurements to clarify if there is sufficient stability.



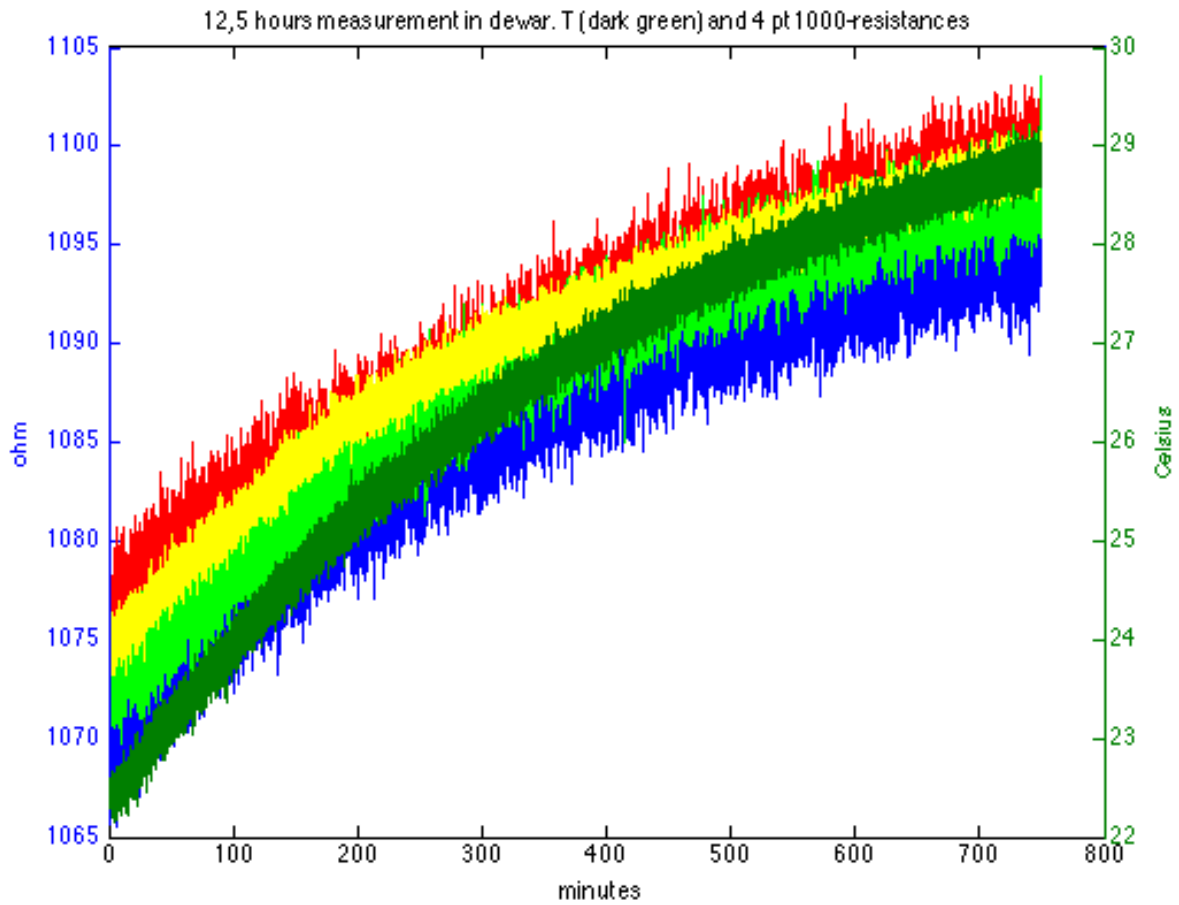
Figur 21. The time interval from 3 to 3,5 minutes are use for statistics. There is still a slight internal heating going on but in this case negligible.

Calibration over an time interval with slowly rising temperatures.

Calibration of sensor 3 and 4 (around 25°C)

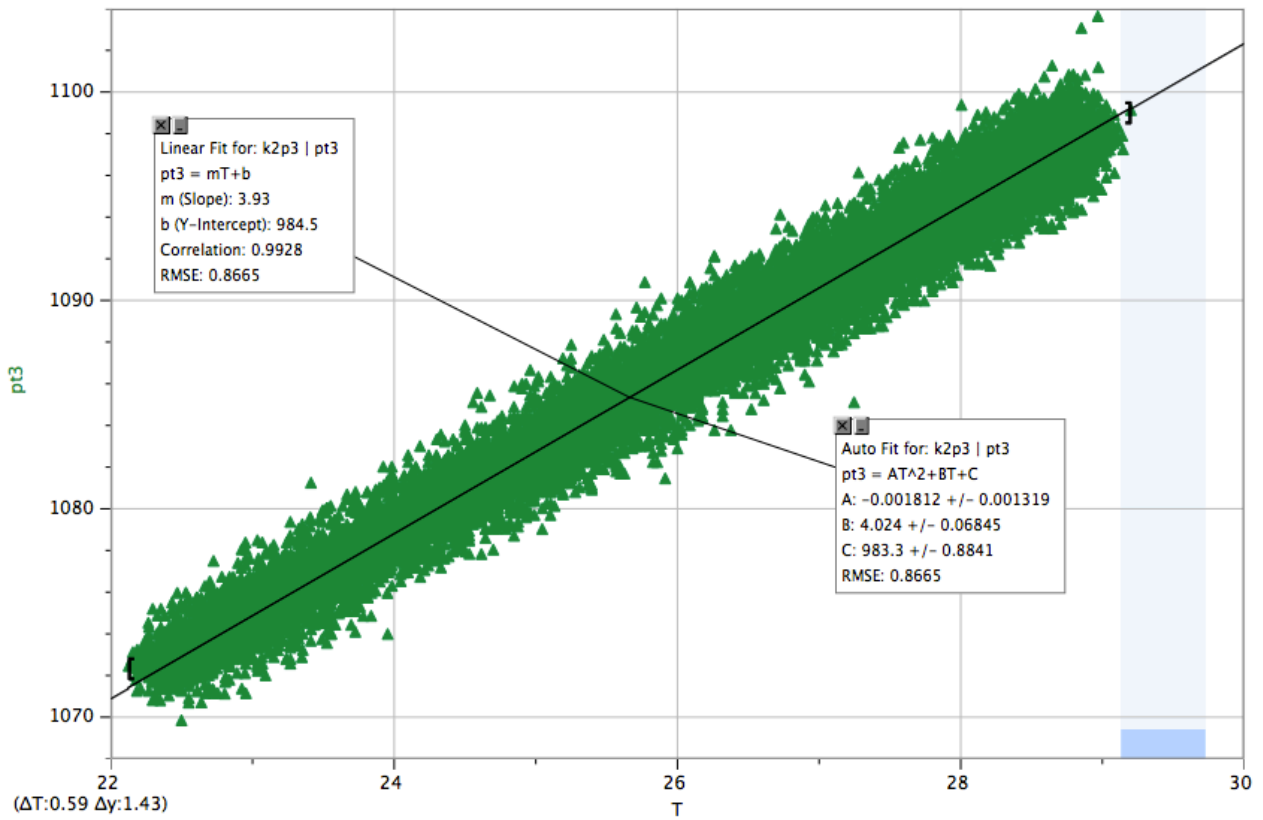
Another and probably better calibration method is attempted by making regression on the sensor-measurements under slowly temperature changes. The sensors are placed in the Dewar for a long time while temperature slowly

converges to the room temperature. Data is logged every second. The calculated temperature and sensor-resistances during the measurement is shown on Figur 22.

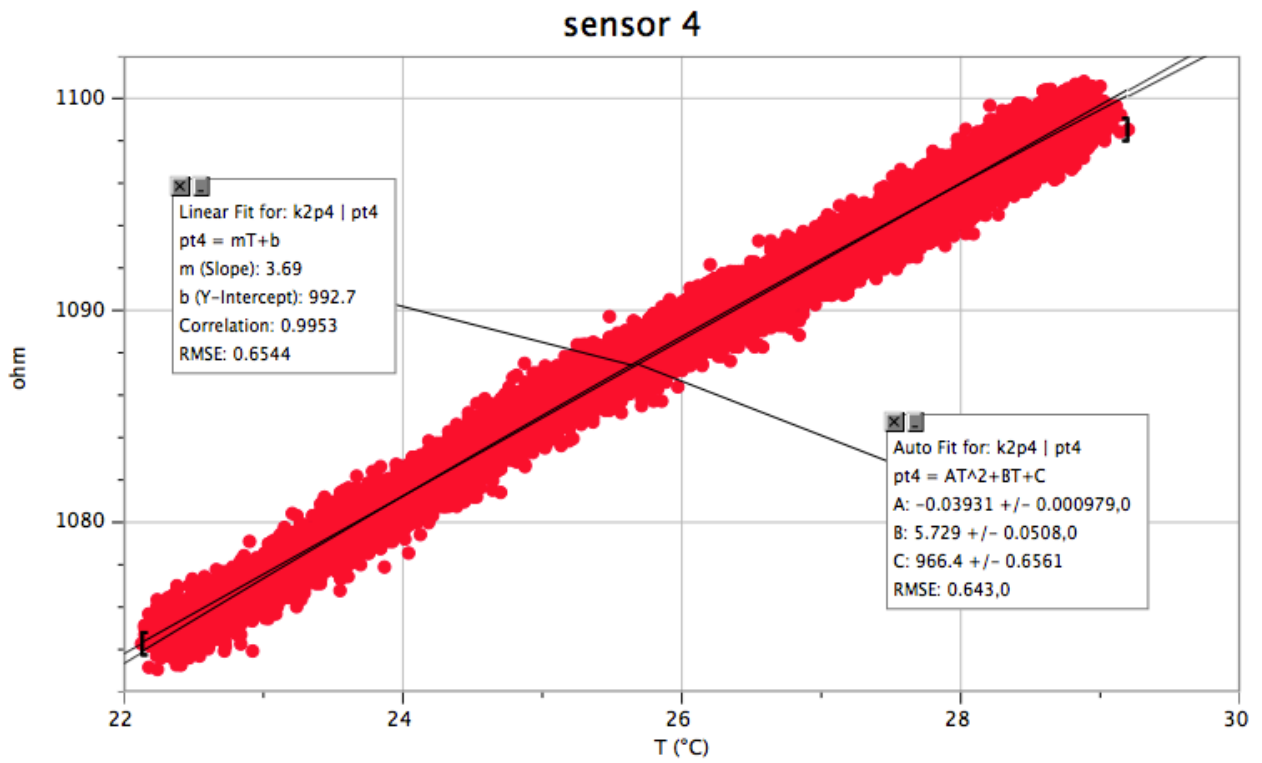


Figur 22. The aggregate of pt-sensors have been immersed in a spirit-dewar for 12,5 hours. Data was logged 1 time per second.

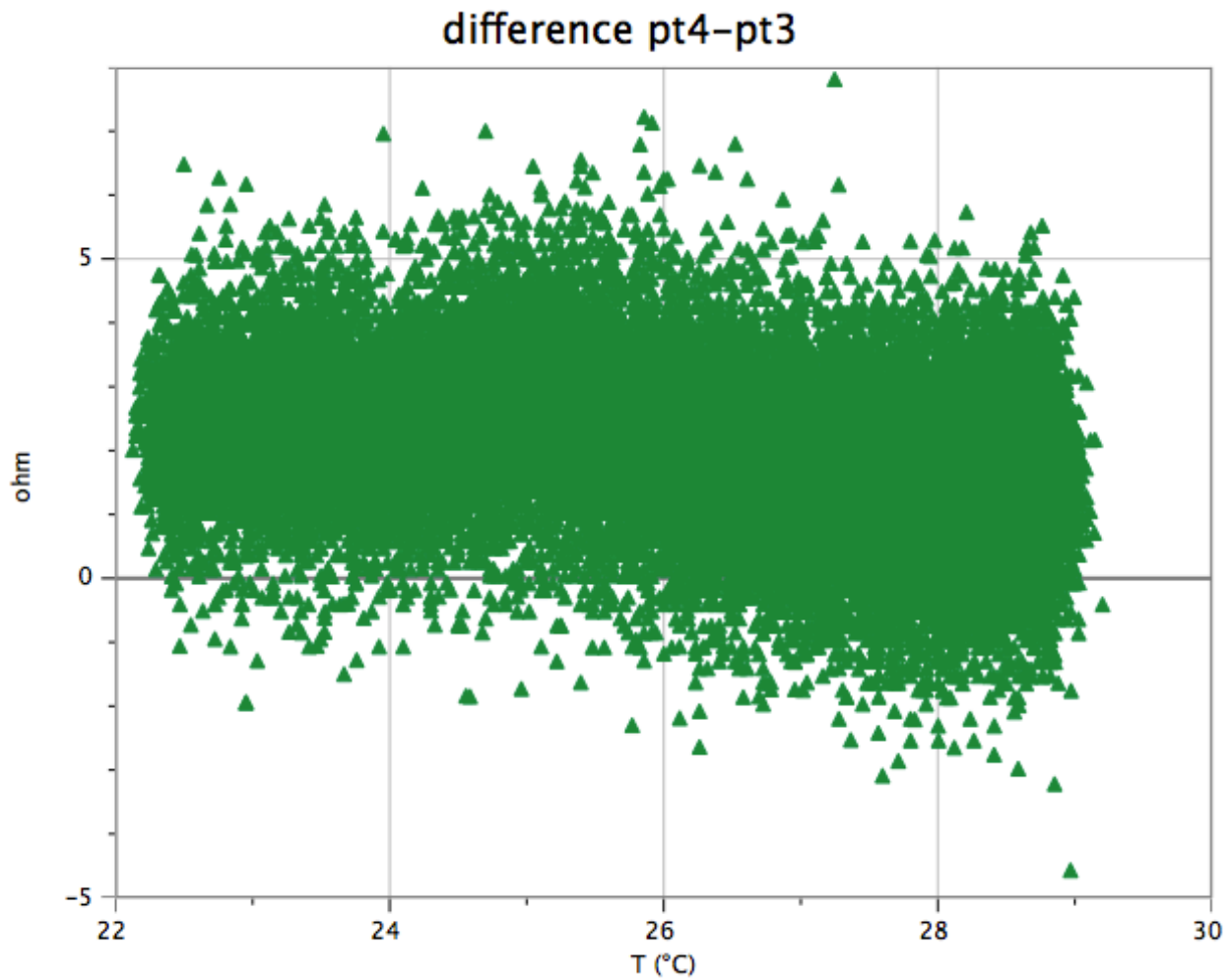
The intention is to calibrate sensor 3 and 4 as they are going to measure temperatures in this range. Regression of R/T are shown on the next figures.



Figur 23. Temperature versus resistance in sensor 3. Data was logged one time a second during 12,5 hours with slowly rising temperature.



Figur 24. Sensor 4 in the same experiment as in Figur 23



Figur 25. Difference between sensor 4 and 3 is plotted to look for possible unstabilities during the measurement. (the x-axis can also be viewed as a distorted time axis since the temperature was monotonically but nonlinearly rising.)

As seen on Figur 23 and Figur 24 a linear correlation can be established between temperature and sensor-resistance. A quadratic fit is tried as well according to the standard formula. In the interval of 22°C to 29°C the linear and quadratic relation deviate much less than 0,1 °C for sensor 3 which is somewhat relieving to see; for sensor 4 the quadratic fit seems to be less appropriate than the linear.

	linear	Quadratic	Callendar
Sensor 3 (25°C)			
$R_0 (\Omega)$	984,5	983,3 Ω	
A or $\tilde{A} (10^{-3}K^{-1})$	3,9919	4,09234	3,9083
B ($10^{-7}K^{-2}$)		-18,4	-5,775
Sensor 4 (25°C)			
$R_0 (\Omega)$	992,7	966,4	
A or $\tilde{A} (10^{-3}K^{-1})$	3,71714	5,7711	3,9083
B ($10^{-7}K^{-2}$)		-396,0	-5,775
Sensor 1 (-30°C)			
$R_0 (\Omega)$	959,7		
A or $\tilde{A} (10^{-3}K^{-1})$	3,3042		3,9083
B ($10^{-7}K^{-2}$)			-5,775
Sensor 2 (-30°C)			
$R_0 (\Omega)$	954,4		
A or $\tilde{A} (10^{-3}K^{-1})$	3,3057		3,9083
B ($10^{-7}K^{-2}$)			-5,775

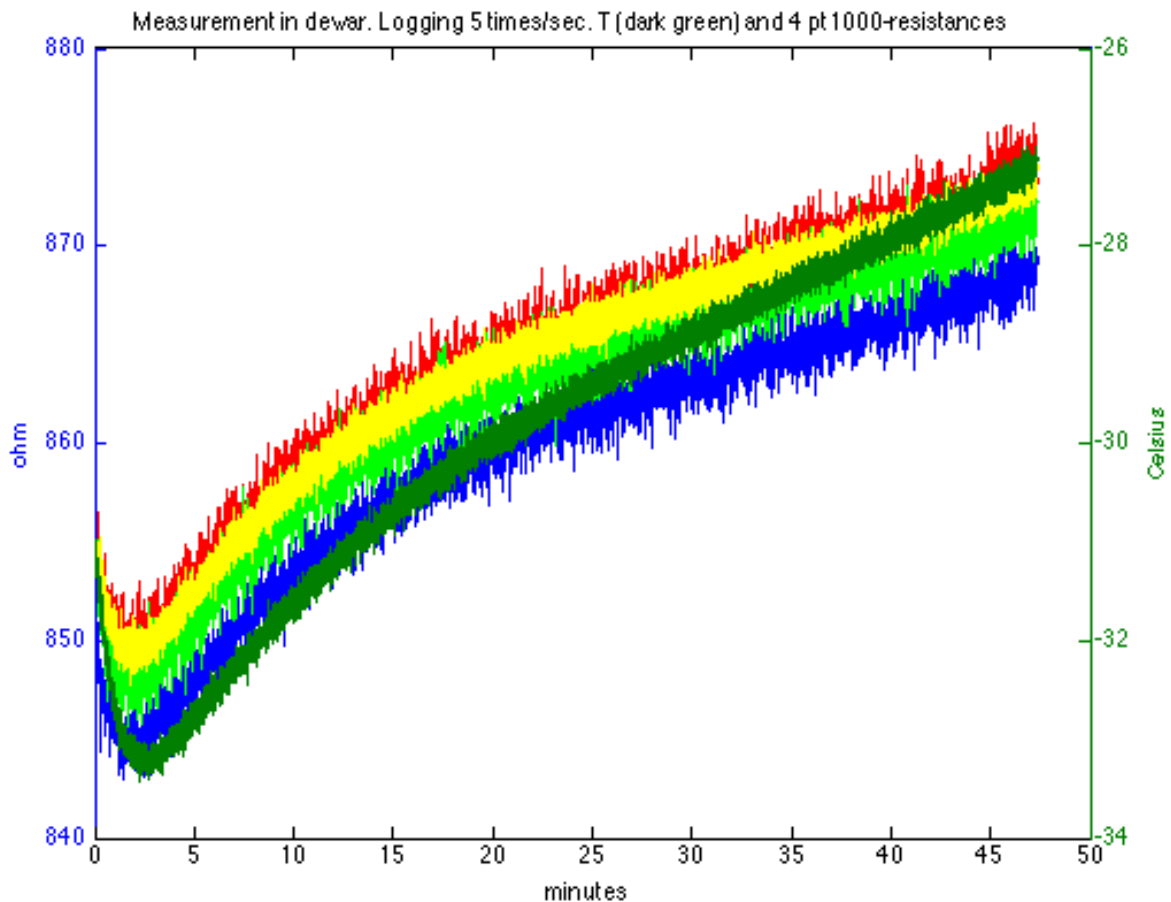
Tabel 2. Regression parameters.

Linear fit $R = R_0 \cdot (\tilde{A}T + 1)$ quadratic $R = R_0 \cdot (AT + BT^2 + 1)$

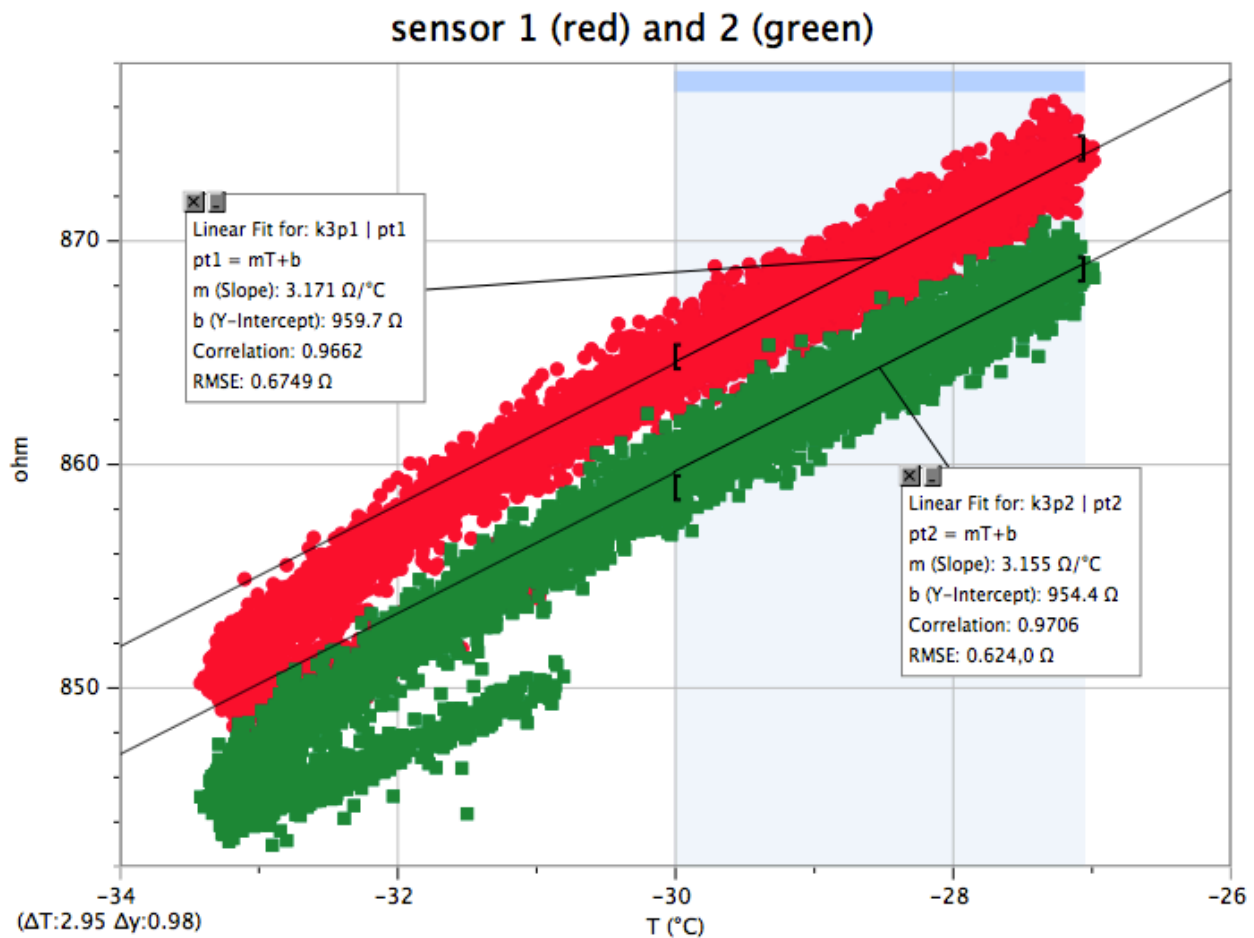
Calibration of Sensor 1 and 2 (near -30°C)

A similar calibration is made for sensor 1 and 2 near -30°C. In this case the temperature rise is steeper so data is now logged 5 times/second. Calculations from the measurements are shown on Figur 26. Conditions seem to be stable while the temperature rises from -30°C to -27°C (in cirka 25 minutes), so regression is done on this interval. Regression to temperature is shown on Figur 27, and regression parameters for both linear and quadratic regression is listed in Tabel 2 for the 4 sensors.

The linear coefficient is close to the coefficient in the Callendar-formula (3,9) for temperatures near 25°C, but for temperatures near -30°C they are lower (3,3) and that is unfortunate since it will give a lower resolution on the temperature measurements. Further it is noticed that R0 deviates significantly from 1000 Ω, which gives the suspicion, that the temperature dependence is not linear over the whole temperature range [-30°C;25°].



Figur 26. As liquid N₂ is added to the spirit, temperature dives and rises quiet sharply after the minimum when the nitrogen is boiled off, while the walls in the dewar is still warmer than its content. From 20 minutes and on stability is assumed – that is while the temperature rises from -30°C to -27°C.



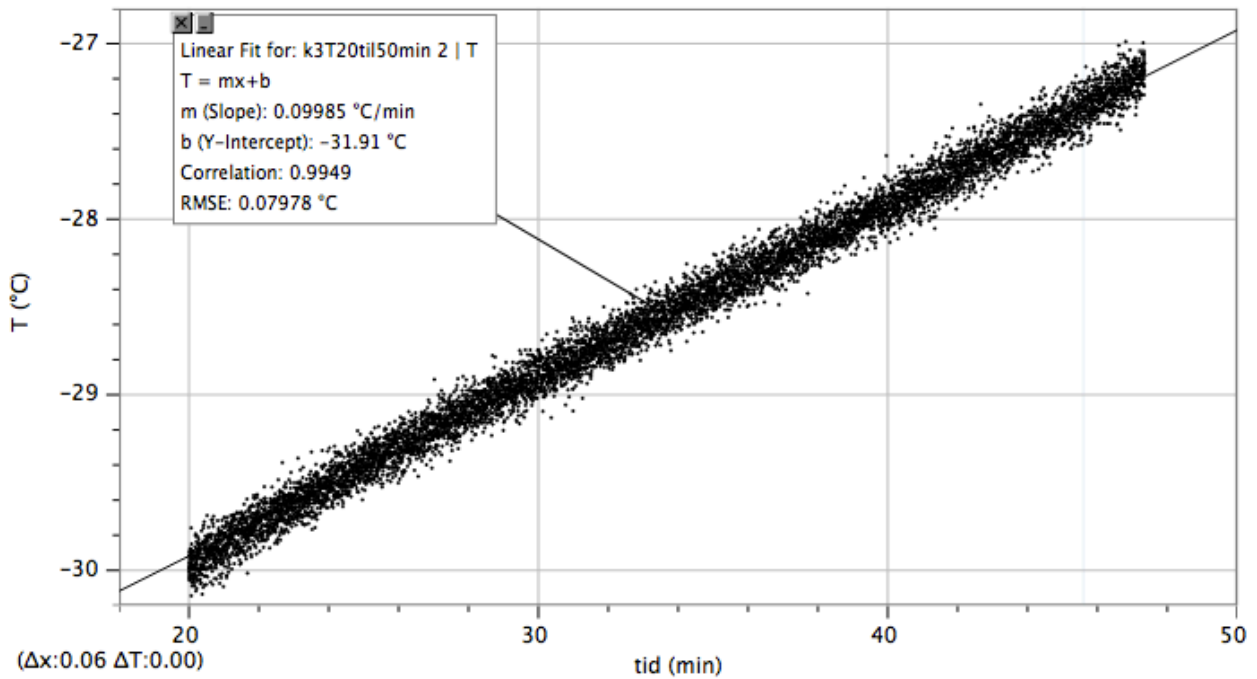
Figur 27. Sensor1 and 2 are calibrated in the temperature interval [-30;-27]°C. The 'hysteresis' is caused by faster reaction times in the small pt1000-sensors compared to the larger pt100-sensor used for temperature calculation.

On the spread and error in the measurements.

It is seen, that there is an not insignificant spread in the measurements (RMSE=0,62 Ω in the regression of sensor 2) and the reason must be considered. How stable are the temperature measurement?

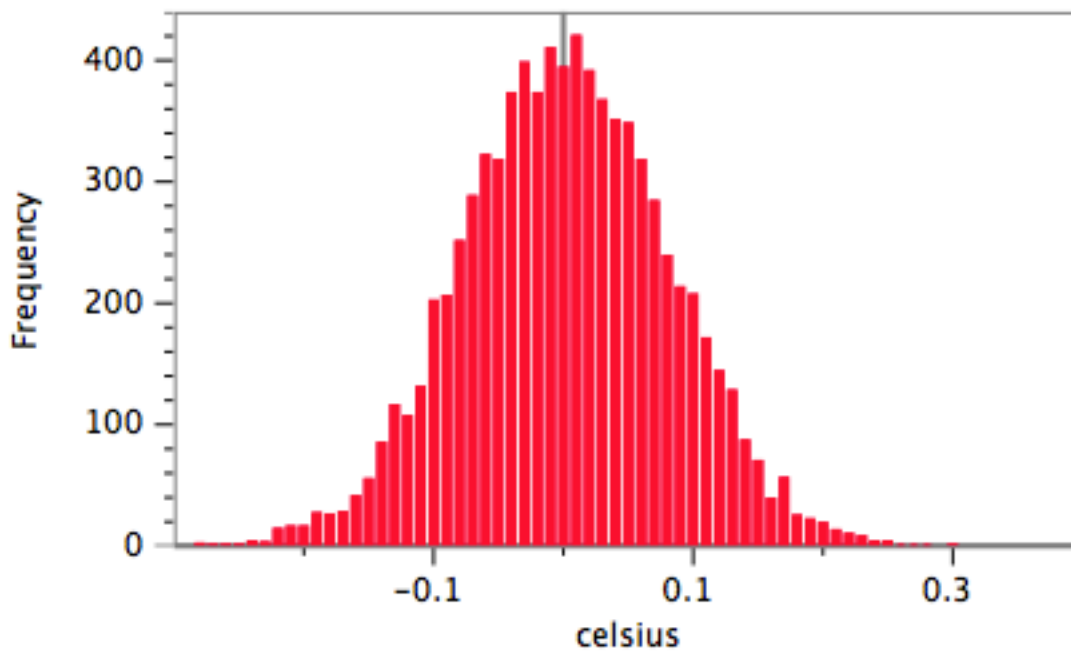
Figur 28 shows a nice linear trend and Figur 29 shows that deviations from the trend is normal distributed as common measure uncertainties should be.

Figur 30, Figur 31 and Figur 32 shows an analysis of the spread in measurements of one pt1000 sensor. It shows no periodicity in the errors (though will it later be tested if there is noise with higher frequency than 2,5 Hz since data here was logged with 5 Hz) . For now it is concluded that the noise is random, the standard deviation on the resistance-measurement is 0,67 Ω, and with a slope in the linear dependence of 3,3 Ω/°C that equalates a standard deviation on the temperature measurement of 0,2 °C.

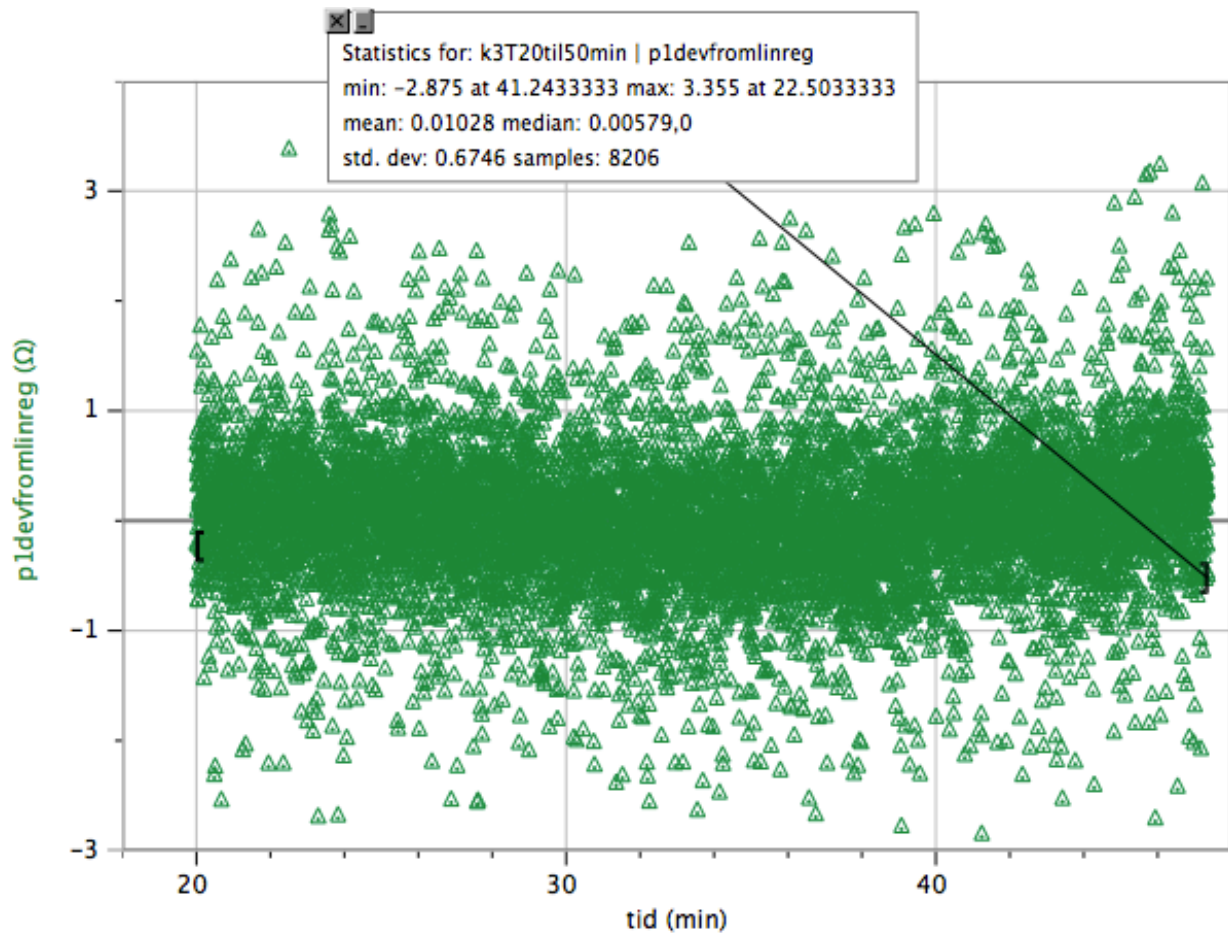


Figur 28. Measured temperature for calibration of sensor 1 and 2.

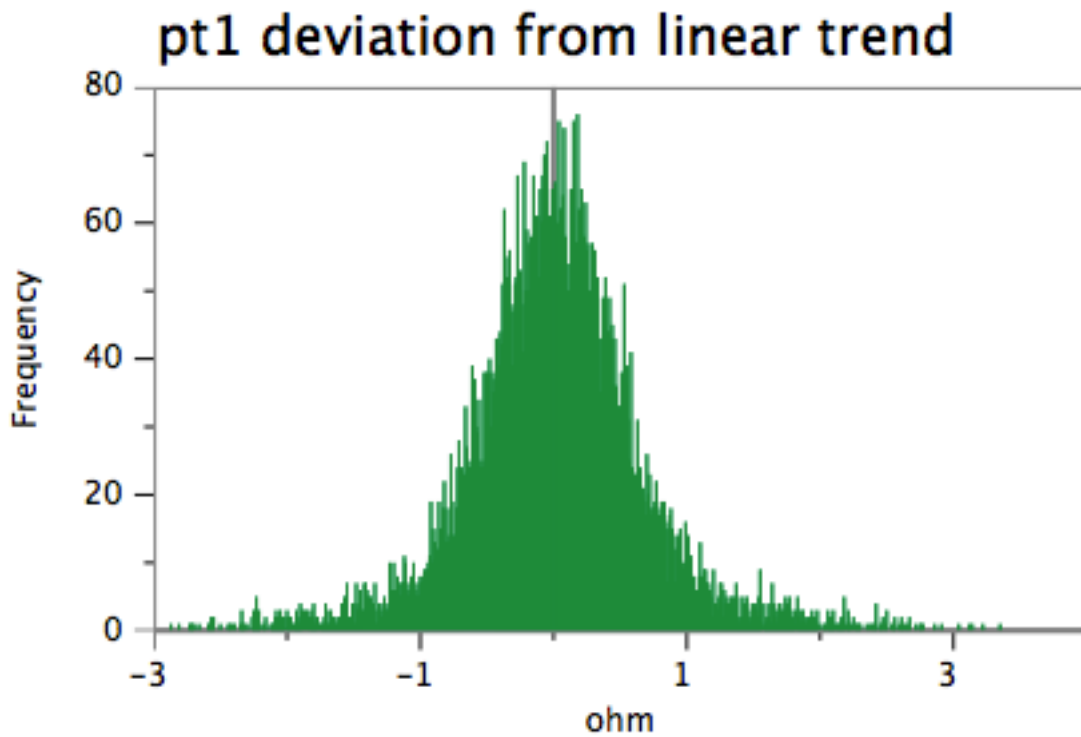
T-measurement deviation from linear trend



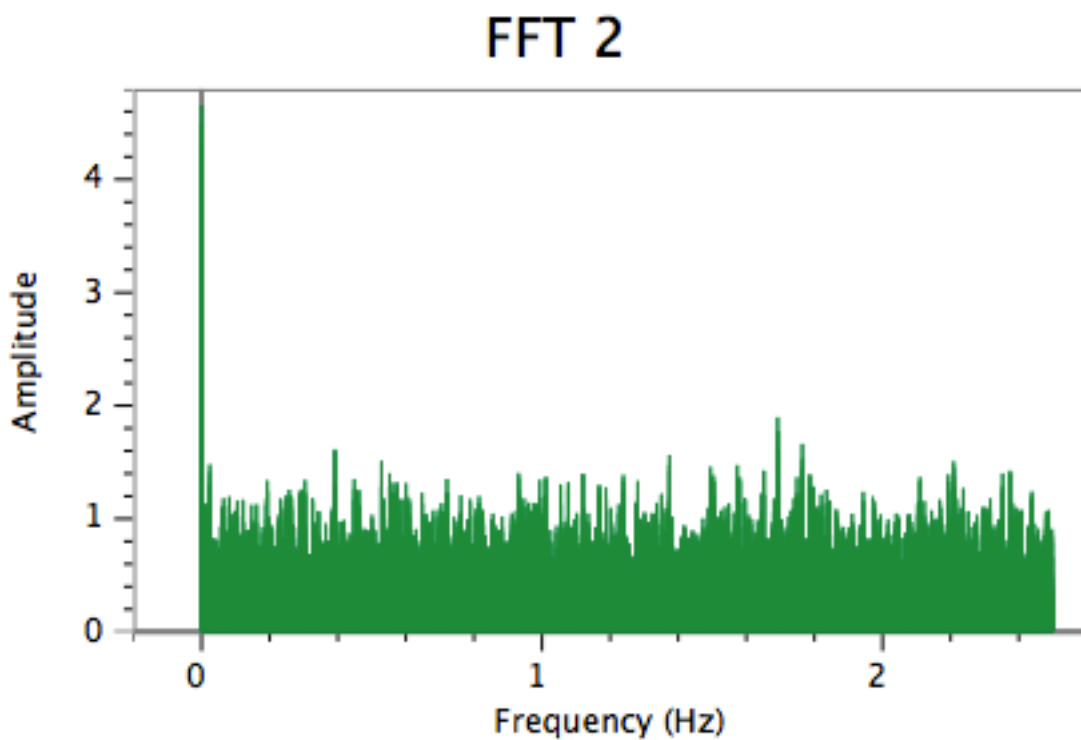
Figur 29. Errors on temperature measurements are normal distributed



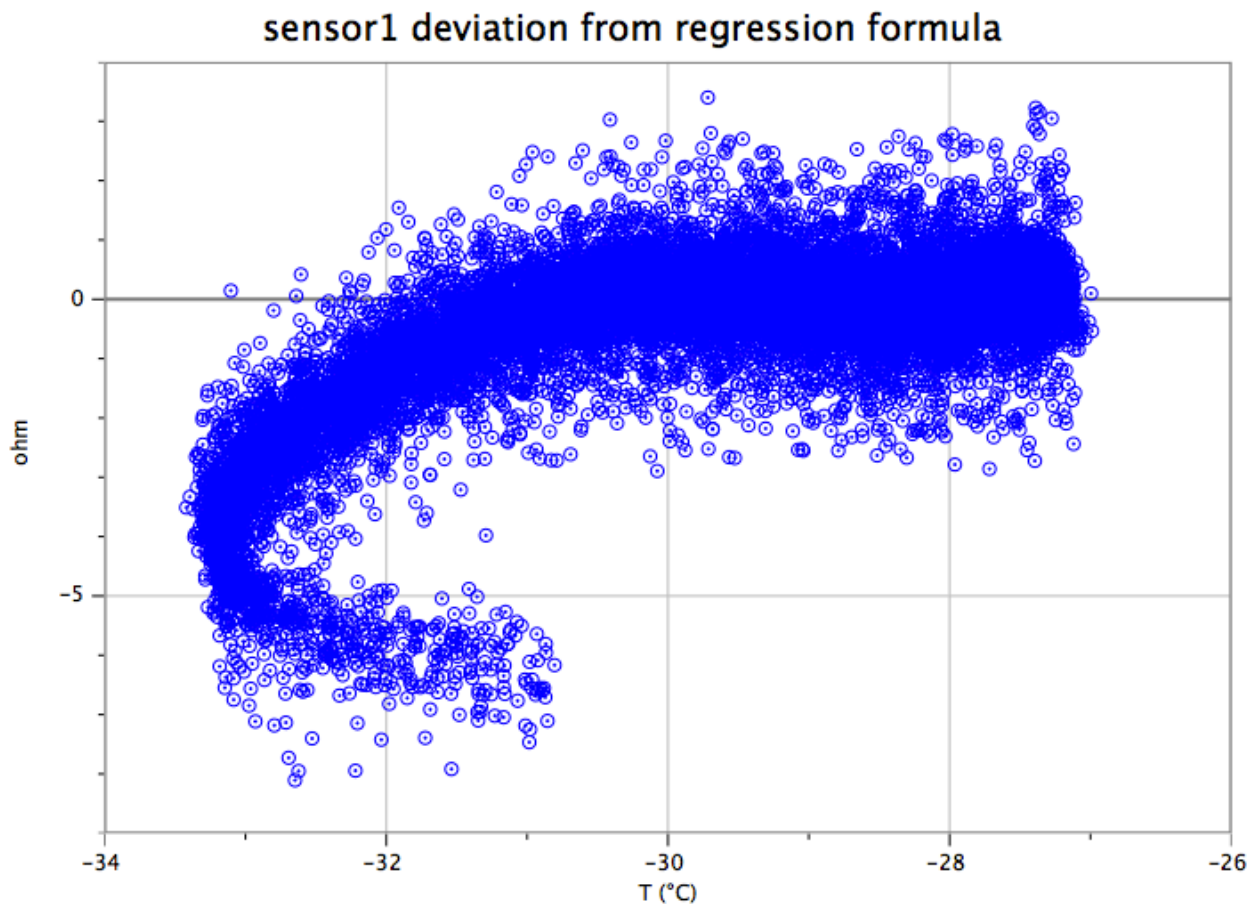
Figur 30. Pt-sensor 1. Deviation from regression formula during the measurement. Std=0,67.



Figur 31. The errors on pt1000 measurements are normal distributed.



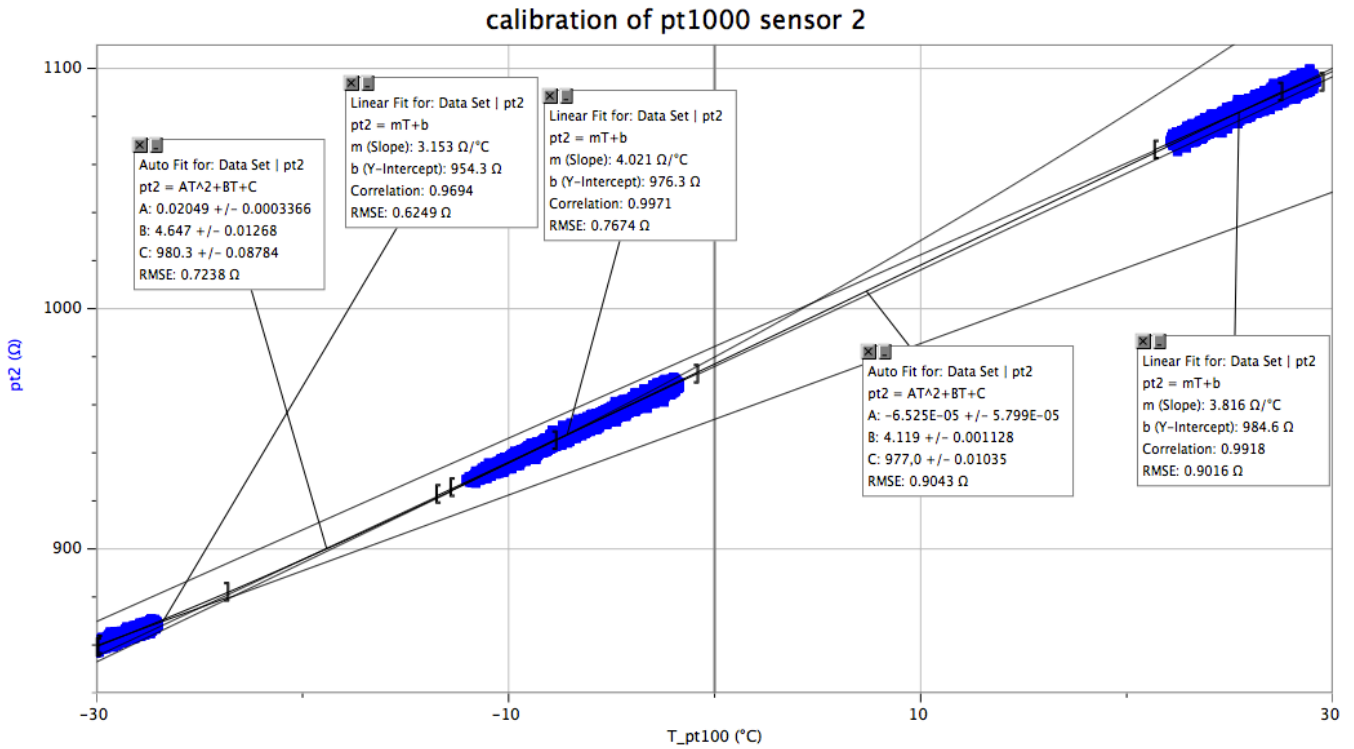
Figur 32. Frequency analysis of the signal shown in Figur 30 shows there is no systematic error (at least with frequency lower than 2,5 Hz) causing the spread.



Figur 33. Measured resistance deviation from the derived sensor formula during the measurement shown on Figur 26. The tail in the lower left is the first 20 minutes before stable conditions were actualized.

Further calibration of pt1000 sensors.

Only the two pt1000 sensors attached to the extraction cell need to be calibrated in the full range [-30°C,30°C]. For measurements on ice it suffices with a calibration near -30°C, but for volume calibration purposes it is useful to measure temperatures on the extraction chamber in the full range.



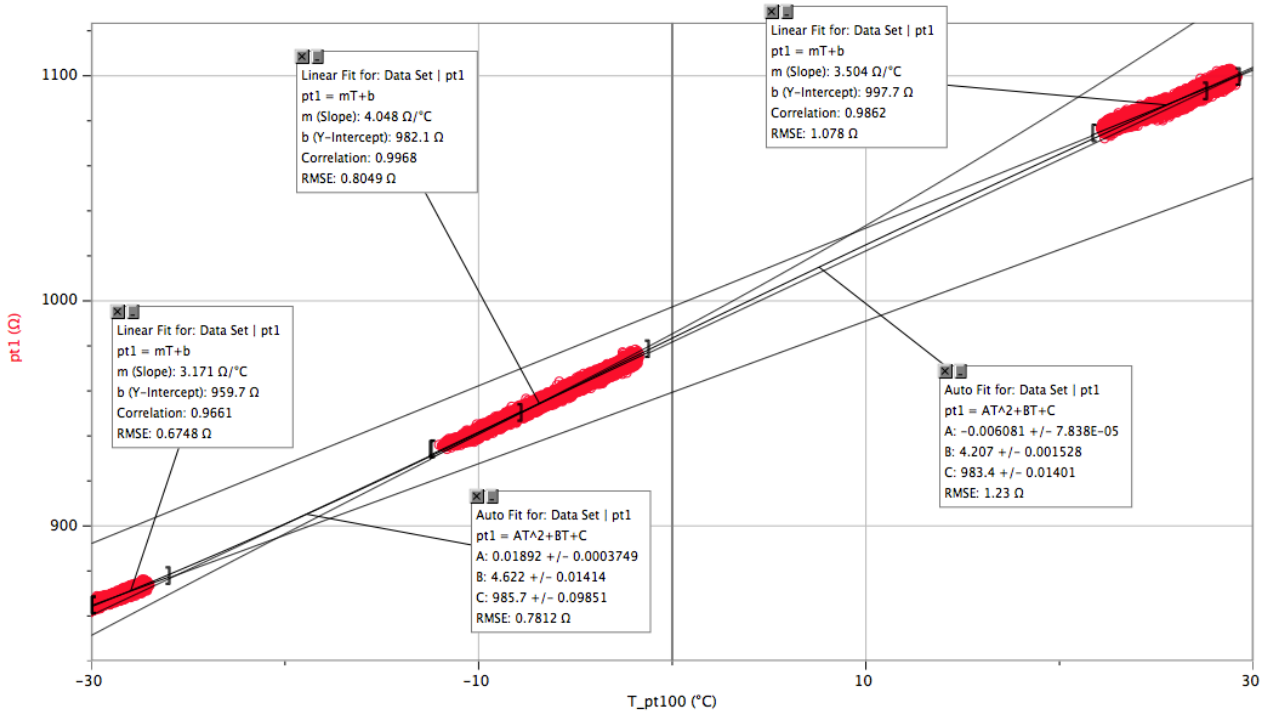
Figur 34. Calibration of pt1000 sensor 2. Measurements are taken in 3 different ranges: [-30°C,-27°C] (8300 datapoints), [-12°C, -2°C] (29000 datapoints) and [22°C,30°C] (45000 datapoints)

Measurements are taken in 3 different temperature ranges: [-30°C; -27°C] (8300 data points), [-12°C; -2°C] (29000 data points) and [22°C; 30°C] (45000 data points). Linear regression is taken on each interval with good correlation. Since the slopes on each regression line are slightly different the temperature dependence can not be assumed to be linear on the whole temperature range. To 'connect' the 3 linear intervals a quadratic fits are made on data points in the temperature ranges [-30°C; -7,7°C] (with 8300 data points in each 'block') and [-12°C; 27,7°C] (with 29000 data points in each 'block'). This summarizes to a function for the temperature dependence of pt-sensor 2 as follows:

$$R_{pt2} = \begin{cases} 3,153 \frac{\Omega}{K} \cdot T + 954,3\Omega & \text{for } T \in [-30^{\circ}\text{C}; -23,5^{\circ}\text{C}] \\ -6,525 \cdot 10^{-5} \frac{\Omega}{K^2} \cdot T^2 + 4,119 \frac{\Omega}{K} \cdot T + 977,0\Omega & \text{for } T \in [-23,5^{\circ}\text{C}; -7,1^{\circ}\text{C}] \\ 4,021 \frac{\Omega}{K} \cdot T + 976,3\Omega & \text{for } T \in [-7,1^{\circ}\text{C}; -6,5^{\circ}\text{C}] \\ -0,002576 \frac{\Omega}{K^2} \cdot T^2 + 4,159 \frac{\Omega}{K} \cdot T + 977,3\Omega & \text{for } T \in [-6,5^{\circ}\text{C}; 26,6^{\circ}\text{C}] \\ 3,816 \frac{\Omega}{K} \cdot T + 984,6\Omega & \text{for } T \in [26,6^{\circ}\text{C}; 30^{\circ}\text{C}] \end{cases}$$

where T is in °C and the intervals are defined by the cuts of the regression functions.

A similar calibration is made of sensor 1:



Figur 35. Calibration of pt1000 sensor 1.

The result summarizes to:

$$R_{pt1} = \begin{cases} 3,153 \frac{\Omega}{K} \cdot T + 959,7\Omega & \text{for } T \in [-30^{\circ}\text{C}; -28,5^{\circ}\text{C}] \\ 0,01892 \frac{\Omega}{K^2} \cdot T^2 + 4,622 \frac{\Omega}{K} \cdot T + 985,7\Omega & \text{for } T \in [-28,5^{\circ}\text{C}; -8,9^{\circ}\text{C}] \\ 4,048 \frac{\Omega}{K} \cdot T + 982,1\Omega & \text{for } T \in [-8,9^{\circ}\text{C}; -6,5^{\circ}\text{C}] \\ -0,006081 \frac{\Omega}{K^2} \cdot T^2 + 4,207 \frac{\Omega}{K} \cdot T + 983,4\Omega & \text{for } T \in [-6,5^{\circ}\text{C}; 26,3^{\circ}\text{C}] \\ 3,504 \frac{\Omega}{K} \cdot T + 997,7\Omega & \text{for } T \in [26,3^{\circ}\text{C}; 30^{\circ}\text{C}] \end{cases}$$

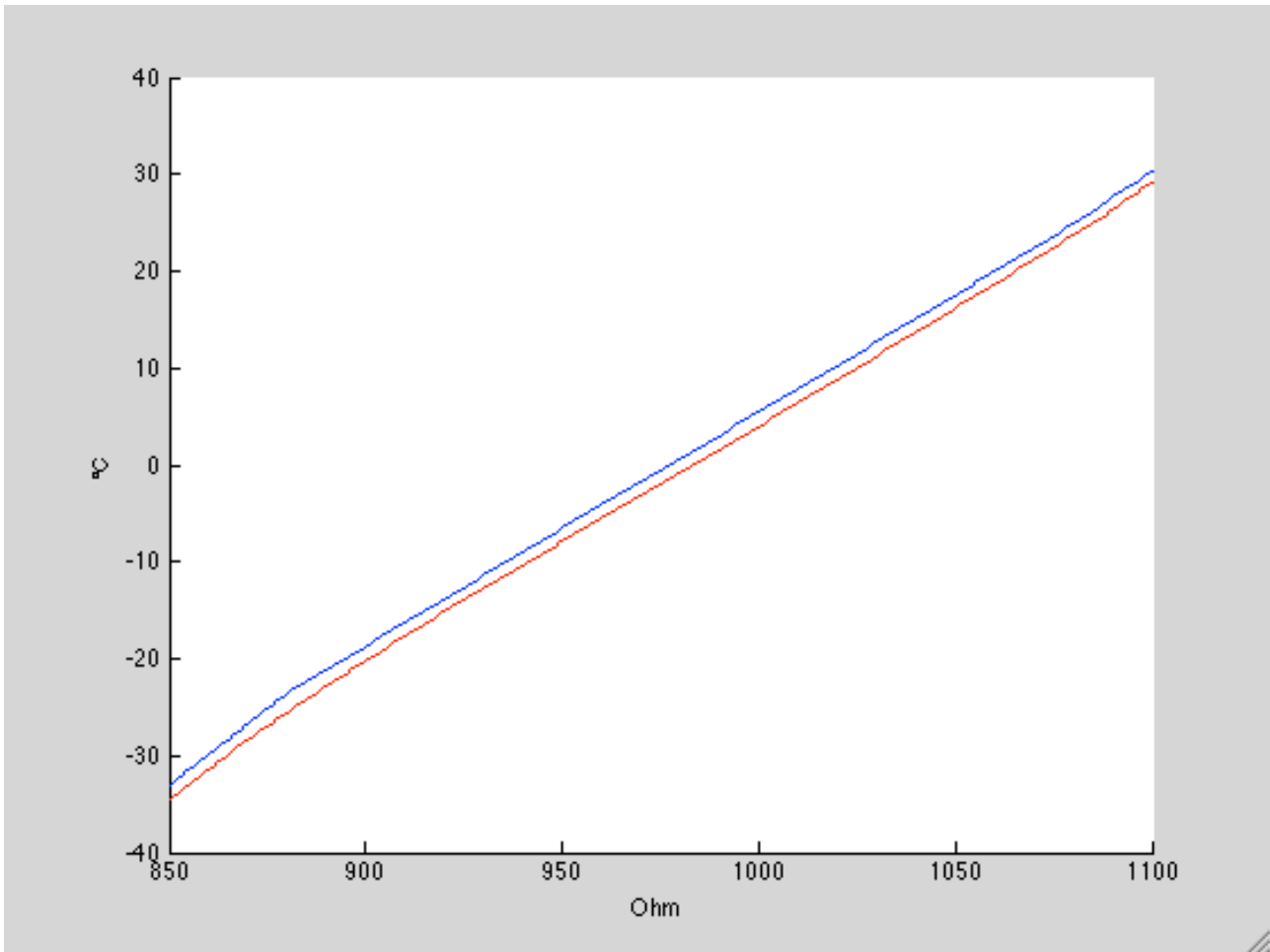
with T in °C.

The inverted functions with the proper solution for the quadratic functions is

$$T_{pt1} = \begin{cases} \frac{(R_1 - 959,7)}{3,171} & \text{for } R_1 < 869,3\Omega \\ \frac{4,622 + \sqrt{21,3629 - 0,0757 \cdot (985,7 - R_1)}}{0,0378} & \text{for } R_1 \in [869,3\Omega; 946,1\Omega] \\ \frac{(R_1 - 982,1)}{4,048} & \text{for } R_1 \in [946,1\Omega; 955,8\Omega] \\ \frac{4,207 + \sqrt{17,698 + 0,0243 \cdot (983,4 - R_1)}}{0,0122} & \text{for } R_1 \in [955,8\Omega; 1089,9\Omega] \\ \frac{(R_1 - 997,7)}{3,504} & \text{for } R_1 > 1089,9\Omega \end{cases}$$

$$T_{pt2} = \begin{cases} \frac{(R_2 - 954,3)}{3,153} & \text{for } R_2 < 880,2\Omega \\ \frac{4,119 - \sqrt{16,9662 + 2,61 \cdot 10^{-4} \cdot (977,0 - R_2)}}{1,3050 \cdot 10^{-4}} & \text{for } R_2 \in [880,2\Omega; 947,8\Omega] \\ \frac{(R_2 - 976,3)}{4,021} & \text{for } R_2 \in [947,8\Omega; 950,2\Omega] \\ \frac{4,159 - \sqrt{17,2973 + 0,0103 \cdot (977,3 - R_2)}}{0,0052} & \text{for } R_2 \in [950,2\Omega; 1086,1\Omega] \\ \frac{(R_2 - 984,6)}{3,816} & \text{for } R_2 > 1086,1\Omega \end{cases}$$

where the units are Ω and $^{\circ}\text{C}$ (and I have omitted writing units on the numbers).

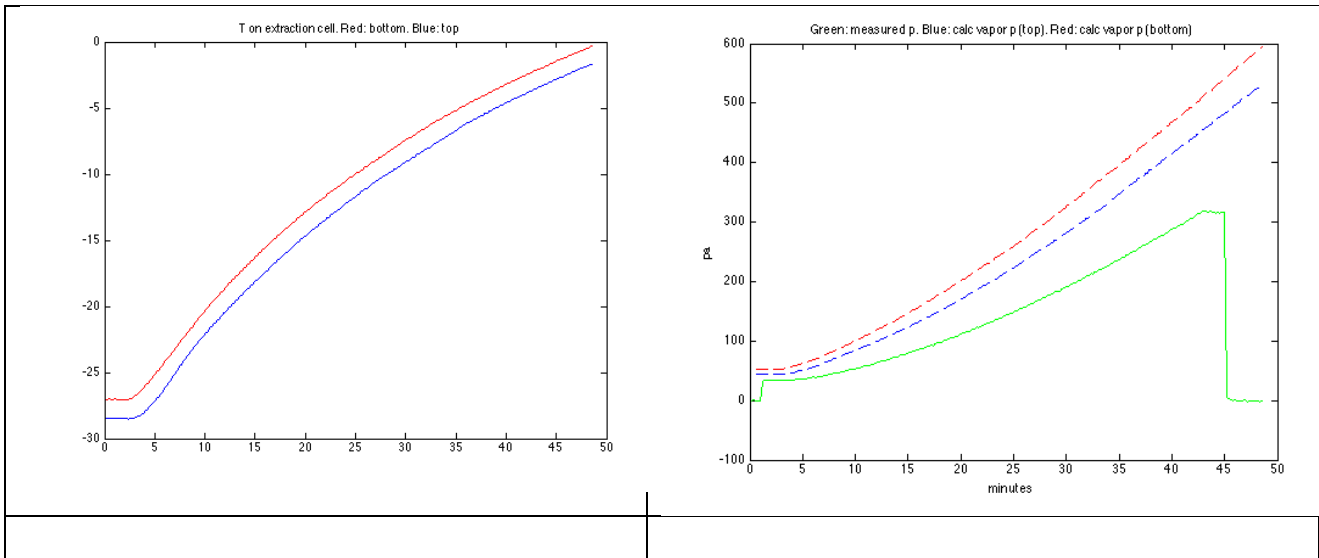


Figur 36. Pt1000-sensor1 (red) and sensor 2 (blue). Established non-linear temperature-functions. (matlab-functions pt1R2T og pt2R2T).

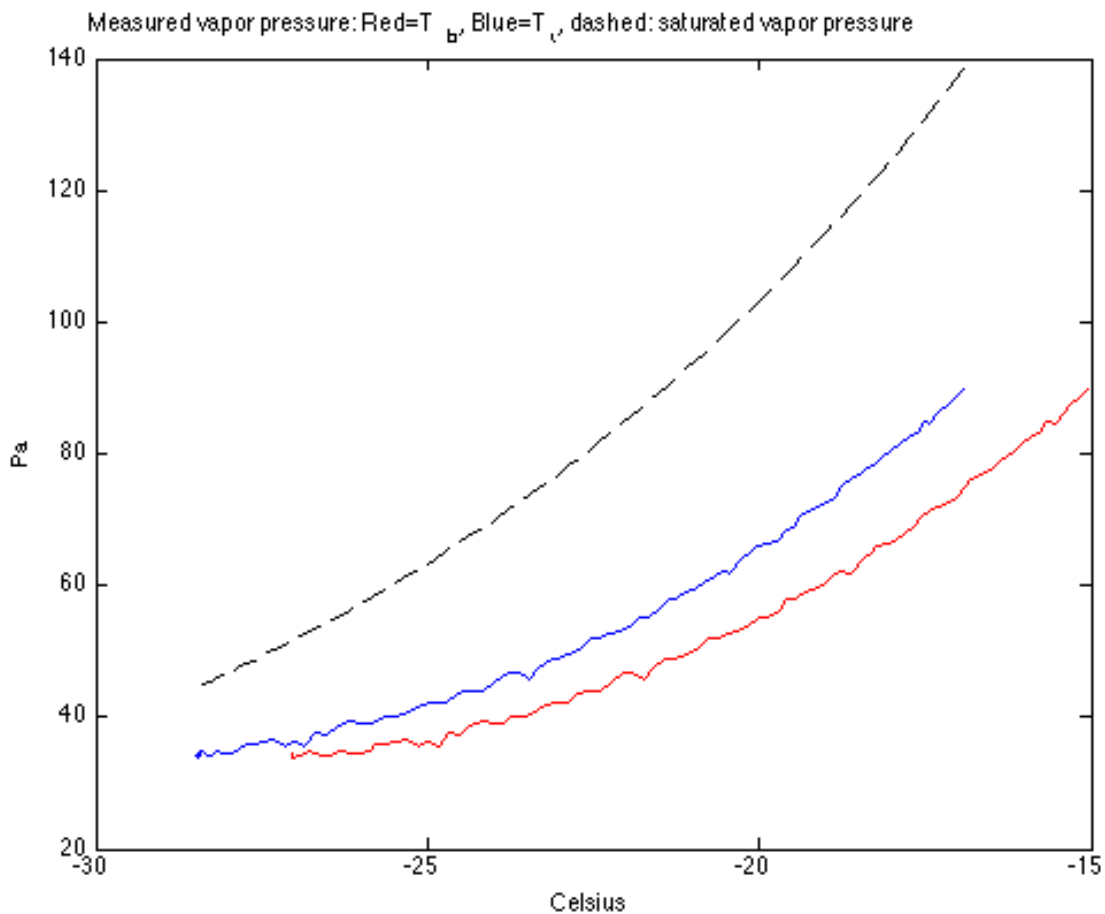
Measuring the saturated vapour pressure – test of the pt1000 calibration. A possible better way of calibrating

To examine the partial pressure of vaporised ice, measurements are taken with frozen demineralised water in the extraction chamber. The water is cooled to a stable temperature and the chamber is evacuated. Valve 7 is opened and the chiller is turned off to let the chamber heat up slowly. On Figur 37 and Figur 38 is shown the temperatures and measured pressure as well as the from eq 1 calculated saturated vapour pressure. It is seen that the measured pressure is below the calculated and the difference increases as the chamber heats; the ice inside is colder than the outer chamber walls where the temperature is measured during heating of course, but already from the beginning a difference of 10 Pa is seen, so we might overestimate the partial vapour pressure by using the saturation formula. The initial vapour pressure shown here occurred few seconds after evacuation. This experiment shows that the temperature sensors

are calibrated wrong. I discover this too late. If I had discovered it earlier I would have used this experiment as a calibration of the temperature sensors rather than a test of the calculated vapour pressure as I original thought it should be.



Figur 37. Left tempertures on extraction cell. Right: measured pressure (green), and calculated saturated vapor pressure (red: T_bottom, blue: T_top).



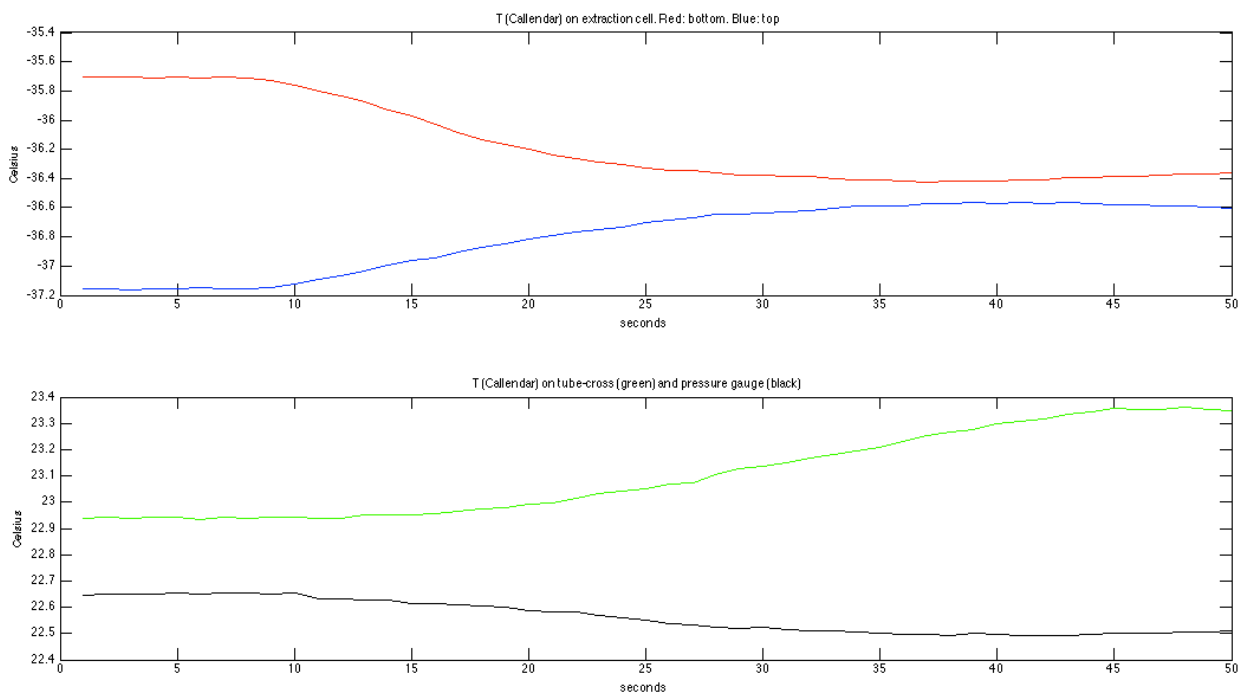
Figur 38. Measured vapor pressure at different T with ice in the evacuated chamber. Red: T at chamber bottom, Blue: T at chamber top, dashed: saturated vapor pressure over ice (eq 1)

Rejecting the sensor calibration

First after some measurements on ice samples I realized that calculating temperatures using the standard Callendar formula is closer to the real temperature than using the formulae derived from calibration (horrible). I compare the tube temperature with an old fashioned quicksilver thermometer placed on the tubes. The temperature on the extraction cell is tested by measuring it as it is cooled to below -30°C with ice inside; after evacuation I measure a pressure assumed to be the saturated vapour pressure (over ice) for the in the chamber given temperature and calculate the temperature from the inverted vapour pressure formula. It seems that the calibrated formulae overestimate the temperature in both extraction chamber and tubes by $3\text{-}4^{\circ}\text{C}$. In the opposite the standard formula is in agreement within 1°C . I recalculate all pt1000 measurement with the standard formula and rely on that from now on.

Stability of electronics

We test the stability of the temperature measurement regarding changes in the room temperature. The sensors are attached to their respective places; the extraction cell is cooled to a stable temperature (-37,1°C). A hair dryer is used on the electronic (Figur 11) for circa 20 seconds. A quicksilver thermometer placed in the air stream showed temperature increase from 22,5°C to 50°C during the 20 seconds. The sensors were shielded with isolating material and it was assumed that their temperatures were constant during this test. Even the less we see changes (both positive and negative) of up to 1 °C in all sensors (Figur 39), caused by changing of the resistor characteristics. The room temperature is often relatively stable around 23°C, but in the afternoon the sun comes in through the westward window and can disturb measurements. In an eventual development of the setup it must be considered to secure a stable temperature in the electronics, but for room temperatures of 23°C ± 3°C, I will from this experiment assume no influence on the measurements.



Figur 39. Stability test of the temperature measurements. Above: T on extraction cell, below: T on tubes and pressure gauge. The sensor temperatures are assumed constant while temperature on the electronic is changed by 30°C.

Pressure measurement

The pressure is measured by an electric instrument of the model BADR Lektra. It measures the pressure difference between two air inlets. The differential pressure can be read on a display with a resolution of 1 Pa. The accuracy is claimed to be 0,075% of 1000 Pa, that is 7,5 Pa. The range is -1300 Pa to +1200 Pa; outside this range it will not measure. This gives the possibility of measuring absolute pressures up to 2500 Pa, by first trapping air in V_{neg} the closed volume at the minus side inlet so that the pressure here is 1300 Pa (this can be measured by evacuating the plus side). In practice it is easy to trap an amount of air by relative quick series of valve work so that the pressure stabilizes at a point in the range 1100 to 1300 Pa. Then pressures up to 2300 Pa can be measured.

The gauge is supplied by 24 V, and its analogue output is obtained by the supply current which is in the range 0-24 mA depending on the pressure difference between the air inlets. The gauge needs a load resistance of 250 Ω serial connected in the supply circuit. To give the best resolution regarding the data loggers, the load resistance is divided in 2 by resistors of 209,89 Ω and 39,59 Ω and the voltage is measured and logged across the 39,59 Ω resistor. The voltage is then in the interval ± 1 V. The pressure gauge also has a display from which the pressure is written with a pen for all point wise measurements.

The pump

The pump is a Pfeiffer and should give a vacuum of 10^{-3} atm. That is 100 Pa, which actually is a non-negligible amount in this setup. It must be assumed that there is a background pressure, p_B , where parts of the line has been evacuated. Since the pressure is measured differential it is not possible to measure this background pressure directly. An attempt to measure it has been done by evacuating the whole line, closing the valves to V_{neg} and V_1 and then cooling the extraction chamber. The pressure fell by only 2 Pa for a temperature decrease of 30 K from which I believe that p_B is less than 40 Pa and could be even smaller since the pressure reduction could partly be caused by vapour condensation. Since all pressure measurements is taken as the differential pressure, the size of p_B will not affect the measurements, as long as it is stable. Closing V_{neg} and pumping continuously on V_{pos} can test this. If the pump is not stable, we will then see p_B fluctuating. I have never observed such effects and must assume that the pump is extremely stable, and that p_B varies less than 1 Pa over long time spans. Hence p_B can be neglected from now on as it will always cancel out of the equations containing p.

Calibration of the pressure gauge

It appeared to be necessary to calibrate the pressure gauge, which a small air-switching test showed:

- 1) Trap dry air in V_{neg} (or V_{pos}) and evacuate V_{pos} (or V_{neg}). Read of Δp_1 .
- 2) Fill V_{pos} (or V_{neg}) until Δp is close to zero. Read of Δp_2 .
- 3) Evacuate V_{neg} (or V_{pos}). Read of Δp_3 .

Then $\Delta p_3 - \Delta p_1 = \Delta p_2$. But the readings from the gauge deviate from this balance, as seen in 3 tests. We let Δp_L denote readings from the pressure gauge (L for Lektra) and the Pa_L ('Lektra-Pascal') be the unit given from the producer calibration (initially supposed to be real Pa).

$\Delta p_{L,1}$ (Pa_L)	$\Delta p_{L,2}$ (Pa_L)	$\Delta p_{L,3}$ (Pa_L)	$\Delta p_{L,3}$ (expected from producer calibration)	a^+/a^-	$\Delta p_{L,3}$ calculated from calibration with Vaisala (Pa_L)
-863	195	1029	1058	1,0348	1029,0
1029	16	-1049	-1013	1,0355	-1048,3
-1049	6	1020	1055	1,0345	1019,7

Tabel 3. Test of the Lektra pressure gauge as described above. The fourth column would equal the third if the readings was a linear function of the pressure difference as expected from the producer calibration.

This shows that the reading is a nonlinear function of the real pressure difference.

To calibrate it a Vaisala barometer is borrowed from DMI. The barometer is a type used for DMI standard observations. It has resolution 0,01 hPa. It was calibrated by DMI in the range of atmospheric pressure and has a precision of 0,05 hPa.

The Vaisala was connected to a plastic bottle that again was connected to the line. Ambient air was let in so that there was atmospheric pressure in the whole system, and then it was closed. V_{neg} was then closed (valve 1 closed and trapping a reference pressure, p_{ref} , in V_{neg}), so variations in the pressure would occur at V_{pos} and at Vaisala simultaneously. The pressure is read of Vaisala (p_V) and we must establish the relation between $p_V - p_{ref}$ and Δp_L . With a screw clamp on the

bottle the common pressure was regulated (Figur 40). It was possible to reach sufficiently stable pressures for sufficiently long timespans in this way, though fluctuations of up to 5 Pa was unavoidable since at temperature change in the flask of 0,1K correspond to a pressure change of circa 33 Pa. Therefore the whole calibration must be done relatively quickly since small temperature changes in V_{neg} will cause to big errors. A calibration was done in 16 minutes. The reference pressure in V_{neg} was taken and controlled by establishing a differential pressure close to 0 ($\Delta p_L=0$) first and last during the calibration. First $\Delta p_L=2 \text{ Pa}_L$ and $p_V = 1003,70 \text{ hPa}$. Last $\Delta p_L = 1 \text{ Pa}_L$ and $p_V = 1003,60 \text{ hPa}$.

Since 1 Pa_L is very close to 1 Pa (as seen on Figur 42), we can assume that: First $p_{ref} = 1003,68 \text{ hPa}$ and last $p_{ref} = 1003,59 \text{ hPa}$. The room temperature was near 23°C (see Figur 41) and a temperature change (decline) in V_{neg} of $0,027^\circ\text{C}$ would actually cause such a change of 9 Pa in p_{ref} . The temperature was not measured directly on V_{neg} but on the Lektra gauge and the tubes at V_1 (Figur 41). Changes of less than $0,06^\circ\text{C}$ is seen to occur, but the to sensors are ambiguitic about the sign. A completely stable temperature in a room with electric machines and humans producing energy is not possible. Under these circumstances I have assumed $p_{ref} = 1003,63 \text{ hPa}$ during the calibration and an uncertainty of 10 Pa.

The readings from the 2 gauges are shown on Figur 42 and the 1-1 correspondence shown as a dashed line. Though a good linearity is seen, we must seek a better relation that can explain the test in Tabel 3. We try to split the measurements for $\Delta p_L > 0$ and $\Delta p_L < 0$. There could be a reason for that since inside the gauge a sensible diaphragm is bended one or the other way with respect to the pressure difference. The result is shown on Figur 43 and Figur 44. From this we conclude the following on how the Lektra is used for measurements:

Let air be trapped in V_{neg} to a reference pressure $p_{ref,L}$ (negative sign) and the reading from Lektra is Δp_L . The pressure at V_{pos} is then given by

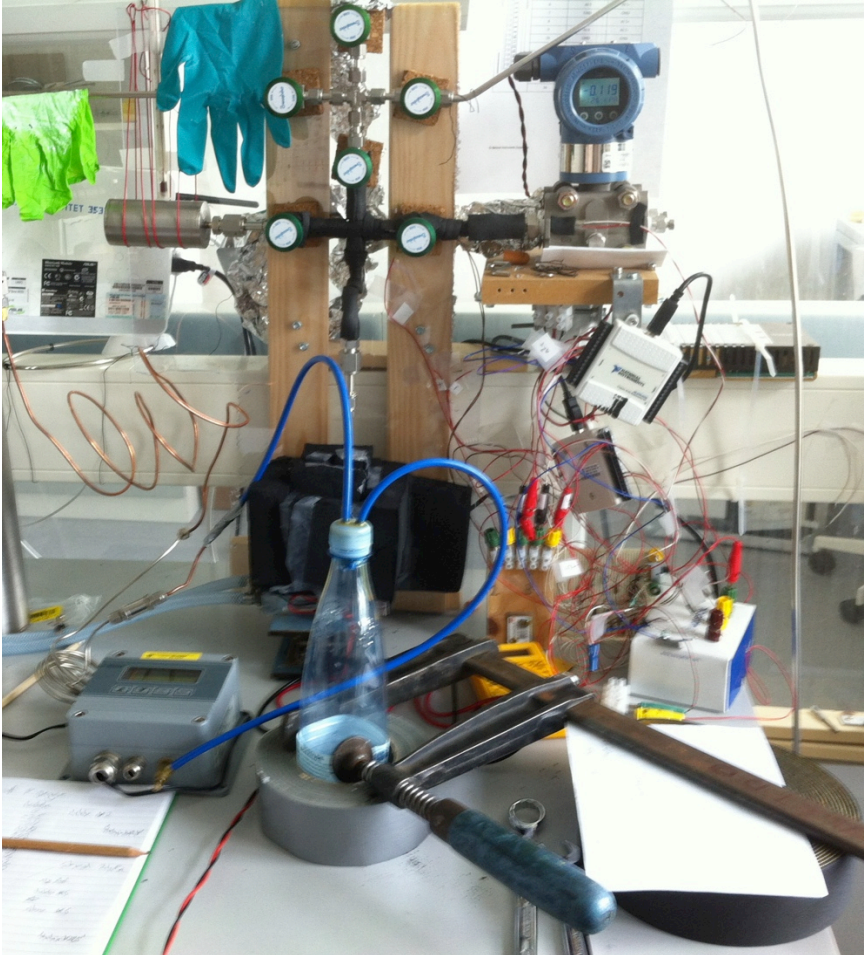
$$p = \begin{cases} 1,0255 \frac{\text{Pa}}{\text{Pa}_L} \cdot (\Delta p_L - p_{ref,L}) & \text{for } \Delta p_L \leq 0 \\ 1,0255 \frac{\text{Pa}}{\text{Pa}_L} \cdot (-p_{ref,L}) + 1,0612 \frac{\text{Pa}}{\text{Pa}_L} \cdot \Delta p_L & \text{for } \Delta p_L > 0 \end{cases} \quad (\text{eq 10})$$

eq 10

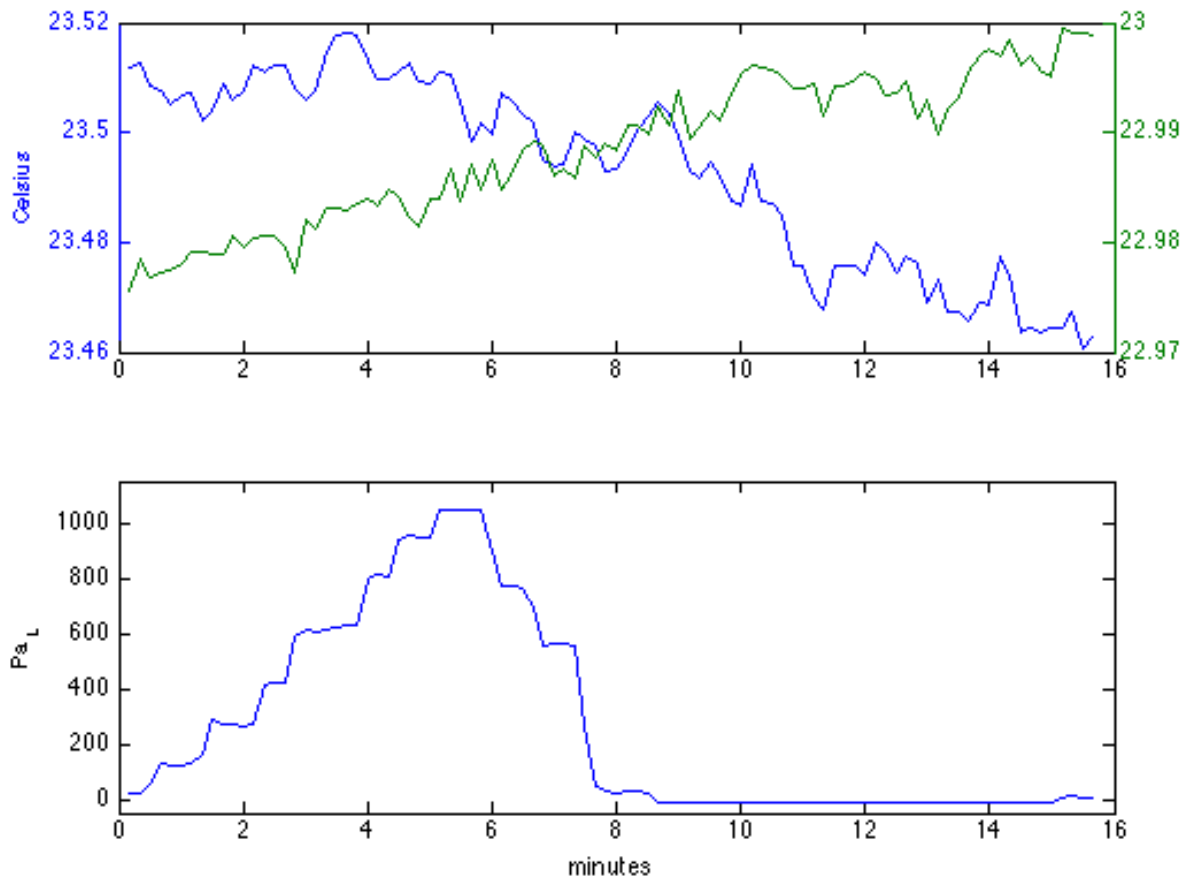
To test this we look at the measurements in Tabel 3. If a is split in a^- and a^+ as in eq 10, we can calculate the ratio a^+/a^- since it must hold that:

$$a_3 \Delta p_{L,3} - a_1 \Delta p_{L,1} = a_2 \Delta p_{L,2}$$

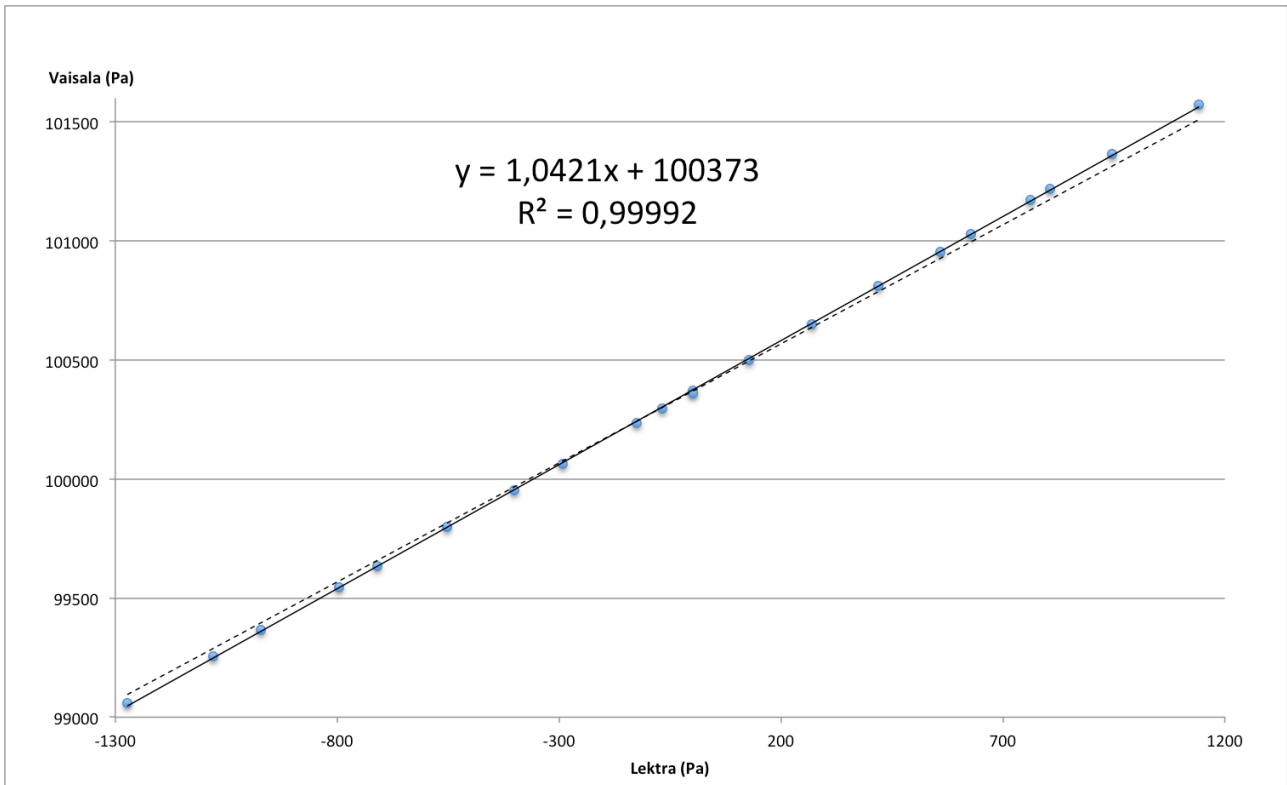
where the a 's are either a^+ or a^- according to the sign of their Δp_L . The a^+/a^- ratios is shown in the table and are very close to $1,0612/1,0255=1,0348$. Further we can test eq 10 by calculating Δp_1 and Δp_2 from $\Delta p_{L,1}$ and $\Delta p_{L,2}$ and then $\Delta p_3 = \Delta p_1 + \Delta p_2$ and then use the inverted eq 10 to calculate $\Delta p_{L,3}$. Comparing this to the measured $\Delta p_{L,3}$ shows a high agreement as shown in Tabel 1.



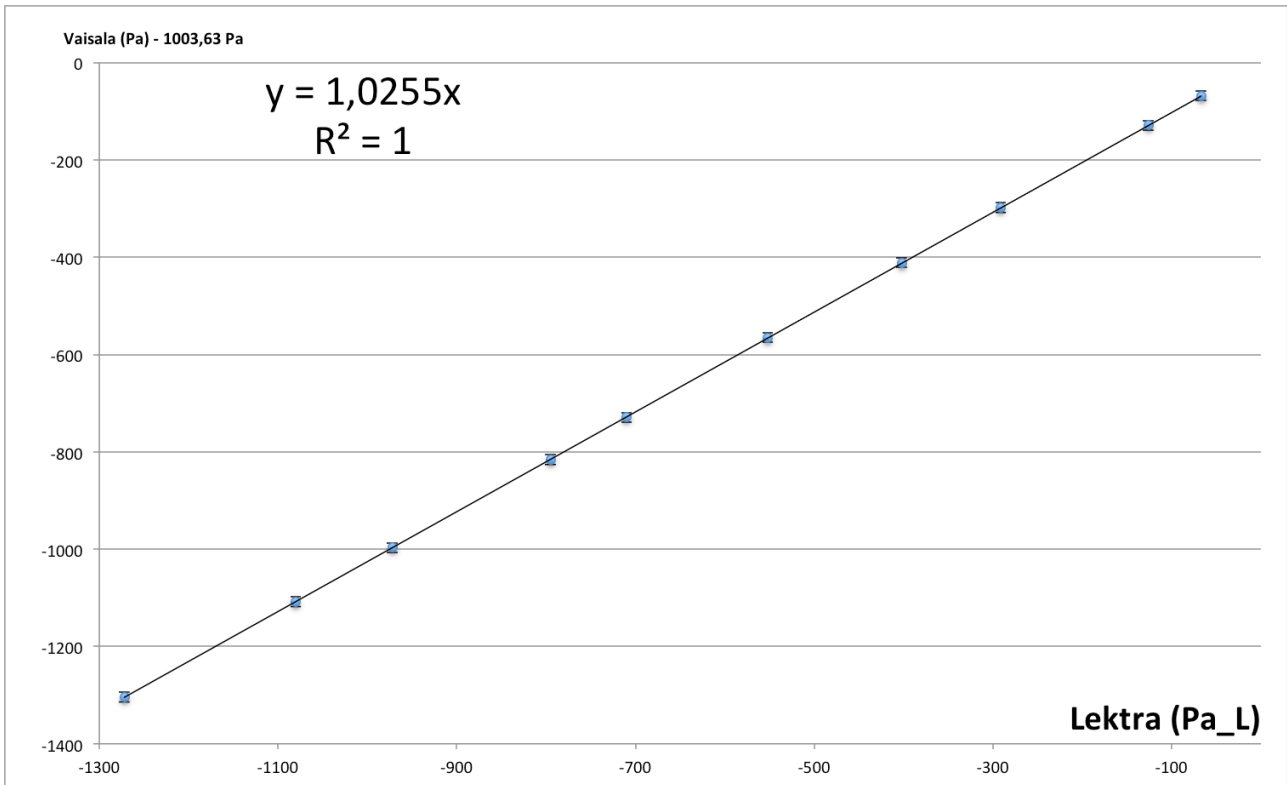
Figur 40. Calibration of the Lektra pressure gauge (upper right) with the Vaisala Barometer (lower left) and a plastic bottle.



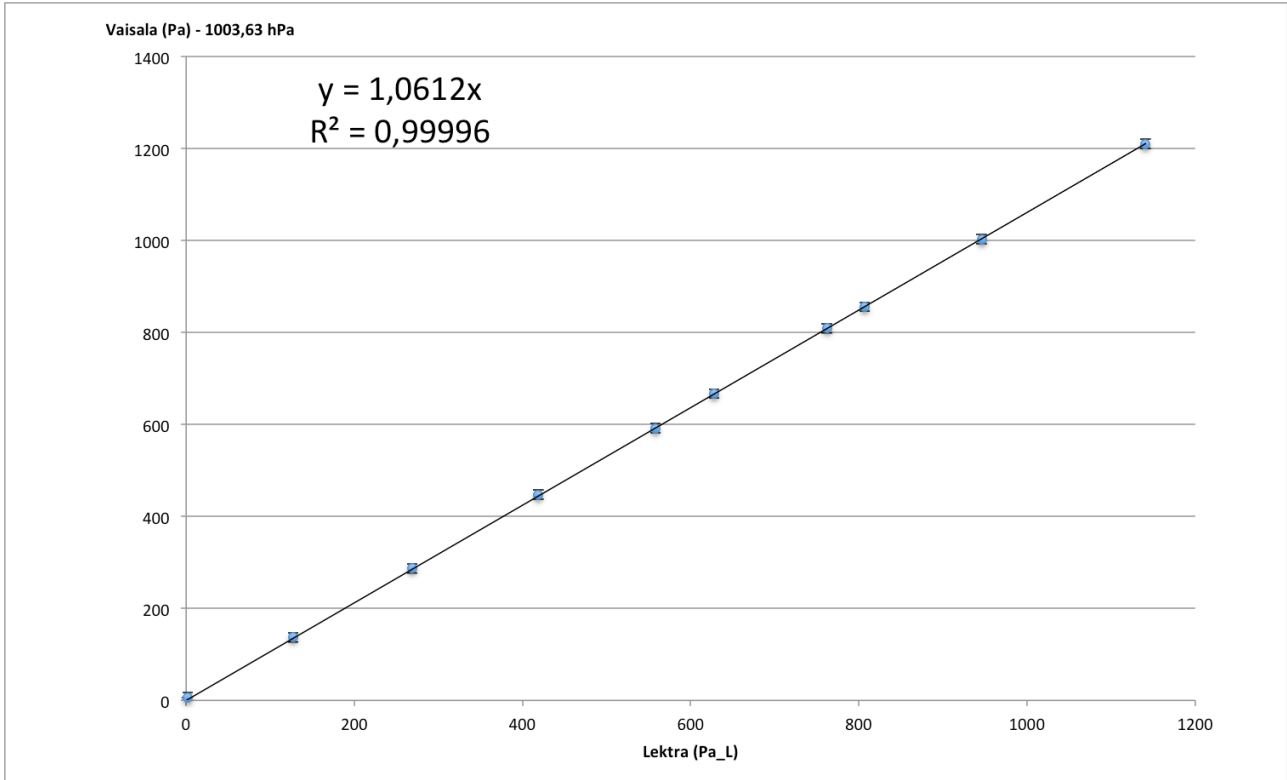
Figur 41. Upper: Blue declining (left scale): Temperature on cross, green rising (right scale): temperature on Lektra gauge. Lower auto logging of Pa_L (not positive for negative pressure differences)



Figur 42. Readings of the Lektra gauge (differential pressure with a reference pressure of 1003,63 hPa) against the Vaisala (full pressure). Error bars are set with ± 10 Pa (same size as the point markers). The dashed line shows the 1-1 correspondence that would hold if Lektra was perfectly calibrated (assuming Vaisala is perfectly calibrated).



Figur 43. Reading of $p_v - p_{ref}$ against Δp_L . Regression line is forced to intersect (0,0) or it would intersect in 0,7 Pa. Error bars show ± 10 Pa.



Figur 44. Reading of $p_v - p_{ref}$ against Δp_L . Regression line is forced to intersect (0,0) or it would intersect in 1,2 Pa. Error bars show ± 10 Pa.

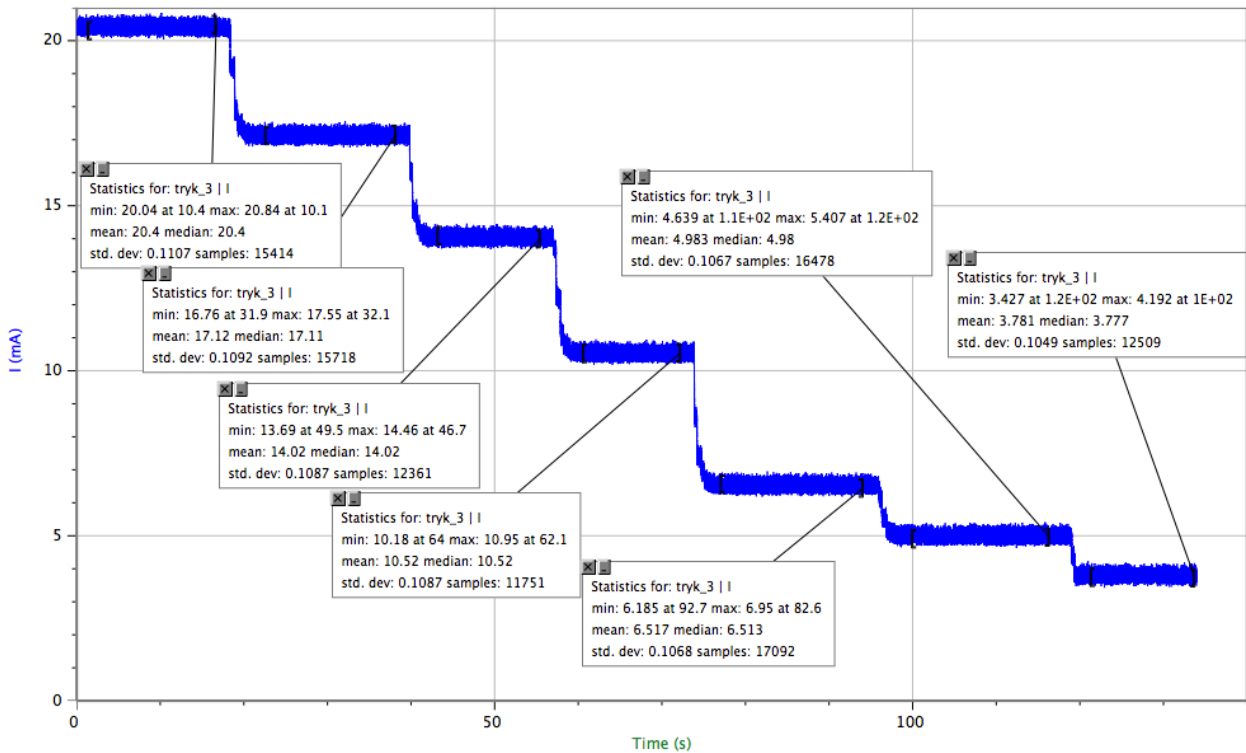
Automatic logging with the pressure gauge

The relation between input current and pressure is obtained by making a series of different stable pressures, measuring and noting the display pressure (see figures below). For each stable pressure 10000 to 20000 samples were logged, and the mean calculated. In each case the standard deviation was in the interval [0,10 mA to 0,12 mA], so the error is less than $\frac{0,12 \text{ mA}}{\sqrt{10000}} = 0,0012 \text{ mA}$, which is within the size of the accuracy determined by the data logger (see below). The current is calculated from the measured voltage, plotted against the display values and a regression function is obtained (see figure below). From this the current-pressure-relation is found to be

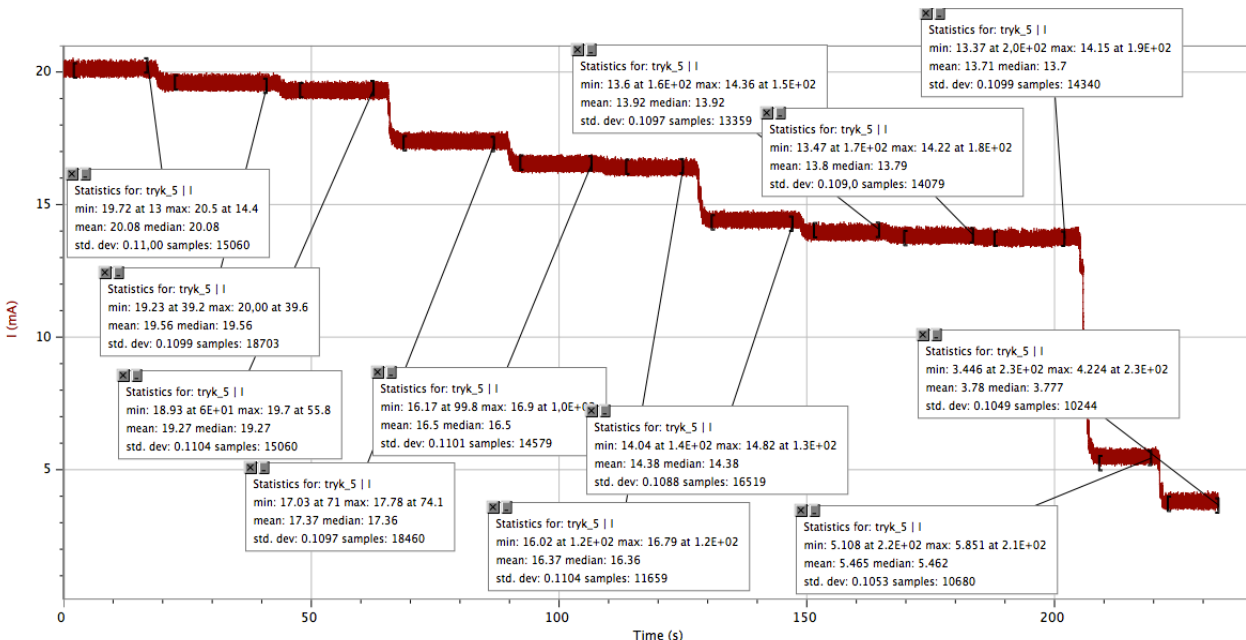
$$p = 62,5 \frac{\text{Pa}}{\text{mA}} \cdot I - 249,4 \text{ Pa}$$

where I is given in mA. On the figure is seen that the data points begin to depart from the regression line when the pressure rises above 1000 Pa and for pressures below 0 Pa. These points are excluded from the regression, and the relation can assume to hold only for pressures in the range +60 Pa to +960 Pa. Does the precision of the data logger hamper the precision of the pressure measurement? Since the accuracy on the data logger is 1,53 mV, the accuracy on the I-measurement is $\frac{1,53 \text{ mV}}{39,59 \Omega} = 0,039 \text{ mA}$, which in turn gives an accuracy on p of 2,4 Pa which is lower than the 7,5 Pa of the pressure gauge itself.

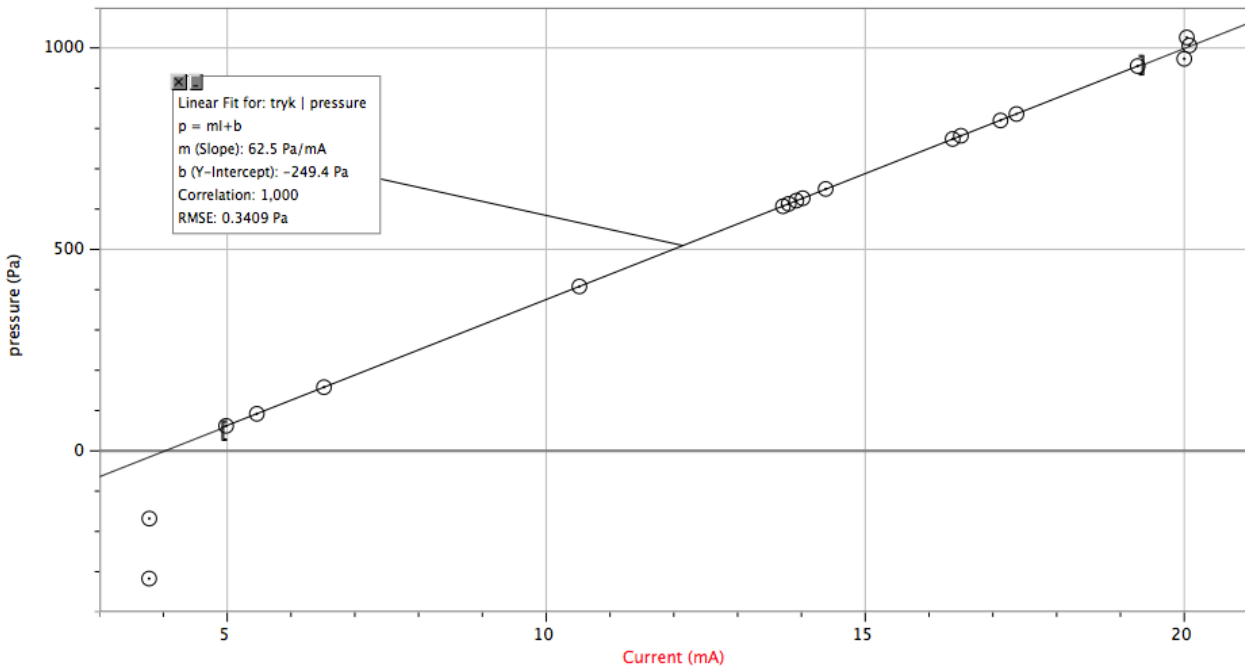
Of course pressure directly as a function of the measured voltage could be made, but I prefer a current-pressure relation that should hold also in case of a later change in the load resistance. A somewhat annoying property or lag of property of the instrument is that the current is only variable when the pressure difference is positive, so there is only possibility of logging the pressure in the positive interval, though pressures in the negative range can still be read of the display.



Figur 45. Establishment of the p-I relation of the pressure gauge. The display readings for the steps in Pa are: 1026, 820, 627, 408, 158, 62, -317. (file: pressuregaugecalibration.cmb1)



Figur 46. Establishment of the p-I relation for the pressure gauge. The display readings for for steps in Pa are: 1006, 973, 955, 836, 782, 774, 650, 621, 613, 607, 92, -168. (fil: pressuregaugecalibration.cmb1)



Figur 47. Linear regression of the means of the steps shown on the previous figures. Only points with pressures in the range [60 Pa, 960 Pa] is included in the regression. (fil: pressuregaugecalibration.cml)

Dimensions of the setup

We need a precise measurement of the main volume, V_M , in which the air is trapped, that is the full volume of the extraction chamber, V_{ex} , the connection tubes and the inner volume of the pressure gauge, V_{tub} , (see diagram). Further we need the measure off an appendix volume, V_{app} , needed under certain circumstances. The dimension of the extraction chamber was thought to be as small as possible, that is, to fit an ice sample with the smallest possible excess space. This will give the highest possible pressure to measure from the trapped air and following the smallest uncertainty on the measurement. As the ice samples was considered to be cubes with side length 3 cm, it was decided that the inner dimension of the extraction chamber should be 32mm x 32mm x 32mm = 32,768 cm³ to fit the ice samples. The actual volume can be estimated to be a bit smaller than this for two reasons: 1) On the floor of the chamber there are soldered 3 small spikes, on which the ice sample can rest, to avoid trapping laboratory air beneath the ice, and 2) the corners are rounded. The first estimate of the volume is therefore 32 cm³ at room temperature. Further we must correct this volume for contraction of aluminium when it is cooled to minus 30 degrees.

The thermal expansion coefficient for aluminium is $2,3 \cdot 10^{-5} \text{ K}^{-1}$. It follows that an aluminium box of $32,768 \text{ cm}^3$ at $25 \text{ }^\circ\text{C}$ will shrink with $0,12 \text{ cm}^3$ when cooled to -30°C . Since the precise calibration of the volume is conducted at room temperature this correction must be applied when measurements are conducted at -30°C .

The tubes are $\frac{1}{4}$ " stainless steel; their inner diameter is $5,3 \text{ mm}$ which gives them an inner volume of $0,22 \text{ cm}^3/\text{cm}$. A first and not very accurate measure give that 64 cm tube connects the extraction chamber and the pressure gauge, that is $14,1 \text{ cm}^3$. Thereto come the dead volumes of the pressure gauge and the valves which could be a few cm^3 . A first estimate of the volume V_M is therefore close to 50 cm^3 . Further calibration as shown in the following gives though $V_M = 60,52 \text{ cm}^3$ indicating that the inner volume in the pressure gauge was larger than expected. To match the accuracy of the pressure gauge ($0,075\%$), the volume V_M should be estimated with an accuracy of $0,05 \text{ cm}^3$

Valve corrections

All valves are hand operated bellow valves. The valves are closed by screwing the bellow into the inner space. This diminishes the inner volume. In a measurement with air trapped in V_M the pressure increased from $p_1 = 2335 \text{ Pa}$ to $p_2 = 2337 \text{ Pa}$ when a valve in the system was closed. Let the volume difference on open and closed be δV . Then $p_1 V_1 = p_2 (V_M - \delta V)$. Hence

$$\delta V = \left(1 - \frac{p_1}{p_2}\right) V_M$$

In this case $\delta V = 0,0856\%$ of V_M . That is $0,052 \text{ cm}^3$, which must be considered as a correction every time a valve is closed in a closed system.

Leak corrections

It is not easy to build a completely leak tight set up. After this setup was built small leaks different places were detected and some tubes and connection had to be shifted. Before measurements the ice samples must be left 4 hours in the evacuated V_{ex} , melting and refreezing, and it is important that leaks cause minimal errors. In the end acceptably small leaks survived in the system and their sizes were estimated by evacuating the whole system for 22 hours, closing all valves, leaving it for 25,5 hours and finally open valves and evacuating the different volumes one by one keeping track of the pressure change. Following pressure rises were detected:

V_{neg} : 1 Pa
 V_{center} : 0 Pa
 V_{pos} : 5 Pa
 V_{app} : 0 Pa
 V_{ex} : 15 Pa

Especially V_{app} and V_{cyl} has proven to be very leak tight and even left closed for more than a week, no pressure was measure in these volumes.

The only leak that must be corrected for is the leak in V_{ex} that gives rise to a pressure increase of 0,59 Pa/hour. For all samples the time from closing valve 7 to the pressure measurements must be noted and the partial pressure from the intruded air subtracted. Since the test was done in room temperature the partial pressure would be lower when V_{ex} is cooled to -35°C. On the other hand the ice sample reduces the air space in V_{ex} giving the leak air intrusion a higher partial pressure. From (eq 13) the proper correction would be in the range

0,59 to 0,79 Pa/hour for the size of ice used. I will choose to correct all measurement with 0,7 Pa/hour. That is usually not much more than a correction of 2 Pa on a sample measurement which is less than 0,3% even for the smallest ice samples worked with.

The leaks in V_{pos} and V_{neg} are negligible; V_{pos} can be evacuated right until the pressure measurement. The measurement itself takes 5 minutes and leaks can be neglected during this short time space.

Volume calibration

To measure or calibrate the volume, V_M , with highest possible accuracy, I follow a method from (Lipenkov, 1995). Another and larger volume, V_{cyl} , is fabricated (a steel cylinder), so that we have to unknown volumes V_M and V_{cyl} . The 2 volumes are connected with valve2. Then V_M is filled with dry air to ambient pressure, p_a , while V_{cyl} are evacuated. Now $p_a V_M = nRT$. Then the valve is opened, the air is expanded to fill out the complete volume $V_M + V_{\text{cyl}}$ and the pressure, p , is measured. Assuming that the temperature is constant, we have $p_a V_M = p(V_M + V_{\text{cyl}})$. Since there is two unknown in this equation it only gives the relation between the two volumes – not the exact values. We need at least one more equation. To that end we do the same measurement again, but now with a steel ball inside the extraction cell. If the volume of the ball is B_1 we have

$$p_a(V_M - B_1) = p(V_M - B_1 + V_{cyl}) \quad (\text{eq 11})$$

eq 11

Now we get an exact solution of V_M and V_{cyl} . Even more measurements with balls of different sizes, B_1, B_2, \dots can be introduced in further measurements to refine the calibration of V_M .

The extraction chamber as well as the calibration cylinder was fabricated in the institute workshop.

The pressure gauge sets a limit on the measure range since its ranges is ± 1200 Pa. Therefore the calibration cylinder must have a volume that gives pressures in this range when air at atmospheric pressure (970 hPa to 1050 hPa was considered as a possible range for atmospheric pressure) in the extraction cell is expanded into the cylinder.

From the size of the extraction cell plus the estimated volume of the connection tubes, it was estimated, that the calibration cylinder volume had to be around 2700 cm^3 in order to do the calibration procedure as described. Finally the cylinder has height = 34 cm and diameter = 10 cm, which gives the volume 2669 cm^3 (or between 2617 cm^3 and 2727 cm^3 if I assume an uncertainty on the diameter of 1 mm). The rest of V_2 constitutes of approximately 64 cm tubes $\sim 14 \text{ cm}^3$ + dead volumes in valves. So the first estimate of V_2 is about $2685 \pm 70 \text{ cm}^3$. This gives expected pressure measurements in the range $0 \text{ hPa} < p < 19 \text{ hPa}$, during the described calibration procedure, which is in the range of the pressure gauge.

Dry air for the calibration is made by drying laboratory air. (see figure) The air is taken through a filter ($0,5\mu\text{m}$) and down in a tube folded to a coil. Coil and filter is placed in a Dewar with liquid nitrogen in the bottom covering the coil but not the filter. The tube proceeds up through the dewar lid, forms another coil outside and ends in the line connected to V_1 by valve 5. When valve 5 is open air is sucked through the filter – I assume that this air consists mainly of evaporated N_2 with a low vapour content – cooled in the coil and condensing its vapour, leaving the dewar almost dry, heated in the coil outside the dewar to room temperature and going into V_M . Valve 5 is only slightly opened, so it takes several minutes to fill V_M . The air is then moving in very slowly, so it is assumed that it has been cooled to -196°C in the dewar and attained room temperature again before entering V_M . Another concern was that a too fast air stream could bring ice crystals suspended in the air with it into V_M . Between experiments air is sucked through the system (only through volumes V_B and V_D) with the coil removed from the Dewar to get rid of ice formed in the coil.

The ambient pressure was at first estimated by taken the sea level pressure at Kastrup Airport 10 km away, which is accessible and updated every 10'th minute on the DMI homepage; from this pressure was subtracted 300 Pa (since the CIC matrikel is located 12,5 meter above sea level and the laboratory is 10-12 meter above the ground). To this pressure estimate there was some misbelief: air condition in the laboratory would change the pressure in the room as well as draft in the building and wind gusts could make rapid variations; as the air in V_1 is sealed the second valve 5 is closed, the 10-minutes mean pressure could be erratic to use. The scale of rapid pressure variations in the room was tested by trapping air at room pressure in V_{neg} and letting valve 5 be open; during 2 minutes there was pressure fluctuations in the range 15 Pa. To get rid of these pressure worries, we borrowed a very precise (with resolution 1Pa and accuracy 10 Pa), electronic Vaisala barometer from DMI, which is read of in the same moment valve 5 is closed.

Also when valve 5 to the dry air inlet is closed the pressure rises. When it is open the pressure in V_M is assumed to be in equilibrium with the ambient pressure in the laboratory. I have closed and opened it several times and seen, that when it is closed the pressure in V_M rises with a value in the range 12 Pa to 30 Pa. (30 Pa when the valve is closed quickly and with 12 Pa when it is closed slowly.) This can only be measured when the pressure in V_{neg} is atmospheric, and therefore not in actual measurements. I must then close the valve slowly assume that a correction of 12 Pa should be added.

3 steel balls are used, B_{15} , B_{20} , and B_{25} with industrial standard sizes for the diameters 15 mm, 20 mm and 25 mm. The extraction cell can contain B_{15} and B_{25} at the same time. This allows for 6 different measurements: with empty extraction chamber, or with the chamber containing B_{15} , B_{20} , B_{25} , $B_{15}+B_{20}$ or $B_{15}+B_{25}$. The result is seen in Figur 48: the lines intersecting in one point defining the two unknown volumes. Since in the first attempts to calibrate the volumes the intersecting point was not exactly so sharp defined as wanted, I thought it could be caused by errors in the ball sizes. The balls were measured with a millimetre screw to give the same sizes with accuracy 0,0025 mm. Also they were weighed and the density is calculated according to the standard sizes. There exists different kinds of steel with different densities; the producer description of these balls did not inform the density, but I assume that their actual density are very similar so that a deviance in densities would reveal that some volumes deviate from their standard size. The ball volumes is thus described as $B = \tilde{B} + b$, where \tilde{B} is the standard volume and b is the apriori unknown deviance which is assumed to be limited as shown in Tabel 4.

Ball	Diameter (mm)	Volume (cm ³)		Mass (g)	density (g/cm ³)
		\tilde{B}	limits for b		
B ₁₅	15±0,0025	1,7671	±0,00088	13,785	7.8007
B ₂₀	20±0,0025	4,1888	±0,0016	32,643	7,7929
B ₂₅	25±0,0025	8,1812	±0,0025	63,796	7,7978

Table 4. Properties of steel balls use for volume calibration.

(eq 11) then takes the form

$$p_a(V_M - \tilde{B} - b) = p(V_M - \tilde{B} - b + V_{cyl})$$

or

$$V_M - b - AV_{cyl} = \tilde{B} \quad (\text{eq 12})$$

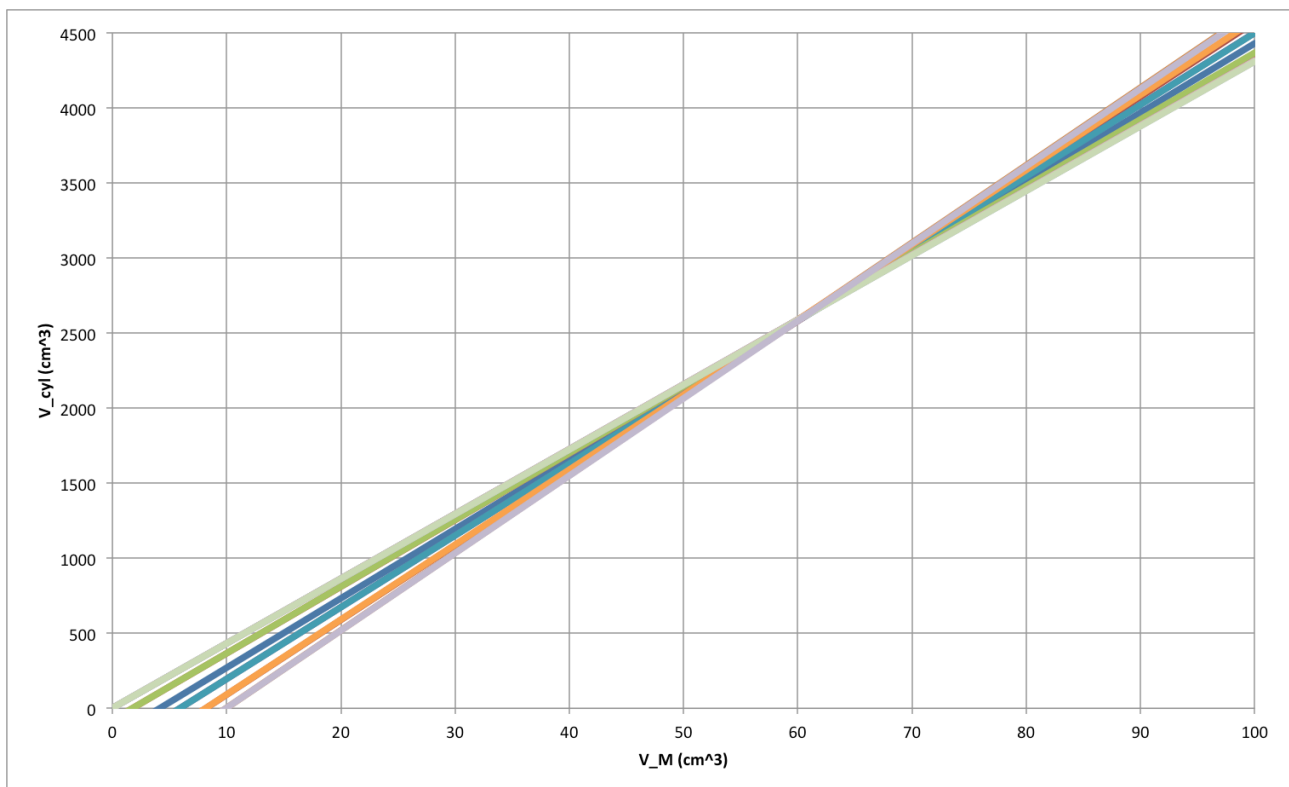
eq 12

where $A = \frac{p}{p_a - p}$ comes from pressure measurements. With different combinations of balls we get an over determined system of 6 equations with the 5 unknown volumes ($V_M, V_{cyl}, b_{15}, b_{20}, b_{25}$):

$$\left\{ \begin{array}{l} V_M - 0 - A_1 V_{cyl} = 0 \\ V_M - b_{15} - A_2 V_{cyl} = \tilde{B}_{15} \\ V_M - b_{20} - A_3 V_M = \tilde{B}_{20} \\ V_M - b_{25} - A_4 V_{cyl} = \tilde{B}_{25} \\ V_M - (b_{15} + b_{20}) - A_5 V_{cyl} = \tilde{B}_{15} + \tilde{B}_{20} \\ V_M - (b_{15} + b_{25}) - A_6 V_{cyl} = \tilde{B}_{15} + \tilde{B}_{25} \end{array} \right.$$

To check the reproducibility more than one measurement with each of these combinations are conducted. 14 independent measurements are shown on Figur 48. Zooming in on the intersecting point (Figur 49) we see that V_M is 60 to 61 cm³, but from the graph it is not possible to estimate it with the wanted precision of 0,05 cm³. Two of the lines deviate particular from the others and these two measurements are assumed to be erratic and will not be included in the volume estimation. Error intervals on one experiment are shown with dashed lines. They are calculated by assuming a precision of 30 Pa on the

ambient pressure, p_a , (10 Pa for the pressure gauge, 10 Pa for the correction on valve closing, and 10 Pa for pressure fluctuations in the room or height correction), and a precision of 7 Pa on the secondary measurement, p . It must be noticed that the error is mainly caused by the 7 Pa on p equivalating a relative precision of circa $7 \text{ Pa}/2000 \text{ Pa}=0,35\%$, whereas the relative precision on the ambient pressure is circa $30 \text{ Pa}/1000 \text{ hPa}=0,03\%$. It is seen that with the given errors the 2 deviating lines must be excluded as erratic, and the rest is confined in the error intervals (not shown but having the same size as the one shown).



Figur 48. Calibration of two volumes defined by the intersecting point of the lines from 14 independent measurements. The intersection with $V_{cyl}=0$ shows the composite volume of the steel balls.

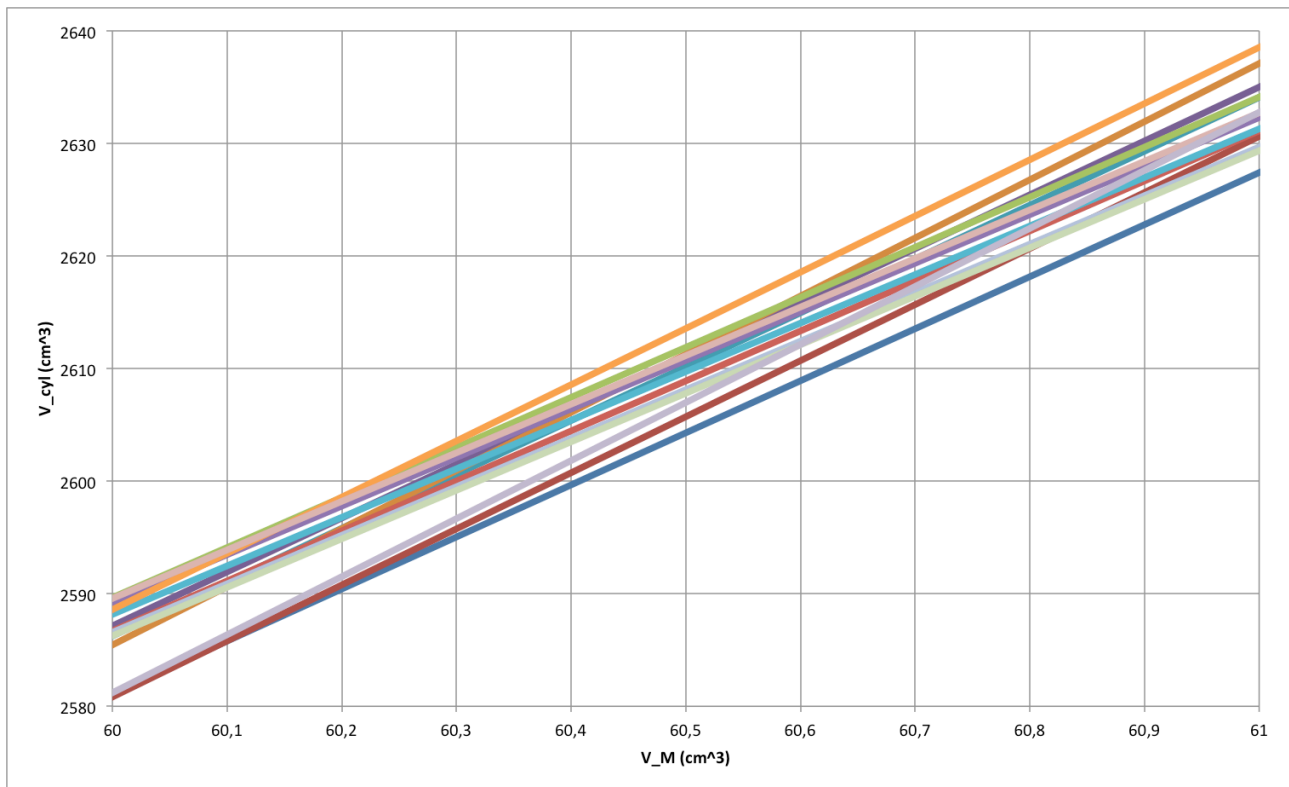


Figure 49. Calibrating V_M (and V_{cyl}) – zooming in on the intersecting point in Figure 48. The intersecting point cannot be read of directly with desired precision. A RMS solution gives $V_M=60,52 \text{ cm}^3$.

A RMS solution for the equation system and the 14 measurements gives:

$$V_M=60,52 \text{ cm}^3$$

$$V_{cyl}=2610,2 \text{ cm}^3$$

$$b1=0,00088 \text{ cm}^3$$

$$b2=-0,0016 \text{ cm}^3$$

$$b3=0,0025 \text{ cm}^3$$

This indicates that standard sizes for B1 and B3 are underestimated and B2 is overestimated. The densities that follows is 7,7968 7,7959 and 7,7955 closer to each other than the values calculated from the standard sizes, which makes these ball correction plausible.

The error on V_M is taken as the span for $V_{cyl}=2610,2 \text{ cm}^3$ ($0,2 \text{ cm}^3$) for the 14 measurements $\frac{0,2 \text{ cm}^3}{\sqrt{14}} = 0,05 \text{ cm}^3$ as desired.

Appendix Volume and additional calibration

For ice samples of 27 cm^3 as intended, the released air will induce a pressure out of our pressure gauge range (up to 3 times). To this problem we can think of 3

solutions: 1) we can gradually trap a sufficient amount of air in V_{neg} – first fill V_{neg} to -1000 Pa, then fill V_{pos} to +1000 Pa (then the pressure is 2000 Pa in V_{pos}), then fill V_{neg} to -1000 Pa (then $p= 3000$ Pa in V_{neg}) and so on until $p=5000$ Pa in V_{neg} . This of course gives risk of errors every time we fill, and it is not only annoying not to be able to measure the pressure p when we evacuate V_{ex} with ice sample inside, it is also impossible to detect pressure changes in V_{neg} due to temperature changes – the higher pressure in V_{neg} the bigger error will follow in the measurement with the same relative pressure change in V_{neg} . Consequently this method will only be used as a last alternative 2) We will only measure on sufficiently small ice samples. This has the drawback that the smaller amount of released air gives a relatively smaller accuracy, and further the cut bubble effect will be relatively larger with possibly larger errors. 3) Therefore we have got and appendix volume, V_{app} , produce. This volume is connected to V_M and can be select on or off by a valve. This volume is calibrated by filling dry air into $V_{app}+V_{tub}$ to a measurable pressure, p_1 , closing valve 5, evacuating V_M , opening valve 5 and expanding the air into V_M and measure the pressure, p_2 , again. This gives (for constant temperature during the process), that $V_M = \left(\frac{p_1}{p_2} - 1\right) V_{app}$. 12 measurements of this scheme were made with different content of calibration balls in V_{ex} (Figur 50). This could also be used as calibration of V_M but the uncertainty would be higher than the calibration above, and it is seen (Figur 50), that V_M would be slightly smaller than found from the calibration above. Instead we take the found $V_M=60,52$ cm² to calculate V_{app} (Figur 51). From the 12 measurements we get:

$$V_{app} = 118,28 \pm 0,07 \text{ cm}^3 \text{ given } V_M = 60,52 \text{ cm}^2$$

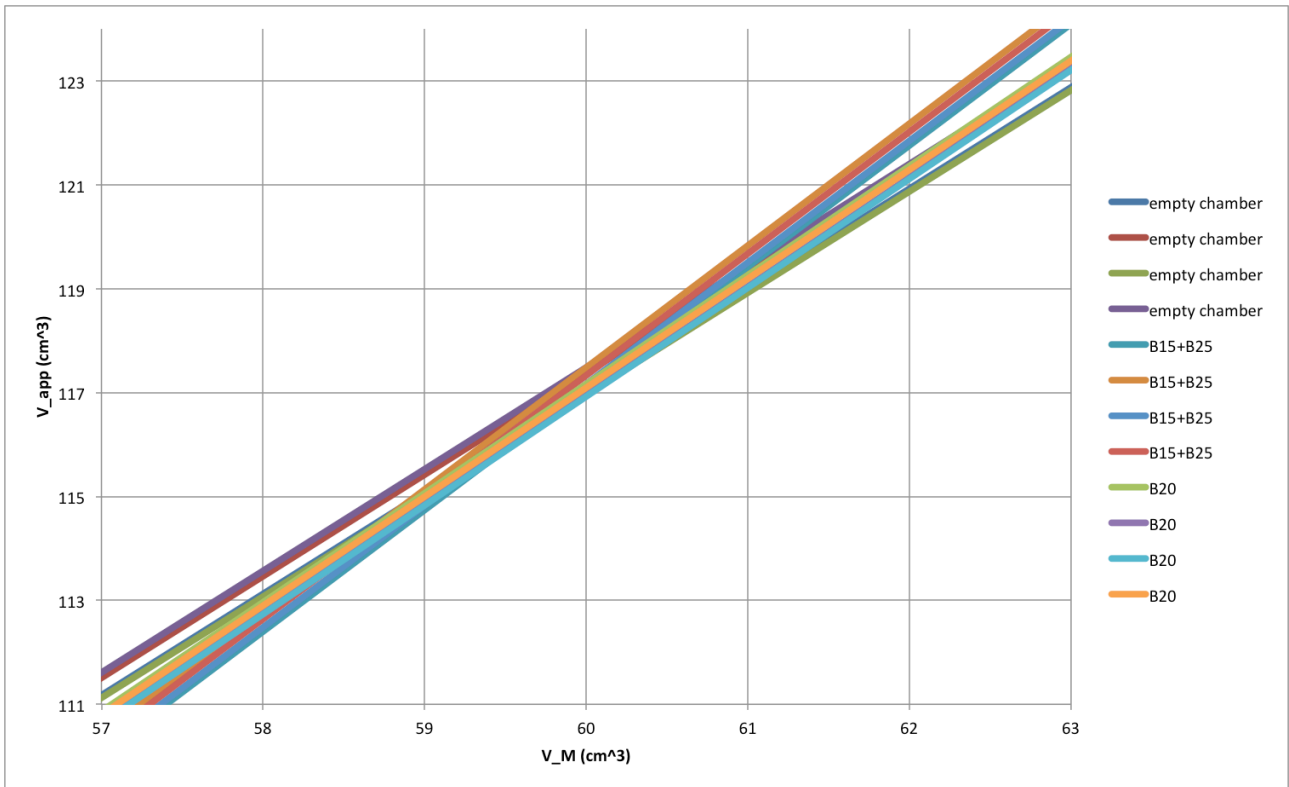


Figure 50. Calibration of V_{app} (and V_M). 12 independent measurements.

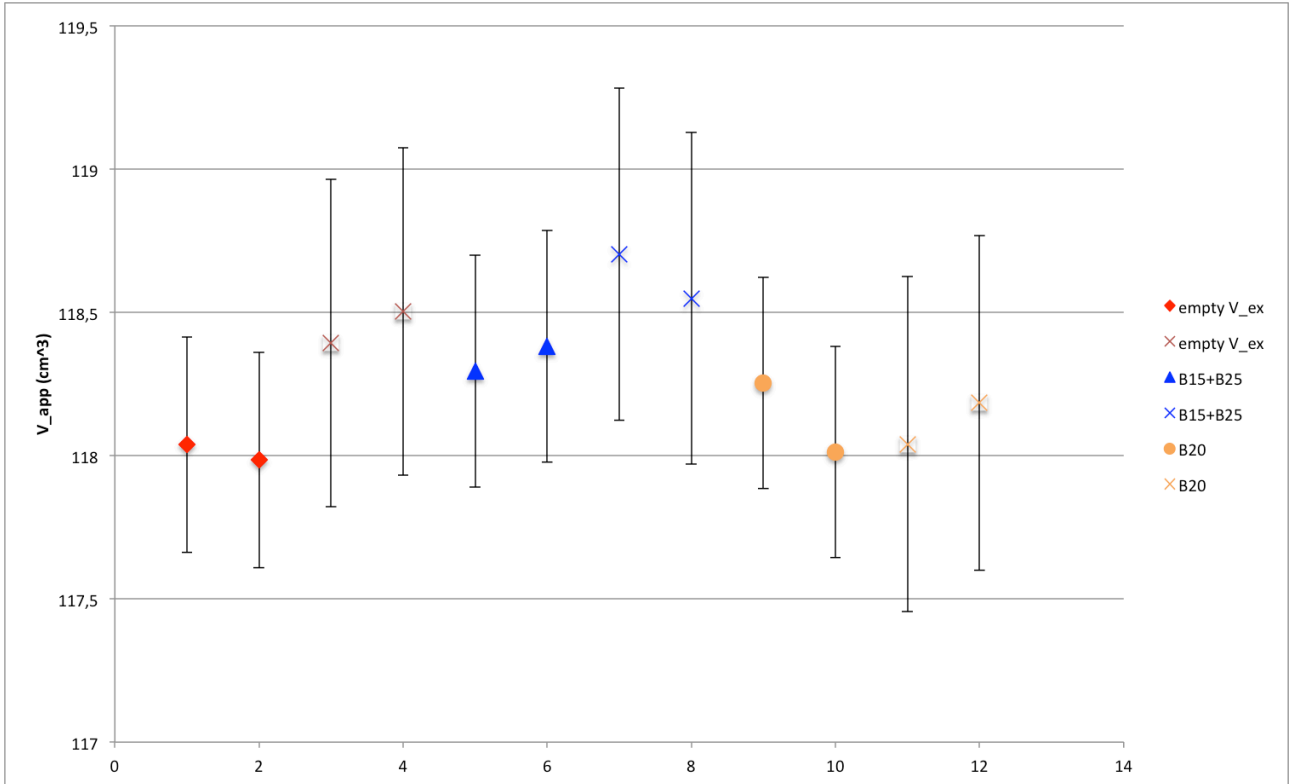
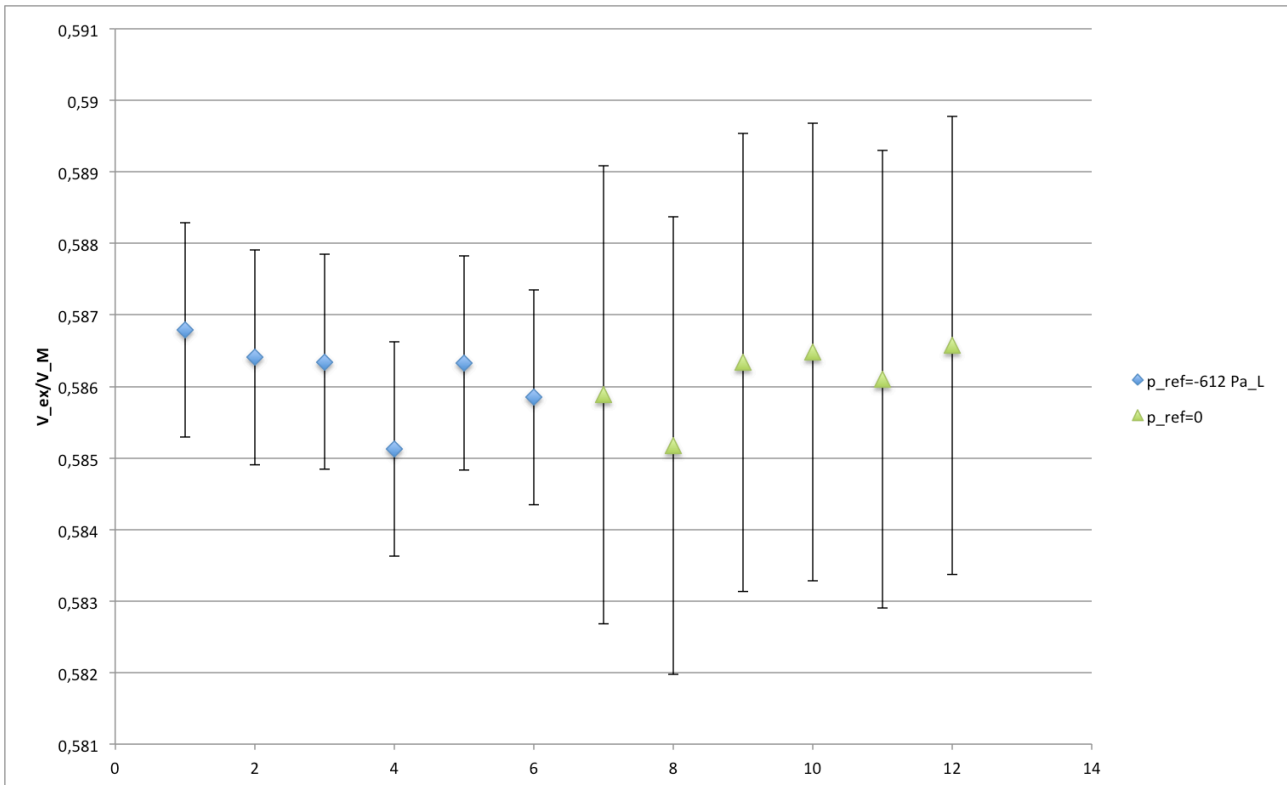


Figure 51. Calibration of V_{app} given $V_M=60,52 \text{ cm}^2$.

Calibration of V_{ex}

V_M is partitioned in $V_{ex} + V_{tub}$. These volumes are calibrated by trapping air in V_M , reading the pressure, closing valve7 (preserving the pressure in V_{ex}), evacuating V_{tub} , and expanding the in V_{ex} trapped air into V_{tub} . We then get the ratio V_{ex}/V_M .



Figur 52. Calibrating V_{ex}/V_M . Error bars indicate 2 Pa on the pressure difference between the 2 pressure measurements.

12 independent of these experiments gives mean $V_{ex}/V_M = 0,5861$ and $\frac{\sigma}{\sqrt{12}} = 0,00015$.

That gives $V_{ex} = (60,52 \pm 0,05) \text{ cm}^3 \cdot (0,5861 \pm 0,00015) = 35,47 \text{ cm}^3 \pm 0,04 \text{ cm}^3$.

Finally we have:

$$V_{tub} = \left(1 - \frac{V_{ex}}{V_M}\right) V_M = (1 - 0,5861 \pm 0,00015)(60,52 \pm 0,05 \text{ cm}^3) = 25,05 \pm 0,03 \text{ cm}^3.$$

Summarizing the calibrated volumes needed for measurements

Volume	Size (cm ²)	Accuracy (cm ²)
V_M	60,52	$\pm 0,05$
V_{ex}	35,47 (-0,12 at -30°C)	$\pm 0,04$
V_{tub}	25,05	$\pm 0,03$
V_{app}	118,28	$\pm 0,07$

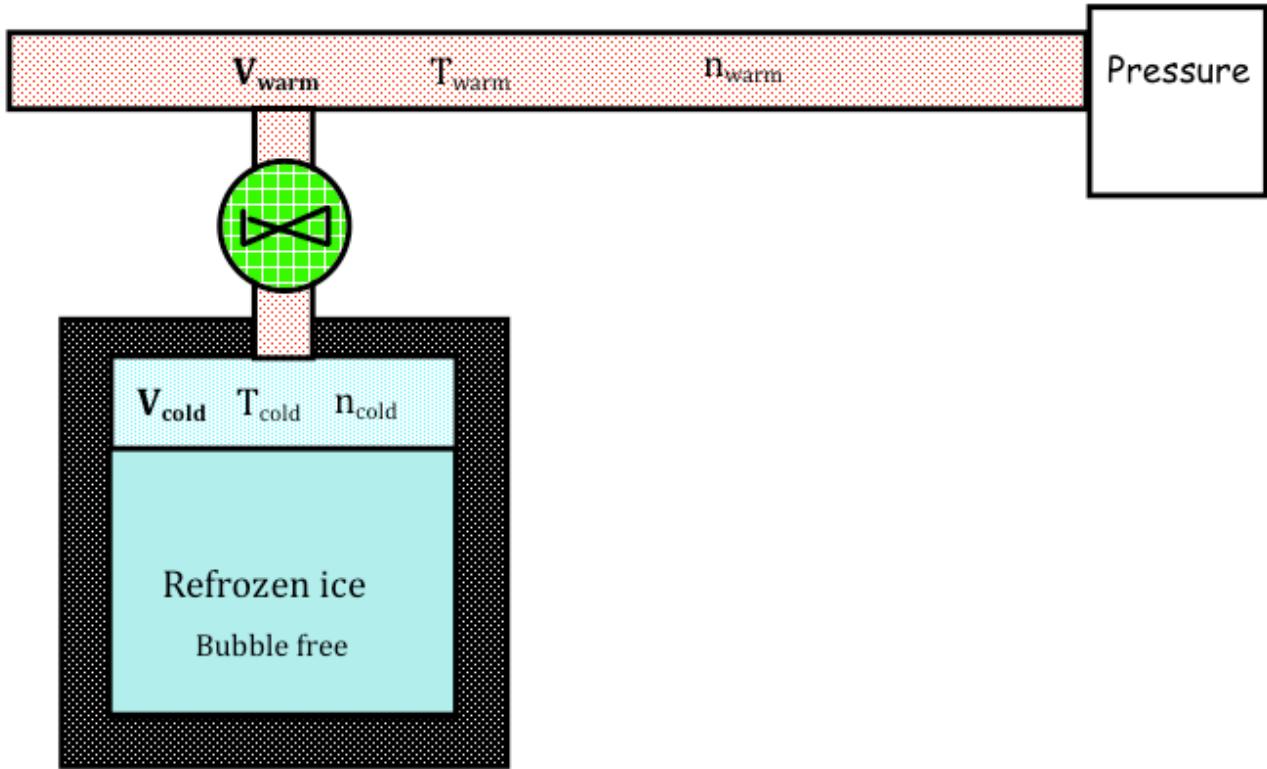
Tabel 5. Calibrated volumes

Measurements on air contained in a volume with variable temperature

When actual measurements are done with refrozen ice in V_{ex} we must consider the volume of the refrozen ice, V_{ice} , and its deprived air is confined in the volume $\tilde{V}_{ex} + V_{tub}$, where $\tilde{V}_{ex} = V_{ex} - V_{ice}$.

By measuring the temperature and pressure to calculate the amount of trapped air, we can safely assume that the pressure is constant through the whole volume, but we must deal with the complication, that the temperature varies across the total volume $\tilde{V}_{ex} + V_{tub}$. We have two temperature sensors attached to V_{ex} and two sensors on V_{tub} . Further we can determine the temperature inside V_{ex} by the vapour pressure. The simplest concept would be to assume the temperature constant in each volume taking the mean of the two sensors on each, or maybe only take the upper sensor on V_{ex} in account, since that is where the air is. The assumption of two separate air masses with homogenous temperatures is not unreasonable, if we consider what happens with the air: It is first contained in \tilde{V}_{ex} , cooled to -30°C and thereby drought. Then the valve connecting \tilde{V}_{ex} and V_{tub} are opened; preferably the valve are just slightly opened – which can be done with some fingerspitzengefühl – so the air expands slowly (that could be a couple of minutes) into V_{tub} . In V_{tub} it expands, cools adiabatically, but quickly heats up by contact with the tube walls. I assume that the flow is turbulent enough in the process of filling the tubes, so contact with the walls will quickly bring the air in temperature equilibrium with the surrounding tube. I assume that the flow from \tilde{V}_{ex} will prevent any heated air in V_{tub} to go back into \tilde{V}_{ex} and mix with the remaining air – this could bring air warmer than -30°C in contact with the refrozen ice and thereby raise the vapour pressure unestimably. Further I assume, that when the expansion is complete and pressure equilibrium in $\tilde{V}_{ex} + V_{tub}$ is attended (pressure=p) no mixing of air between \tilde{V}_{ex} and V_{tub} is going on during the measurement; since the warm air is located above the cold air the conditions should be very stable in this sense. Finally I will make a small correction to the volume division. Since the valve for practical purposes cannot be wrapped in isolation material as the extraction cell,

a small piece of tube below the valve, δV , will belong to the high temperature part; thus we have $V_M = V_{\text{cold}} + V_{\text{warm}}$, where $V_{\text{cold}} = \tilde{V}_{\text{ex}} - \delta V$, and $V_{\text{warm}} = V_{\text{tub}} + \delta V$. The number of mole of trapped air molecules, n , is divided so $n = n_{\text{cold}} + n_{\text{warm}}$, and the fraction $n_{\text{cold}}/n_{\text{warm}}$ is proportional to $T_{\text{tub}}/T_{\text{ex}}$.



Figur 53. Conceptual sketch of 2-airmass-assumption.

When pressure, p , is in equilibrium, it follows that

$$\begin{aligned} p(\tilde{V}_{\text{ex}} - \delta V) &= n_{\text{cold}}RT_{\text{ex}} \\ p(V_{\text{tub}} + \delta V) &= n_{\text{warm}}RT_{\text{tub}} \end{aligned}$$

and hence

$$p = \frac{nR}{\frac{(\tilde{V}_{\text{ex}} - \delta V)}{T_{\text{ex}}} + \frac{(V_{\text{tub}} + \delta V)}{T_{\text{tub}}}} \quad (\text{eq 13})$$

eq 13

We test (eq 13) with dry air in V_M , empty extraction cell, and open valve 7. The cell is cooled to -30°C , while pressure and temperatures are logged – (see Figure 54).

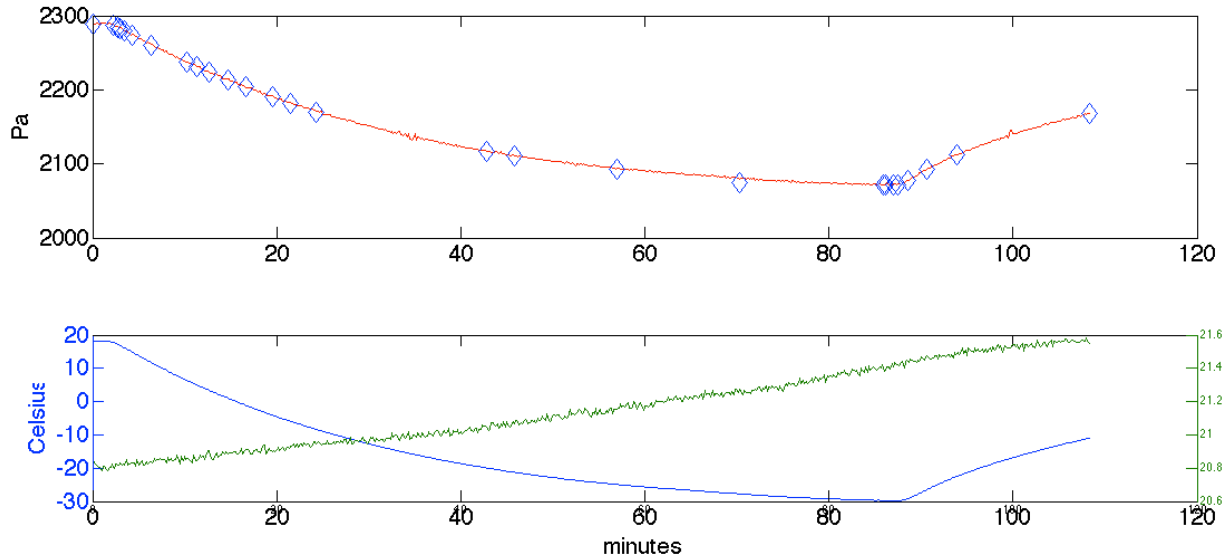
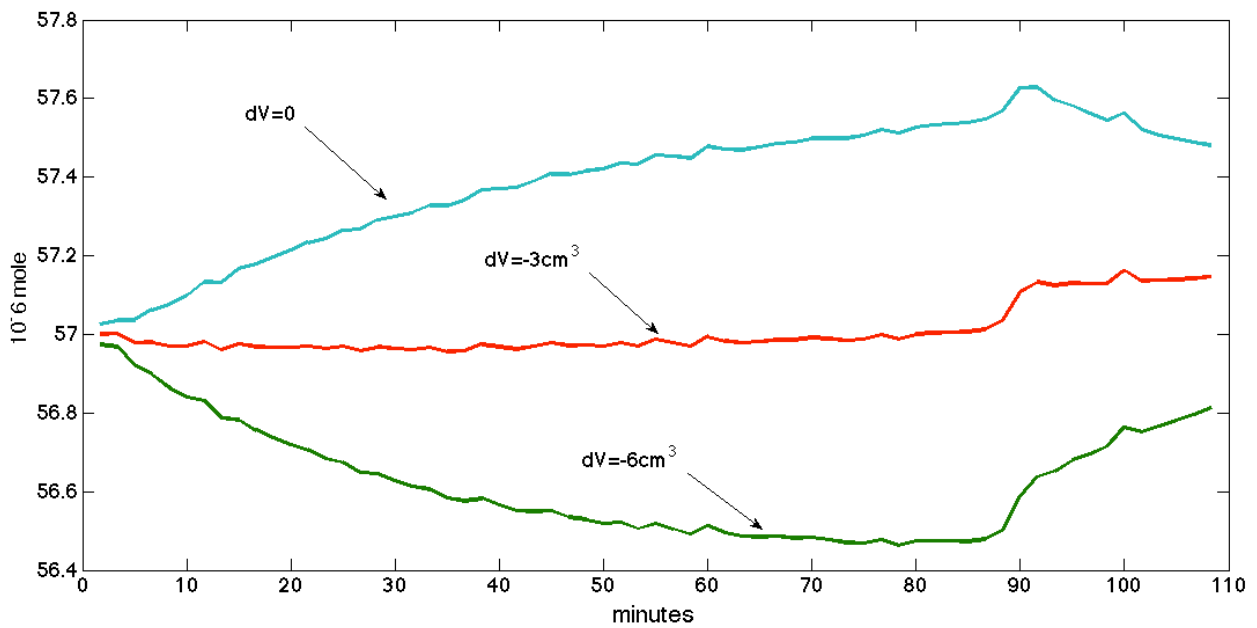


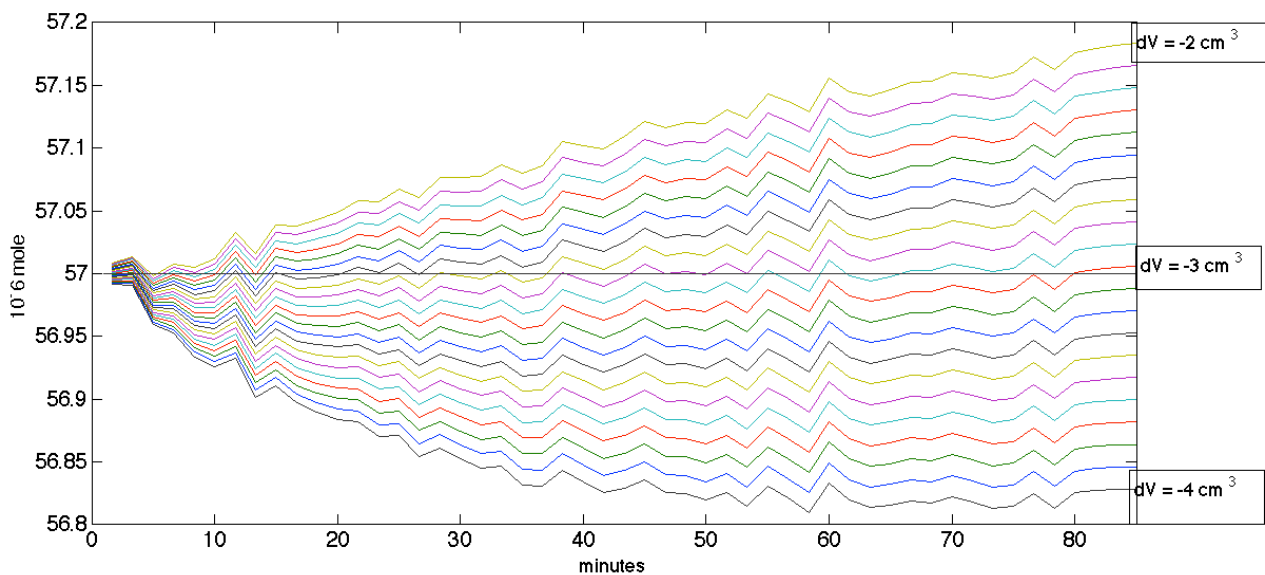
Figure 54. Cooling dry air in the empty cell. Above: pressure (red line: auto logging, blue marks are display readings pedantic pencil noted during the experiment). Below: Temperature on top of the cell, T_{ex} , (blue, left scale) and on pressure gauge, T_{tub} , (green, right scale).

We isolate n in (eq 13) and assume to get a constant value independent of time. Calculations of n throughout the experiment is shown on Figure 55 for 3 different values of δV . It is seen that for $\delta V = -3 \text{ cm}^3$, we get a relatively constant calculation of n , whereas for $\delta V = 0$ or $\delta V = -6 \text{ cm}^3$, we get a deviation that grows to 1% as the cell is cooled from $+20^\circ\text{C}$ to -30°C . Thus the volume correction is important. Further it is seen that when the temperature rises after 90 minutes (the chiller is turned off) the calculation of n jumps, probably because the cell is heating quickest from the bottom and the air inside is warmer than the outside lid of the cell and the temperature sensor; this indicates that it is important to keep a stable temperature for several minutes before real measurements.

To select a precise value for δV , we show a spectre of δV in the interval $[-2 \text{ cm}^3 ; -4 \text{ cm}^3]$ (Figure 56). The best value is $\delta V = -3,0 \text{ cm}^3$ for which (eq 13) gives $n = 57,00 \cdot 10^{-6} \text{ mole}$ for both $+20^\circ\text{C}$ and -30°C . During the whole cooling history the n -calculation deviate less than 0,08% from this. The deviation could well be caused by the lag time in temperature equilibrium.



Figur 55. Calculation of air molecules in the system from the dry air experiment (Figur 54).



Figur 56. With $\delta V = 3,0 \text{ cm}^3$, (eq 13) gives a stable measure of the air content in V_M while V_{ex} is cooled from $+20^\circ\text{C}$ to -30°C .

It was the intention to do more dry air experiments of this kind with steel balls in the extraction cell to reduce the volume simulating refrozen ice, to see if (eq 13) would still hold, but the time went.

From this we can consider the expected pressure range during ice sample measurements. (Lipenkov 1995) found air contents in the range 0,087 to 0,117

cm³ (STP)/g ice. That is $3,57 \cdot 10^{-6}$ to $4,80 \cdot 10^{-6}$ mole/g. The density of refrozen ice is 0,9200 g/cm³ at -30°C (according to www.engineeringtoolbox.com), so every cm³ of refrozen ice has released $3,88 \cdot 10^{-6}$ to $5,22 \cdot 10^{-6}$ mole air. Regarding the range of the pressure gauge the preferable pressure would be in the range 1500 Pa to 2000 Pa. For a sample that in refrozen form has the volume $V_{ice} = 9 \text{ cm}^3$ (near 1/3 of the extraction chamber) and assuming $T_{tub} = 25^\circ\text{C}$ the pressure formula above (eq 13) gives pressures in the range 1487 Pa to 2001 Pa. To that we must add the saturated vapor pressure over ice at -30°C which is 38 Pa. Ice samples much bigger than 1/3 of the chamber volume will give pressures out of the gauge range. As the initial intention was samples of $3 \text{ cm}^3 \times 3 \text{ cm}^3 \times 3 \text{ cm}^3$ (that was before we bought the pressure gauge – eventually it could be substituted with another gauge with wider range) we have let an extra chamber of 50 cm³ fabricate; this can be connected to V_{tub} and thereby give pressures in the proper range in case of bigger samples.

A schedule for measurements should be: 1) measure the pressure for the released air. 2) Evacuate V_M , close valve 4 and measure the vapor pressure while keeping same temperature in both measurements. Then the correction for vapor pressure can be done as a direct measurement.

Summarize of calculations

For measured m_{ice} , T_{ex} , T_{tub} , p , we use (from eq 13)

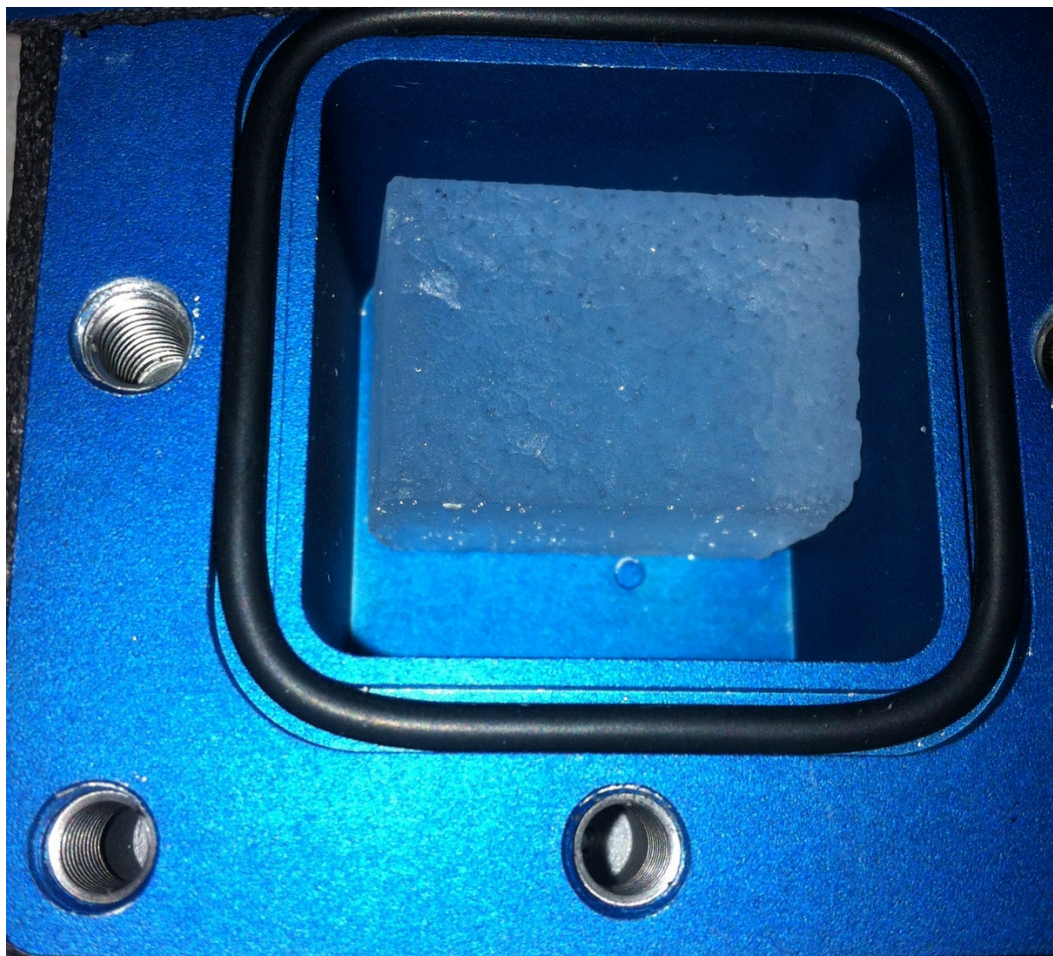
$$\bar{n} = \frac{p}{R} \left(\frac{V_{ex} - \frac{m_{ice}}{\rho_{ice}} - \delta V}{T_{ex}} + \frac{V_{tub} + \delta V}{T_{tub}} \right) \quad (\text{eq 14})$$

eq 14

where p is corrected for vapour pressure. We can use (eq 9) to find n from \bar{n} or measure two times. The air content, n/m_{ice} , can then be given in mole/g ice or alternatively in the unit cm³ air (STP)/g ice which is related to the first as:

$$V = \frac{n}{m_{ice}} R \frac{273K}{1013 \text{ hPa}} \cdot 10^{-6} \quad (\text{where } m_{ice} \text{ is in g}).$$

Ice core measurements



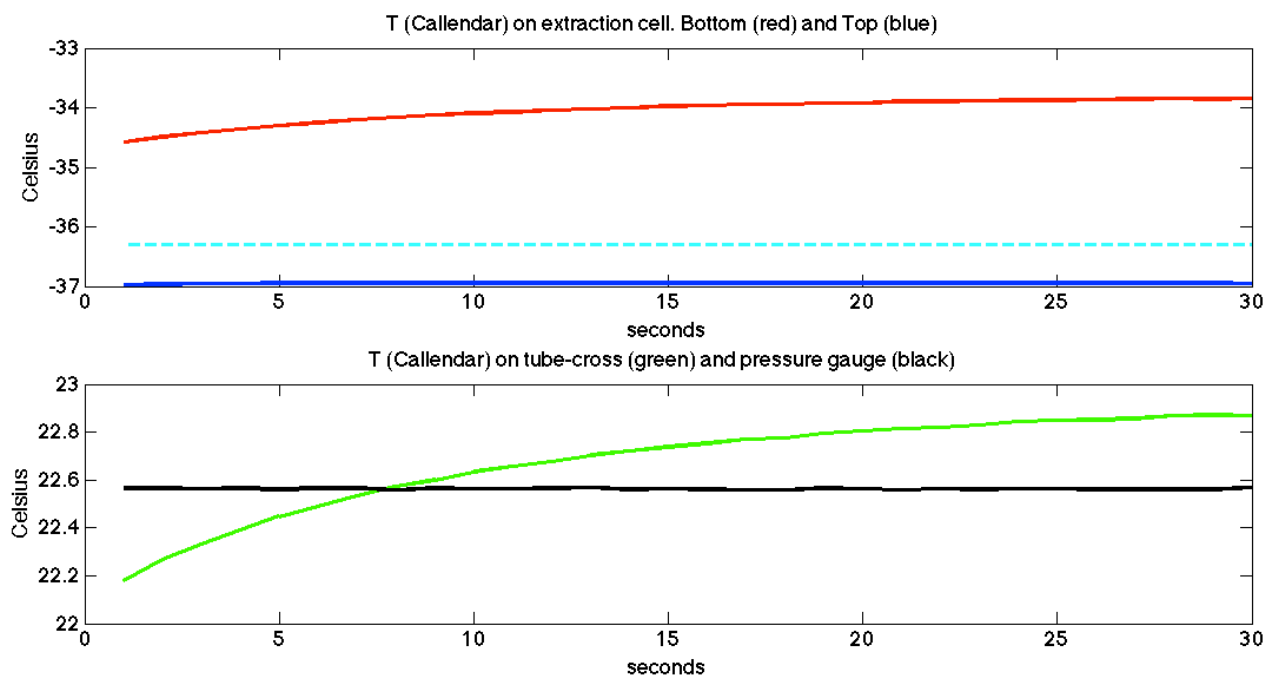
Figur 57. A piece of ice core has just entered the extraction cell in the freezer.

10 ice samples have been measured. The samples were from Eurocore near GRIP from a depth of 220 m. A piece of circa 20 cm was cut into 15 pieces of rectangular but different sizes. All pieces were weighed and their side lengths were measured for surface area determination. The pieces were kept in the CIC freezer. The schedule for the single measurements was as following:

The day before the measurement the extraction cell was brought to the freezer, so it was cooled to -15°C when the sample was put in. The cell was hermetic closed in the freezer and then brought to the laboratory in a polystyrene box. The transport must be done quick and careful – to slow and premature melting can release air bubble; on the other hand, if one runs up the stairs the sample can rattle inside the cell, edges can break and release air as well.

In the laboratory the chiller was on the forehand cooled down, the cell was put on and connected to the line. The cell was evacuated for 15 minutes, then valve 7 was closed, and the extraction procedure conducted. Temperatures on the cell

have always shown to be well below 0°C while evacuation took place. The heating wire enhanced the melting process after evacuation. Cooling was continued until a constant temperature was reached (Figur 59). The temperature sensors were unplugged for a minute. Valve 7 was opened to led the extracted air out; it was preferably opened as slightly as possible and the air sieved slowly out in circa ½ minute, and the pressure was measured. Temperature sensors were plugged in again and the initial temperature taken to avoid the internal heating problem (Figur 58). The whole main volume was evacuated for 5 minutes and pressure and temperature was measured again. This is expected to give the measure of the saturated vapour pressure over ice at the given temperature, and is used:
 For the first to correct the air measurement for vapour pressure.
 For the second it is used to calculate the temperature (assuming that the air is 100% saturated) as an alternative to the temperature measurement (Figur 58).



Figur 58. Temperatures during pressure measurements. Above: temperatures on extraction cell and from the 5 minutes later measured saturated vapour pressure calculated temperature (dashed). Given an accuracy of 1 Pa on the saturated vapour pressure, the error on the here from calculated temperature is $\pm 0,5^{\circ}\text{C}$. Bottom: temperatures on tubes and pressure gauge. The sensors were connected in the moment the measurement was taken. 2 sensors are significantly affected by internal heating.

During the measurements 2 of the temperature sensors (1 on the bottom of the cell and 3 on the tubes) showed to be affected by internal heating (Figur 58). Further sensor 1 showed to be drifting. I had difficulties with fasten them tightly enough to the cell and tube and have moved and replaced them in between some of the measurements. On the other hand the 2 other sensors seemed to be stable so I will rely only on these two for the air content determination. Sensor 4 on the pressure gauge was usually close to the reading of a quicksilver thermometer placed near by. Sensor 2 on the top of the cell is compared to the temperature deducted from the measurement of vapour pressure on (Figur 61) on the 21 measurements of vapour pressure. In the given temperature range the to temperature estimates deviate in mean $1,0^{\circ}\text{C}$ with a low spread. This shows at least that both measures are quiet stable. A priori the pt1000 sensor has a high precision but a low accuracy (since it is not calibrated properly). On the opposite the vapour pressure derived temperature has good accuracy but a lower precision. I will rely on the vapour pressure derived temperature, then, since the pt1000 sensor is not properly calibrated. This could even be a way to calibrate it. Even with a well-calibrated pt1000 sensor the vapour pressure could provide a better estimate for the temperature inside the cell since it probably differ (though not much) from the outside. Assuming an accuracy of ± 1 Pa on the vapour pressure we have a temperature measure with an accuracy of $\pm 0,3^{\circ}\text{C}$ at -32°C decreasing to $\pm 0,55^{\circ}\text{C}$ at -38°C .

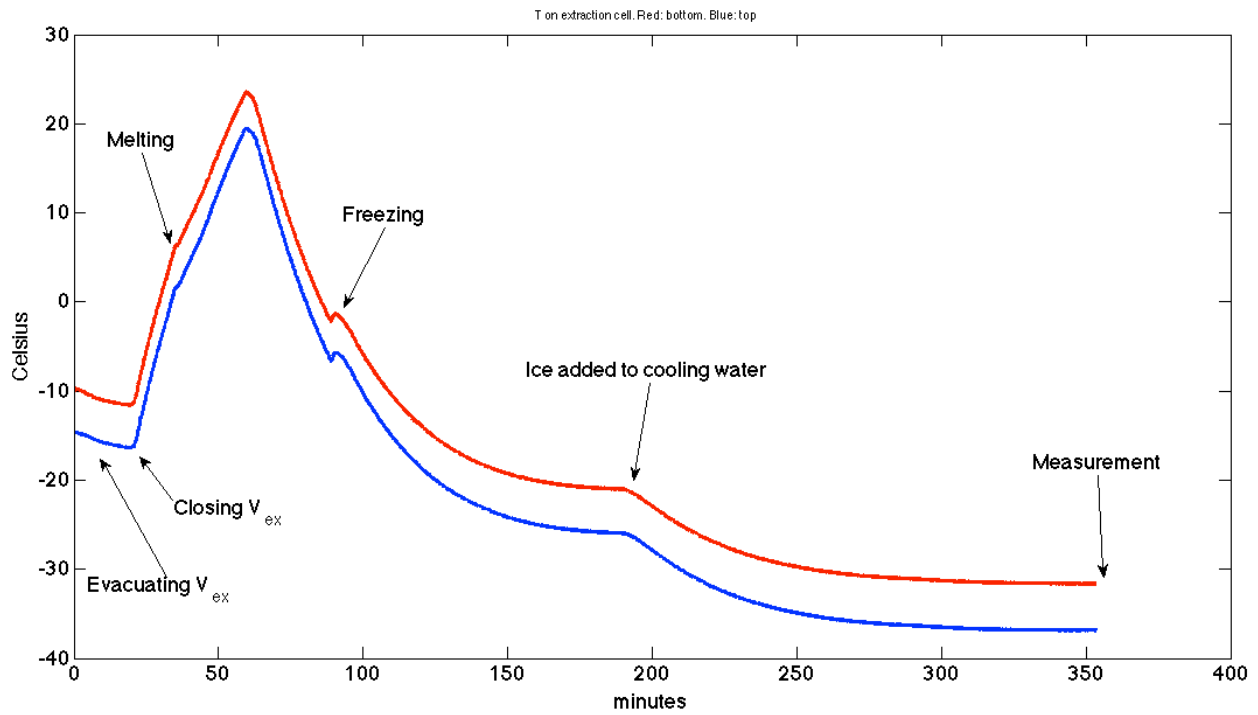


Figure 59. S10 Air extraction before the first measurement.

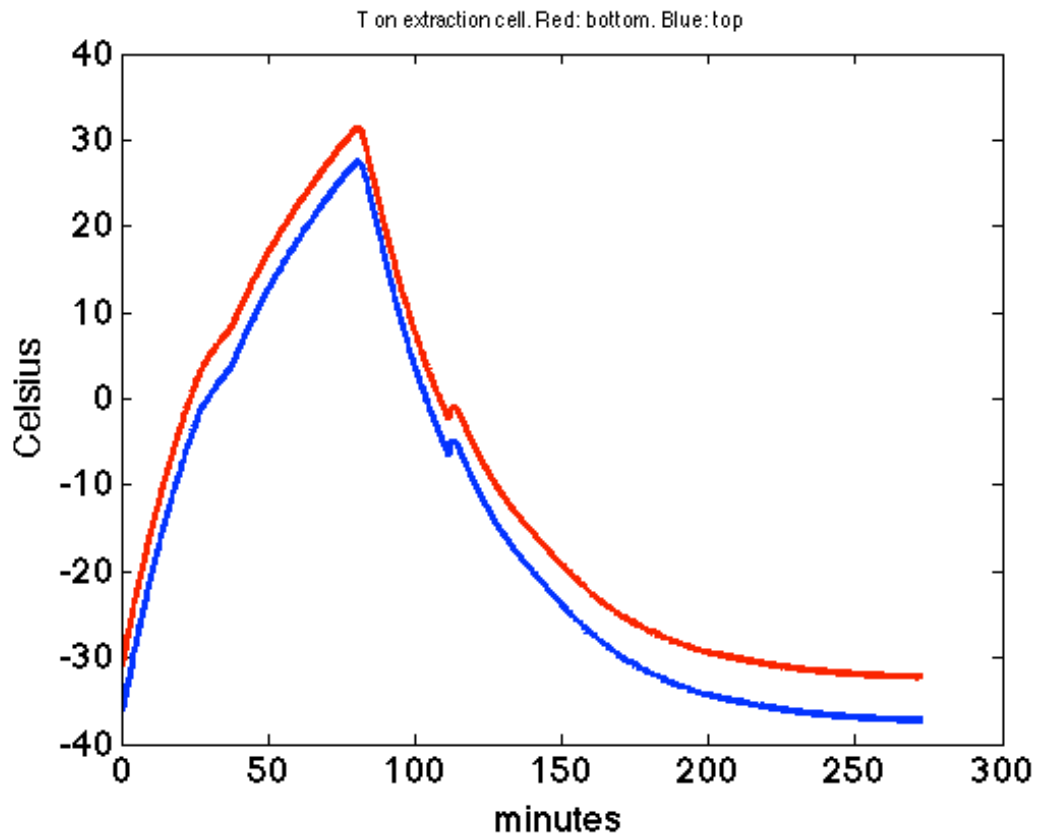
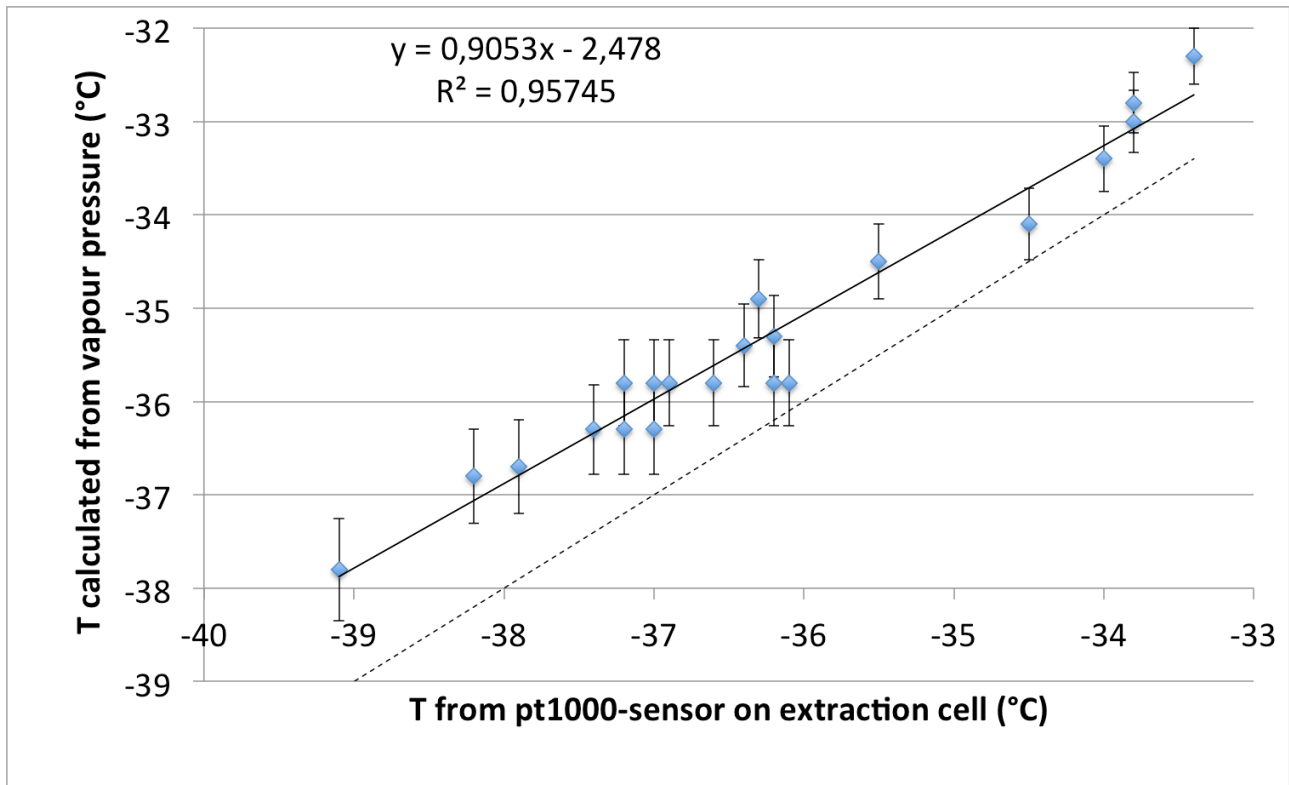


Figure 60. S10. Second extraction. Heating and cooling before second measurement.



Figur 61. Temperature estimation in the extraction cell from 21 measurements done with the pt1000-sensor and by calculating the temperature from the measurement of saturated vapour pressure. The error bars correspond to the error from ± 1 Pa on the pressure measurement giving errors of $\pm 0,55^\circ\text{C}$ near -38°C and $\pm 0,3^\circ\text{C}$ near -32°C . The calculated T consequently gives a lower value than the measured with a mean of $-1,0^\circ\text{C}$. The dashed line ($y=x$) shows the expected calculated T if the measurement gave the correct T inside the cell.

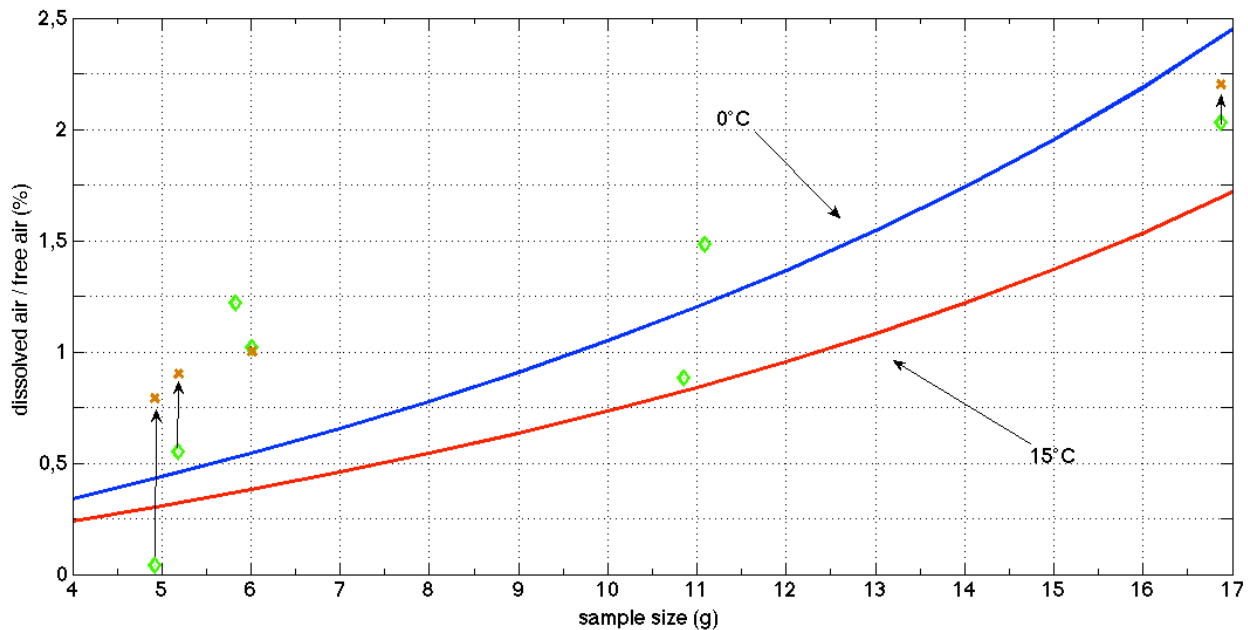
For the problem of dissolved air 7 of the samples were re-melted/re-frozen/re-measured a second time (Figur 60), to extract remnant air and see if it fit the conjecture (eq 9). 4 samples were further measured a third time – then it would be expected no air measurable air was left. The test of extracting remnant air this way is shown on (Figur 62).

First it is noted that 4 of the second extractions gave more air than was expected possible to dissolve. Possibly are the values of Henry constants for O_2 and N_2 too small (a range can be found on Google, which shows that it is difficult to do experiments establishing such constants.) Another explanation could be that some of the degassed air forms small bubbles that stick to the sides of the cell. This phenomenon is observed every day in half emptied glasses of tap water that has heated up to room temperature. A possible method to overcome the problem could be to boil the sample before refreezing; on the other hand it is

preferable not to expose the extraction cell to too big temperature changes, which could cause leaks as the steel and aluminium parts respond different to this. (Lipenkov, 1995) had good experiences with immersing his extraction cell in an ultrasonic bath a 50°C to avoid bubbles.

2 of the 4 third time extraction clearly gave a higher measure than supposed. I must ask myself if the leak was underestimated (see Leak corrections), since more of the second extractions as well give more air than expected, and for the third extraction the sample has always been left overnight in the cell. Especially the leftmost in the diagram is strange since the second extraction gave almost no air from it, but the third gave more. On the other hand it does not look too bad. Most of the second extractions deviate less than 0,5 per cent points from blue line. For the small samples near 5 g the first pressure measurements are circa 750 Pa, so for the next extraction I expect to measure 3 Pa (to hit the blue line), and with an accuracy > 1 Pa this would of course give an significant spread around the line.

For the air content determination I must do something consequently and I decide to use the sum of the first to extractions for the 7 samples and for the 3 only once extracted I add a correction corresponding to the blue line. I will then assume an uncertainty of 0,5% for the question of dissolved air.



Figur 62. 7 samples were measured 2 times (green diamonds) and 4 were further measured a third time (orange x). According to the assumption the green diamonds should lie in the space between the lines and the orange crosses should sprout negligibly from them.

Estimate of the air content

We calculate the air content of each sample from (eq 14) and either sum two sequent extractions or correct for extracted air by (eq 9) assuming $T=0^{\circ}\text{C}$. Assuming that the ice the samples are taken from has a homogenous air content per mass, $n/m=c_1$. But the samples have different surface areas, A_i , and we have cut a number of bubbles proportional to A_i thereby lost some of the air. That is for a given sample

$$n_i = c_1 m_i - c_2 A_i$$

or

$$\frac{n_i}{m_i} = c_1 - c_2 \frac{A_i}{m_i} \quad (\text{eq 15})$$

eq 15

or

$$V_i = \frac{R \cdot 273K}{1013 \text{ hPa}} \frac{n_i}{m_i} = V^* - c \frac{A_i}{m_i}$$

where V_i is the measured air content and V^* is the real air content in STP cm^3/g . We assume to find a linear relation between V_i and $\frac{A_i}{m_i}$ that will give V^* . The 10 samples are shown on (Figur 63).

Individual errors on all measurements

The error bars on the $\frac{A_i}{m_i}$ -axis is taken by assuming an accuracy of ± 1 mm on the sides of the samples; uncertainty on m is neglected.

For the error on the single measurements $M_i \equiv \frac{n_i}{m_i}$ I use the propagation of error formula on eq 9 divided by m . That is

$$M = \frac{\bar{n}}{m} = \frac{p}{mR} \left(\frac{V_{ex} - \frac{m}{\rho_{ice}} - \delta V}{T_{ex}} + \frac{V_{tub} + \delta V}{T_{tub}} \right)$$

Let s denote the error on the different parameters, then the error on the single measurement M_i is given by:

$$s_M = \sqrt{s_p^2 \left(\frac{\partial M}{\partial p}\right)^2 + s_{V_{ex}}^2 \left(\frac{\partial M}{\partial V_{ex}}\right)^2 + s_{V_{tub}}^2 \left(\frac{\partial M}{\partial V_{tub}}\right)^2 + s_{\delta V}^2 \left(\frac{\partial M}{\partial \delta V}\right)^2 + s_{T_{ex}}^2 \left(\frac{\partial M}{\partial T_{ex}}\right)^2 + s_{T_{tub}}^2 \left(\frac{\partial M}{\partial T_{tub}}\right)^2 + s_m^2 \left(\frac{\partial M}{\partial m}\right)^2}$$

(I have omitted the index i above for clarity). The partial derivatives have pedantically been derived, but I shall omit the expressions here.

To this error I add an error of 0,5% of M for the dissolved air uncertainty:

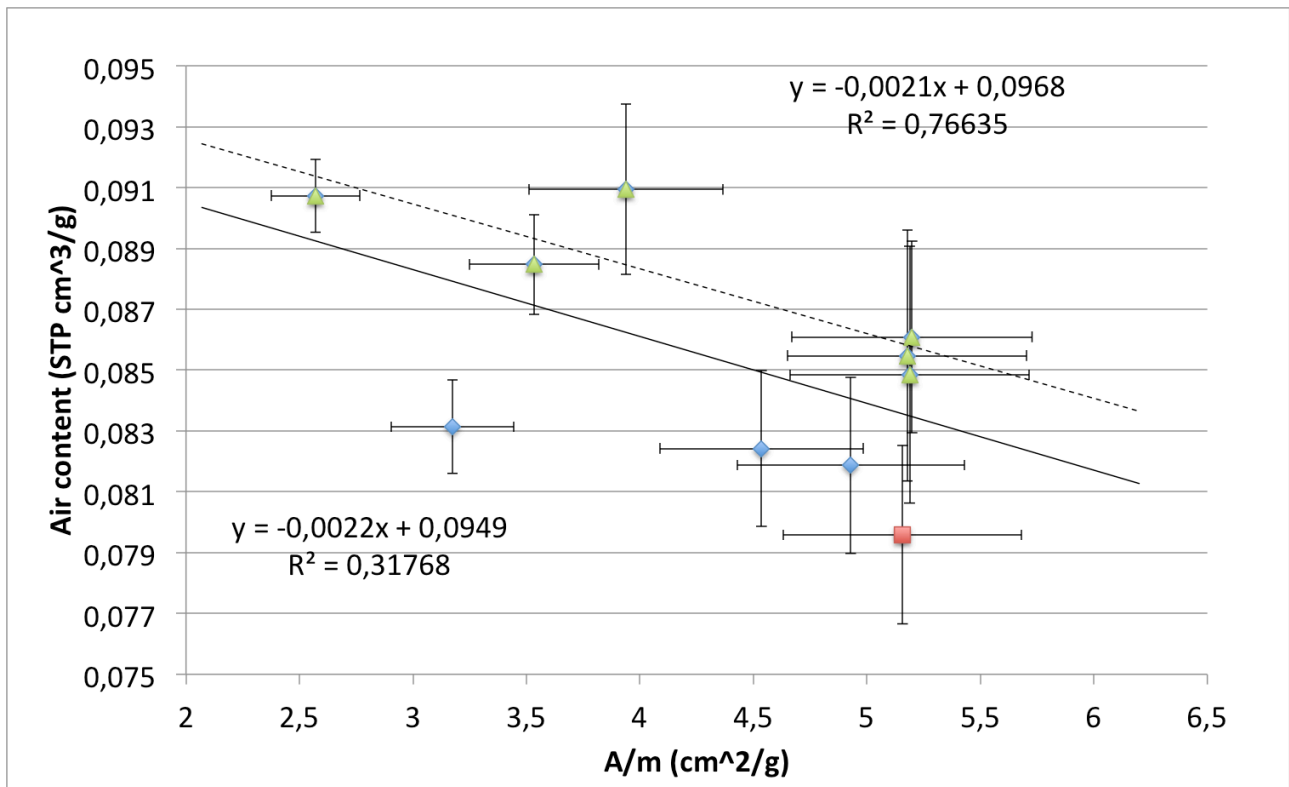
$$s_M^* = s_M + 0,05M$$

and

$$s_V = \frac{R \cdot 273K}{1013 \text{ hPa}} s_M^*$$

For the samples that were extracted twice I calculated error on each and summed them for the final error.

By first glance it can be hard to see what causes biggest uncertainty. The whole expression was put in a spreadsheet, where I can study the influence from the error on the individual parameters changing them one by one, either setting them to zero or raise them to an over number.



Figur 63. Determination of the air content in the 10 samples. Full line: linear regression of all samples. Dashed line: linear regression of green samples.

The errors on the **volumes** are given in (Tabel 5). These errors give a minor contribution to the complete errors.

On the **mass** I have taken $s_m=0,1$ g. The samples were weighed on an apparatus that gave the weigh in g with 2 digits; I had carefully horizontalised it, and it should be very precise, but the reading was not complete stable; I would need a chamber to put above it to avoid draft. The mass error has a pregnant influence on the smallest samples (in the right end) with masses near 5 g, but it hardly influences the largest samples (left side) near 17 g.

The error on the **temperatures** is set to $0,5^\circ\text{C}$. Initially I wanted an accuracy of $0,1^\circ\text{C}$, but as the problems of sensor calibration and stability arose, I must realize it has been higher. Though the temperature error hardly has any effect on the complete error even if I raise it to 1°C .

The error on **pressure** is set to 7 Pa. Actually I regard the accuracy on single pressure measurements as better. For example the 21 vapour pressure measurements in the range 16 to 30 Pa seems to be consistent with temperature (Figur 61). Often I have seen the pressure rise by one Pa when closing a valve,

and it is amazing to imagine how this sensitivity is possible. Then there are the two measurements from two extractions each with a possible error, and the leak correction with a possible error. I would like to say, that each of these 3 terms is ± 1 Pa summing to ± 3 Pa, but as given from the producer I will say ± 7 Pa. The contribution of this is slightly lower than the composite error of $\pm 0,1$ g on m and $\pm 0,5^\circ\text{C}$ on T.

The main contributor to the error on the biggest sample is the **dissolved air** error of 0,05%. On the small samples this error does not make a big impact.

As seen on (Figur 63) the 10 measurements do not provide the linear relation (eq 15) to a degree where a line can be fit within the errors from the single measurements. The regression line divides the points in a low and a high group. From this we must suspect that either the ice was not homogenous or some measurements have been affected by errors not taken into account. The question would be whether these errors have contributed positively or negatively to the air content. Leaks would contribute positively and premature melting, or damaging of the ice samples during sawing or transport to the laboratory would contribute negatively. One sample that surely is erratic is the one marked with red on Figur 63; it was the first sample that was measured. After the measurement the cell was opened and air bubble could be seen in the refrozen ice (Figur 65). I expect the reason was a piece of ice survived the melting; the maximum temperature had been 10°C . In later experiments I got in the habit of heating the cell to 20°C for the melting. Since we must assume that this measurement is underestimated one could suspect that 3 other samples in the low end are also underestimated for some unknown reasons. For the remnant 6 samples (green on Figur 63) it is possible to make a linear fit. Of course linear regression in this case must be criticized: the points are not normal distributed, the points on the right side get an over weight. Further the accuracies are different. Somehow I would like to make a fit that gave the most precise measurements the highest weight.

The most accurate measurement (left most) had sides 3,0 cm x 2,9 cm x 2,2 cm and weighed 16,87 g. It was by the way the only sample where V_{app} had to be added to keep the pressure down. There is room for even larger samples in the cell and it would be interesting to have some measurements of samples as big as possible, which would have the best accuracy.

Correction for the cut bubble effect

Nevertheless we cannot deny there is a slope. Assume it is, as the regression says, $c = -0,0021\text{cm}^2/\text{g}$. That says for every cm^3 surface $0,0021\text{cm}^3$ air is lost due

to bubble cutting. Assume the bubbles are spherical and divided into halves by the cut. That is equivalent to:

for each cm^2 there is:

two bubbles of diameter 1,6 mm

or 8 bubbles of each 1,0 mm in diameter

or 66 bubbles of 0,5mm in diameter.

It would be interesting to study the size and density of the bubbles.

(Lipenkov,1995) says that for samples of 25 g the 'cut-bubble effect' is 10% near the close off and 1% deep in the ice, and that it can be estimated from the size and shape of the bubbles.

We correct all measurements for the air lost by cut bubbles, that is we add $c \frac{A_i}{m_i}$ to the measurements. We must then add $c \cdot s_{A/m}$ to the errors on V^* .

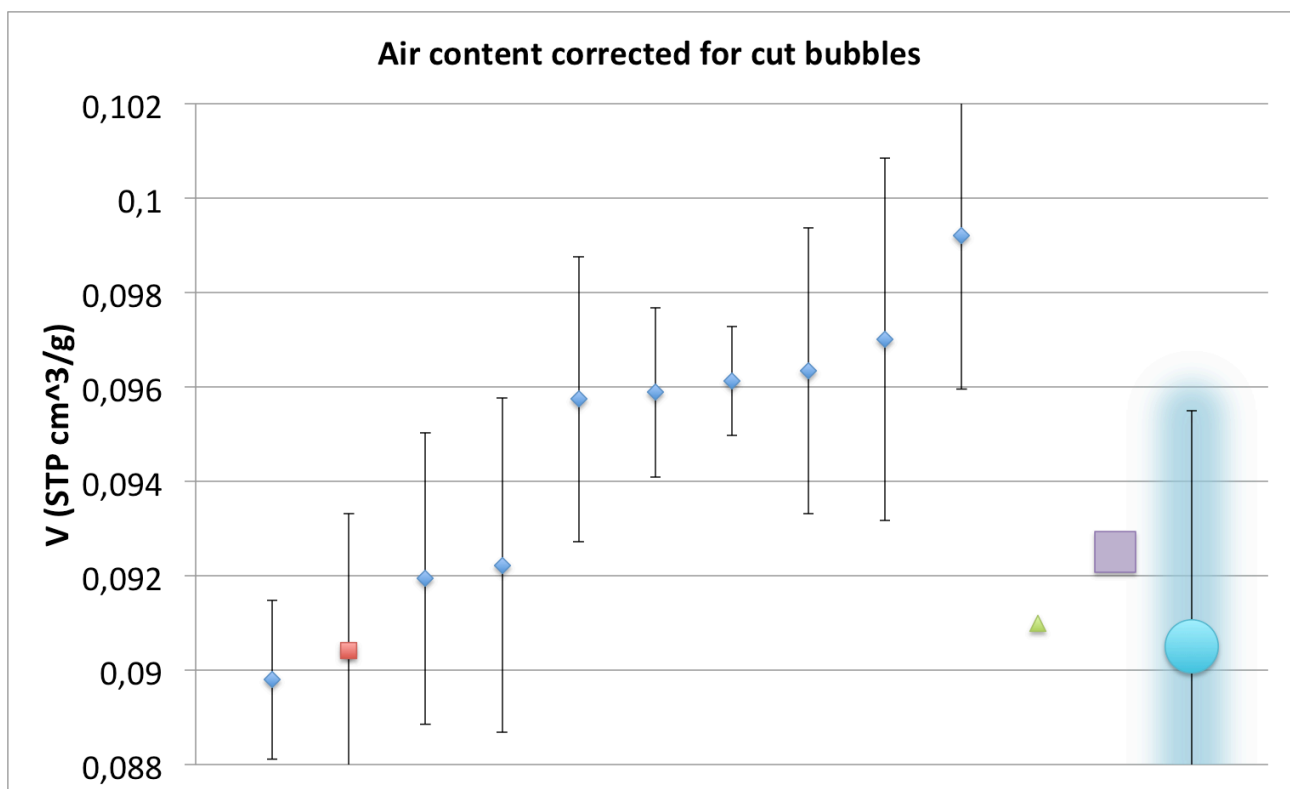


Figure 64. The cut bubble corrected measurements compared with (Raynaud, 1997) to the right: Green triangle ~ Eurocore 160 m depth. Violet square ~ present day at GRIP site. Blue circle ~ last millennium mean and the variation over Holocene marked as shade.

On Figure 64 the samples are sorted after bubble corrected air content. It looks again like the samples fall in two categories: one with mean $V^* = 0,091 \text{ cm}^3/\text{g}$ and another with mean $V^* = 0,097 \text{ cm}^3/\text{g}$. The overall mean is:

$V^*=0,094$ STP cm^3/g but with no samples in the interval $0,092$ to $0,096$ cm^3/g , though the error have now grown.

Comparing with Raynaud is also shown on Figur 64:

(Raynaud,1997) says:

Eurocore 160 below surface: $V=0,091$ cm^3/g

Present day conditions at GRIP: $V=0,092 - 0,093$ cm^3/g

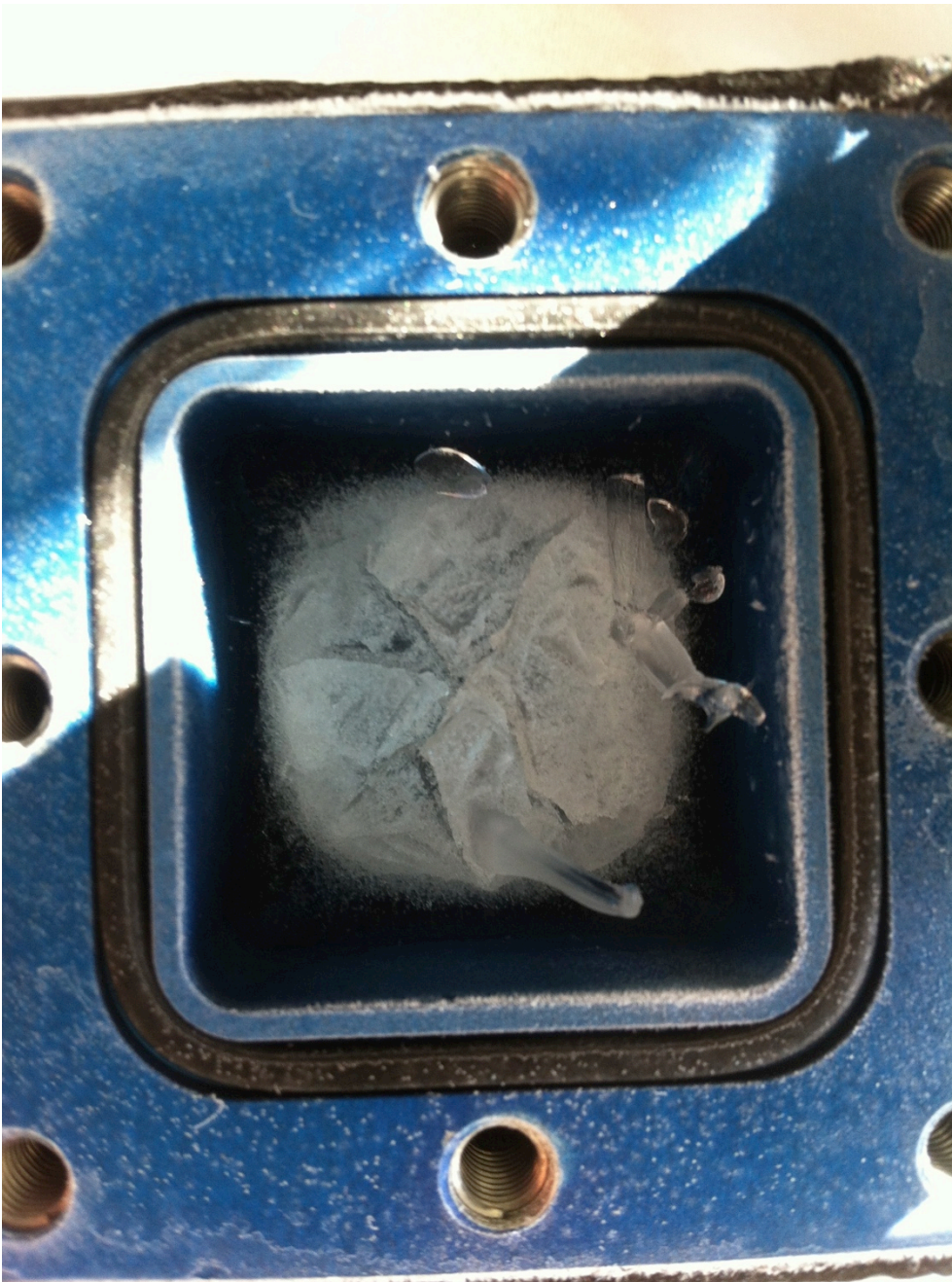
(calculated from an empiric temperature-air content relation)

Mean for last millennia at GRIP: $V=0,090 - 0,091$ cm^3/g
with measurements in the range $0,085$ to $0,095$ cm^3/g .

For the 4 samples with lowest content the agreement with Raynaud very satisfactory (I believe though, that the red coloured sample would be amid the highest group if all air had been extracted). The remnant 6 gives though a higher value than we would expect. The one with highest content actually is an impressive Olympic record of air content ever measured in Holocene ice at GRIP. The mean of all 10 samples is as well a bit over the expectation.



Figur 65. The first sample after the measurement. Not all air was extracted; in the centre air bubbles are seen.



Figur 66. The -30°C cell is opened after 3 successive extractions. Ice stalagmites had grown vertical upwards from the extracted ice surface (seen on the right and bottom) - a visible proof of the importance of drying the air. The cracks radiating from the centre is formed when the aluminium cell contracts and squeezes the ice under the low temperatures.

Possible explanations for the deviation from Raynaud

Why do 6 samples deviate from the expectation? Was it caused by measurement errors? I have thought of following:

- 1) Maybe it can be taken seriously that the samples fall in two groups with different air content. Sometimes strong winds can pack the firn and form an ice layer that **prematurely close off** the firn below (Raynaud, 1997) that following will get a higher air content than the surrounding ice. It is not impossible that the 6 samples are from such a layer, a signature of a polar storm. Unfortunately I cannot reconstruct the adjacency of the samples; the piece they were cut from was not slice from one end, but irregular cut to get rid of a bad side and turned several times to collect all useful pieces. I imagined that it was completely homogenous then, but now it would be interesting to know the original position of the pieces.
- 2) I overestimate the **cut bubble effect** - with a lower slope on Figur 63 I could get air content in the present day range 0,092 to 0,093 cm³/g. The 4 remnant samples would then be too low.
- 3) **Leaks** in the extraction cell. Since it is opened and moved in connection with every measurement there is possibilities for not closing it totally the same way every time. Further the many heating and cooling cycles could damage the thread or the O-ring. But from the many second and third extractions I can refuse that any serious leaks have taken place. They would have been discovered in the second and third extractions, where almost no dry air was in the cell for many hours.
- 4) Air **degassing from the cell walls**. I have often observed that I can pump on the empty cell for several hours. When I close V_M there is a pressure – it could be 5 Pa. I can evacuate again for a while but not get rid of this pressure – it persists like a small background pressure. This same problem does not happen for V_{tub} , which can be perfectly evacuated in few minutes. It can take several days of constant pumping to get rid of this background pressure. A have assumed that it is vapour slowly evaporating from small culverts for example along the O-ring from where the molecules has a long and narrow way into the inner cell. As long as it is only vapour it will though not affect the ice measurements. But if it is also dry air it will have an effect. It could even be that the aluminium walls has an absorptivity for the air molecules. Every time a molecule hits the wall it will not rebound, as assumed in the derivation of the gas equation, but is actually absorbed in the wall while another molecule is expelled. For the evacuated cell there will be an exponential decay in this molecule expelling causing this observed background pressure. For the measurements I always evacuated the cell for only 15 minutes; from then I checked there was a stable

pressure – the saturated vapour pressure, before I closed V_{ex} . I think that this degassing problem could not have such a big influence, but it could be interesting to make a test measurement, where the cell was evacuated for 3 hours before melting of the sample. Though it must then be estimated or measured how much of the sample sublimates.

- 5) Measurements are affected by a **systematic error**. If for example the **temperatures** are consequently underestimated, I will overestimate the air content. How much wrong should the temperatures be to explain the disagreement? To test this I add a constant to all temperatures and recalculate the air content. To increase T_{ex} can in no way bring the result closer to Raynaud. Even if I change T_{ex} to room temperature I increase c without much change in V^* and a worse correlation. Namely the best measurement done with V_{app} is not much dependent of T_{ex} since it only applies 11% of the air space. Then I can try to add T_{tub} . I must increase T_{tub} by 12°C I reach an air content of 0,0929 for the high samples and that with a poorer correlation. That would be in agreement with Raynaud, but it is impossible that that room temperature was wrong with 12°C, I have measured between 22 -25°C for all 21 measurements. So, I can refuse that the disagreement is caused by errors in temperature measurements.

Then I turn to the **pressure** measurement. I correct all pressures with 95%. The result is an air content of 0,092 cm³/g for the 6 high samples and almost same cut bubble effect and correlation. A systematic overestimation by 5% on all pressure measurements could explain the difference. Actually, if I omit the calibration done in Calibration of the pressure gauge the air content would be in better agreement with Raynaud. But it is undeniable that the pressure gauge needed to be calibrated as tests like that in Tabel 3 easily shows, and it is implausible that the DMI-tested barometer should be that erratic. So I will say, that it is not plausible that systematic errors in the pressure measurements causes the deviance.

Could the **volumes** be overestimated? If I reduce all volumes by 3% the result is in good agreement with Raynaud. But V_M is calibrated in to different ways, and from Figur 48 and Figur 50 it is clear that 3% error is impossible. The volume calibration depends of course on the pressure precision, but even the change that came following the pressure gauge calibration only changed the volumes less than 0,5%.

From the above considerations I cannot really explain the high spread in the measurements with errors. If I could I would make a series of measurement on samples with $m > 15$ g, they have the lowest error as the sample on Figur 64 with $V^* = 0,096 \pm 0,001$ cm³/g. To refer to the quick consideration in Effects of variations in ice sheet elevation, this single measurement would determine the close-off height with precision ± 74 m.

To further reduce the error I would change the pt1000 sensors. They would not stick to the cell wall and tubes. There exist a type incorporated in a thread. It would be an improvement if they were screwed into the metal; they would actually be closer to the air, and we would not have to speculate about a possible temperature gradient across the cell wall. I would certainly have a sensor placed on V_{app} , and I would have more sensors on V_{tub} . Then I would make a proper calibration and then establish a relation with saturated vapour pressure and see if it would fit with (eq 1). Possibly I would use (eq 1) to calibrate the pt1000-sensor. A further improvement would be working on the degassing from water; either by finding a way to refreeze from the bottom slowly or experimenting with boiling the sample. This actually causes bigger error than the temperature problem right now for big samples. I would also study the effect mentioned in 4).

Sample	m (g)	dimension (mm x mm x mm)	T _{ex} (°C)	T _{tub} (°C)	p (Pa)	V* (STP cm ³ /g)
1	4,96	31x25x9	-35,8	24,1	701,4	0,0904
2	4,94	31x25x9	-35,4	22,3	748,5	0,0963
3	4,93	31x25x9	-34,9	23,5	743,6	0,0957
4	5,19	31x25x9	-33,4	24,3	762,3	
4b			-32,8	25,0	4,2	0,0922
4c			-32,3	24,4	2,7	
5	10,85	27x27x22	-36,3	22,6	1943,8	
5b			-35,3	22,8	17,2	0,0959
6	4,92	31x25x9	-35,8	22,6	753,1	
6b			-35,8	22,1	0,3	0,0970
6c			-34,1	21,8	5,7	
7+V _{app}	16,87	30x29x22	-36,8	22,7	1005,0*	
7b			-35,8	23,5	73,5	0,0961
7c			-35,8	22,5	6	
8	11,09	29x22x22	-34,5	22,9	1875,1	
8b			-33,0	25,0	27,9	0,0898
9	6,01	29x29x9	-35,8	23,1	894,3	
9b			-36,3	22,2	9,1	0,0919
9c			-37,8	22,1	-0,2	
10	5,83	10x22x29	-36,3	22,1	949,1	
10b			-36,7	22,6	11,6	0,0992

Tabel 6. Measurements. b and c denotes second and third extraction. T_{ex} is derived from vapour pressure measurement. p is corrected for vapour pressure and leak.

Suggestion for changes in the setup

- The **pt1000** sensors should be changed to the thread types.
- The **resistors** should be changed with high quality temperature independent resistors.

- Another extraction cell with **limpid plastic sides** has been manufactured by the workshop. Possibly slowly refreezing from the bottom will work with that (I have not tested it).

Acknowledgements

I will thank a lot of people for a lot of help with this project. Thanks to: Thomas, Bo, Corentin, Peter, Theo, Myriam, Christoffer, Dennis, Preben and Simon have all helped a lot.

Literature

Lipenkov, V. et al: Instruments and Methods. A new device for the measurement of air content in polar ice. *Journal of Glaciology*, Vol. 41, No. 138, 1995.

Raynaud, D. et al: Air content along the Greenland Ice Core Project core: A record of surface climatic parameters and elevation in central Greenland. *Journal of Geophysical Research*, Vol. 102, No. C12, November 30, 1997.

Raynaud D. et al.: The local insolation signature of air content in Antarctic ice. A new step toward an absolute dating of ice records. *Earth and Planetary Science Letters* 261, 337-349, 2007.

Taylor, John R.: *Error Analysis*. Sausalito, 1997.